Ministry of Higher Education and Scientific
Research of the Republic of Algeria
Ahmed Draia University
Faculty of Matter Sciences,
Mathematics and Computer Science
Department of Mathematics and Computer Sciences

THESIS

In view of obtaining the grade of

Doctor in Mathematics

Speciality : Applied Mathematics

Presented by

Abdeldjalil Kadri

Contribution to the modeling and mathematical analysis of some stochastic epidemiological models

Prof.	**Abdeldjalil Slama**	University of Ahmed Draia Adrar, Algeria	Chairman
Prof.	**Ahmed Boudaoui**	University of Ahmed Draia Adrar, Algeria	Supervisor
Prof.	**Tomás Caraballo**	University of Seville, Spain	Examinator
Dr.	**Mebrouk Rahmane**	University of Ahmed Draia Adrar, Algeria	Examinator
Dr.	**Nourhane Attia**	NHS for Marine Sciences and Coastal, Algeria	Examinator

Academic Year: 2024-2025

Dedication

I dedicate this work to my parents:

May they find here the testimony of my deep gratitude and acknowledgment

To my brothers and my sisters, my grandparents and my family who give love and liveliness.

To all those who have helped me - directly or indirectly - and those who shared with me the emotional moments during the accomplishment of this work and who warmly supported and encouraged throughout my journey.

To all my friends who have always encouraged me, and to whom I wish more success.

Thanks!

Abdeldjalil KADRI

Acknowledgements

Praise be to the Almighty God who has given me faith, courage, and patience to carry out this work.

I want to express my deep gratitude to my supervisor **Prof. Ahmed Boudaoui**, for the confidence he has placed in me, through his presence always with me, by his direction, his modesty, his advice, and constructive remarks for the good progress of this work.

I express my sincere gratitude to the members of the jury **Prof. Abdeldjalil Slama**, **Prof. Tomás Caraballo**, **Dr. Mebrouk Rahmane** and **Dr. Nourhane Attia**, for the honor they gave me while accepting to examine my work and taking part in this dissertation and for their time and valuable comments my dissertation.

I would like to thank everyone who helps me to improve my work. and who gave me any remark that helped me to perfect this manuscript.

I express my deep gratitude to my parents, my brothers, my sisters, and my whole family for their encouragement and prayers that allowed me to achieve this modest job. I am very grateful for the confidence they have placed in me.

Finally, I express my gratitude to all those who have contributed in one way or another to the development of this work.

O Allah, send your blessings on your noble messenger, his family, and companions, and bless us in our life.

Contents

List of Symbols

$\mathbf{a.s.}$	**Almost surely.**
$\mathbf{p \vee q}$	**Maximum of p and q.**
$\mathbf{p \wedge q}$	**Minimum of p and q.**
$\mathbf{C^k(U, \mathbb{R}^n)}$	**Space of continuously k-times differentiable $\mathbb{R}^n$-valued functions defined on U.**
$\mathbf{C^{1,2}(\mathbb{R}_+ \times \mathbb{R}^n, \mathbb{R})}$	**Space of all real-valued functions $Q(t, X)$ defined on $\mathbb{R}_+ \times \mathbb{R}^n$ which are once differentiable in $t \in \mathbb{R}_+$ and continuously twice differentiable in $X \in \mathbb{R}^n$.**
$\mathbf{C(U, \mathbb{R}^n)}$	**Space of continuous $\mathbb{R}^n$-valued functions defined on U.**
$\mathcal{L}^p([a, b]; \mathbb{R}^n)$	**Space of $\mathbb{R}^n$-valued $\mathcal{F}_t$-adapted processes $h(t)_{t\in[a,b]}$: $\int_a^b \lvert h(t)\rvert^p dt < \infty$ a.s.**
$\mathcal{M}^p([a, b], \mathbb{R})$	**Space of processes $h(t)_{t\in[a,b]}$ in $\mathcal{L}^p([a, b]; \mathbb{R}^n)$: $\mathbb{E}\int_a^b \lvert h(t)\rvert^p dt < \infty$.**
$\mathbf{L^p(\Omega, \mathbb{R}^n)}$	**Space of $\mathbb{R}^n$-valued random variables$Y$ with $\mathbb{E}\lvert Y\rvert^p < \infty$.**

All other symbol will be clarified upon its first occurrence.

List of Tables

List of Figures

Chapter 1

General introduction

Historically, infectious diseases have often manifested as catastrophic plagues, with some persisting to the present day while new ones continue to arise. Recent instances of developing diseases globally encompass West Nile virus, Zika virus, Influenza, HIV, Hepatitis virus, and most recently, COVID-19 (see [13, 38, 88]). These diseases are frequently induced by infectious agents, including bacteria, viruses, fungi, or parasites, and can disseminate by multiple avenues, such as direct human contact, environmental exposure, interactions with animals, or bug bites. Without appropriate control mechanisms, such diseases can escalate into epidemics or even worldwide pandemics, as evidenced by the COVID-19 situation. The dissemination and intensity of communicable diseases are inconsistent; their advancement is contingent upon various factors, including the pathogen's nature, the affected population's characteristics, and environmental influences such as climate, healthcare infrastructure, ecological changes, and seasonal fluctuations.
Mathematical modelling is an essential element of epidemic preparedness strategies, facilitating the prediction of outbreak dynamics and the assessment of potential interventions (see [33, 82]). As modelling can be performed remotely, researchers can aid in preparedness and control efforts without the necessity of physical presence in the field (see [38, 47]). Furthermore, it reduces dependence on costly and ethically intricate experiments. In this thesis we will explore some of the ways in which mathematics can be used to understand infectious disease dynamics, and attempt to expand the methodological inventory available to infectious disease modellers.

1.1 A brief history of epidemic models

The definition of infectious illness epidemiology began with John Graunt's 1662 work, "Natural and Political Observations made upon the Bills of Mortality." This foundational work engaged

with the communal Bills of Mortality, detailed records of mortality data and causes in London parishes, originating from 1592 and systematically recorded from 1603. The exemplary data in these records enabled Graunt's astute examination of death trends, producing new understandings of the relative mortality risks linked to different diseases and representing the initial move towards a whole theory of competing hazards.

In the 18th century, smallpox was a prevalent and enduring disease. The initial mathematical model in epidemiology was thus shaped by Daniel Bernoullis (1700-1782) investigation of the impacts of smallpox inoculation [85]. Variolation, a technique for developing immunity by exposing persons to a benign strain of the virus, was implemented to provide enduring protection, however it carries a little risk of infection and fatality. Since that time, several efforts have been undertaken to elucidate the effects of certain epidemics on the population; nonetheless, the non-linear dynamics of their transmission remained inadequately comprehended until the twentieth century. W. H. Hamer in 1906, was the first observer of the phenomenon wherein a declining number of vulnerable persons can result in the extinction of the measles epidemic. He established the inaugural conventional epidemiological framework for modelling illness prevalence [85]. Similarly, S. R. Ross using mathematical modelling in 1911 to evaluate the efficacy of various therapeutic strategies against malaria [2]. W.O. Kermack and A.G. McKendrick in 1927, produced a comprehensive model for the transmission of epidemics through direct contact. They evaluated their model with empirical data from the spread of the Bombay epidemic during 1905 and 1906 [14]. Their theory was essential in the eradication of Smallpox in the 1970s [33]. By the conclusion of the twentieth century, mathematical epidemiology gained prominence in the formulation of public health policies. A multitude of contributions has been made to the modelling of certain epidemics, with the majority of these research depending on diverse assumptions grounded in deterministic formulations. Since the commencement of the 21st century, numerous epidemics have emerged (see [13, 37, 47, 132]). This renewed interest in mathematical modelling enhanced the Kermack-McKendrick model and incorporated novel hypotheses based on the attributes of each epidemic.

1.2 Mathematical modeling

A mathematical model depicts a system using mathematical concepts and language. The development of such models is referred to as mathematical modelling. These models elucidate system dynamics, assess the impact of various components, and predict future behaviours. Their forecasting capacity is very advantageous for decision-making. This thesis concentrates on the modelling of infectious diseases and their spread among populations. Mathematical modelling is

a multifaceted methodology applicable across several disciplines, including biology, physics, and economics.

The modelling approach, depicted in Fig.1.1 [82], converts a biological scenario into a mathematical problem, commencing with a precise system description and a defined research objective. The system is represented by variables and parameters linked by relationships, emphasising only pertinent elements for precision. Upon formulation, the model can be scrutinised with mathematical instruments, calibrated to data, employed to estimate parameters, and simulated to evaluate the influence of each parameter on the answer.

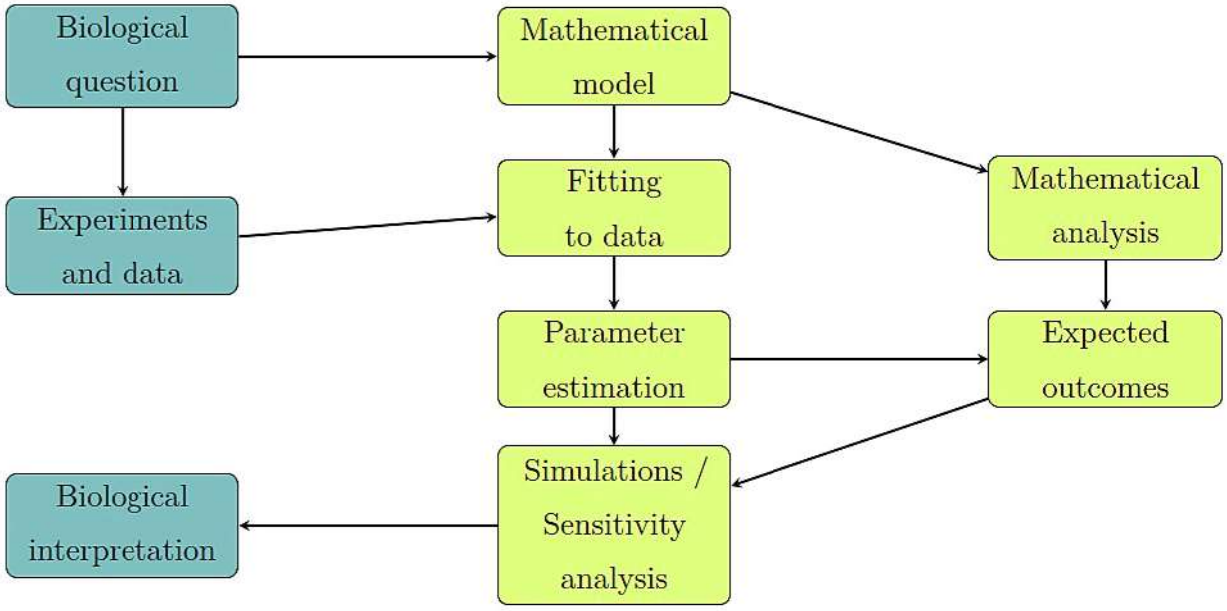

Figure 1.1: Modeling diagram.

1.3 Deterministic epidemic models: a prelude to mathematical modeling using compartemental approach

This section describes the process of developing a mathematical model for disease transmission using a compartmental approach. We begin by dividing the host population into distinct, non-overlapping groups-referred to as compartments-based on the disease's progression. For a basic infectious disease, these compartments may include: people susceptible to infection S, infected individuals I, people that have recovered from infection R. Figure (1.2) illustrates the transmission process.

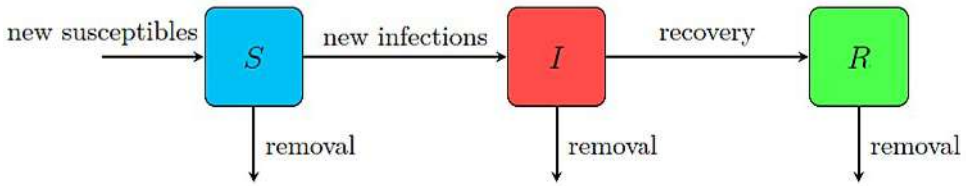

Figure 1.2: Transfer diagram for a SIR compartment model.

In this diagram, arrows depict the movement of individuals between different compartments. The term "removal" encompasses the departure of individuals due to death or migration.
The purpose of modeling is to monitor the population of hosts within each of the three compartments at any given time t. These quantities are represented as $S(t)$, $I(t)$, and $R(t)$, respectively. We examine a brief time interval $[t, t + \Delta t]$ and analyze the net change in the number of people within each compartment. In the transfer diagram, arrows depict the direction of people movement. The net change in a compartment is determined by the number of people entering it minus those exiting during the given time interval. By using this principle to each compartment, we derive the following equations:

$$\begin{aligned} \Delta S(t) &= [\text{new susceptible}] - [\text{removal from } S] - [\text{new infections}], \\ \Delta I(t) &= [\text{new infections}] - [\text{removal from } I] - [\text{transition into } R], \\ \Delta R(t) &= [\text{transition from } I] - [\text{removal from } R]. \end{aligned} \tag{1.1}$$

Dividing both sides of (1.1) by Δt and taking the limite as $\Delta t \to 0$, we derive the following system

$$\begin{aligned} S'(t) &= [\text{new susceptible}] - [\text{rate of removal from } S] - [\text{incidence rate}], \\ I'(t) &= [\text{incidence rate}] - [\text{rate of removal from } I] - [\text{transition rate into } R], \\ R'(t) &= [\text{transition rate from } I] - [\text{rate of removal from } R]. \end{aligned} \tag{1.2}$$

By representing all terms on the right-hand side as functions of $S(t)$, $I(t)$, and $R(t)$, we derive a system of differential equations that constitute our mathematical model. The formulation of these functions is determined by the assumptions made about disease transmission and the flow of individuals between compartments. Below we will show examples of some classic deterministic models.

1.4 Some classical epidemic model

1.4.1 The SIR model without demography (Kermack-McKendrick model)

To illustrate how the rates in equation (1.2) depend on $S(t)$, $I(t)$, and $R(t)$, we introduce the following hypotheses regarding disease transmission and host population dynamics.

- Horizontal Transmission: disease spreads through direct contact between individuals.
- Homogeneous Mixing: individuals interact randomly, and the incidence rate follows the Law of Mass Action ($\beta I(t)S(t)$, where β is the transmission coefficient).
- Proportional transfer rates: movement between compartments depends on population size (e.g., recovery rate is $\gamma I(t)$).
- No latency period: individuals become infectious immediately upon infection.
- Permanent immunity : no reinfection; recovered individuals stay immune.
- Closed population: no births, deaths, or migration; no new susceptibles enter. Since there is no influx or removal, the total population remains unchanged.

These assumptions allow the conceptual model in Figure (1.2) to be converted into the explicit model shown in Figure (1.3)

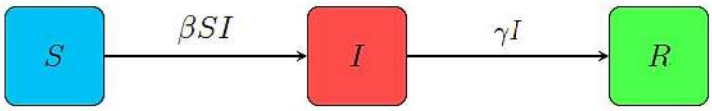

Figure 1.3: Transfer diagram for a simple SIR model.

Substituting all terms in (1.2) by our mathematical descriptions, we derive the following model [85]:

$$\begin{aligned} S'(t) &= -\beta SI, \\ I'(t) &= \beta SI - \gamma I, \\ R'(t) &= \gamma I. \end{aligned} \tag{1.3}$$

To ensure well-defined mathematically, this model (1.3) is initialized with the following

$$S(0) = S_0 > 0, \;\; I(0) = I_0 > 0, \;\; R(0) = R_0 \geq 0.$$

Since $S(t), I(t)$ and $R(t)$ denote the number of people, they are expected to take nonnegative values. Constants β and γ are model parameters, and they are assumed to be nonnegative since

they denote rate constants. If the values of model parameters β and γ are known, then for each set of initial conditions S_0, I_0 and R_0, model (1.3) has a unique solution $(S(t), I(t), R(t))$ that produces a prediction for the time course of the epidemic for $t > 0$. The region

$$\mathbb{R}^3_+ = \left\{(S,I,R) \in \mathbb{R}^3 : \quad S \geq 0, I \geq 0, R \geq 0\right\}$$

is positively invariant w.r.t. model (1.3).
If the epidemic is ever to take off, $S_0 > \frac{\gamma}{\beta}$. In other words the initial number of susceptibles must exceed the quantity $\frac{\gamma}{\beta}$.

A fundamental quantity in mathematical epidemiology is the basic reproductive ratio, commonly denoted R_0. This quantity is defined to be the expected number of subsequent cases produced by a single infectious case in a population which has had no previous exposure to infection [51].
In the context of the model (1.3), R_0 can be expressed as $R_0 = \beta.S_0.\frac{1}{\gamma}$ can be interpreted as

average number of effective contacts of a single infectious host	· initial susceptible population	· mean infectious period .

When $R_0 > 1$ the epidemic takes off while there is a minor outbreak when $R_0 \leq 1$.

1.4.2 The SIR model with demography

To incorporate demographic factors into the Kermack- McKendrick models , the birth and death processes are assumed to have the same rate constant μ, and the disease is not fatal. The total population is kept as a constant, which is already scaled to 1. The updated transfer diagram is presented in Fig. 1.4, resulting in the following model (1.4) [85]:

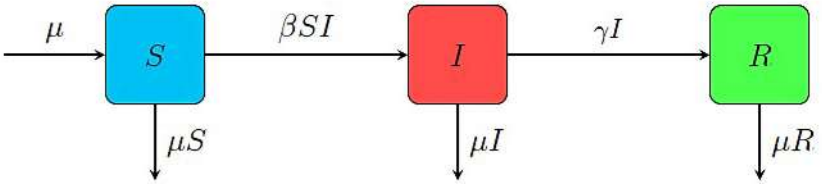

Figure 1.4: Transfer diagram for a SIR epidemic model with demography.

$$\begin{aligned} S'(t) &= \mu - \beta SI - \mu S, \\ I'(t) &= \beta SI - \gamma I - \mu I, \\ R'(t) &= \gamma I - \mu R. \end{aligned} \tag{1.4}$$

The feasible region for model (1.4) is:

$$\Pi_{SIR} = \Big\{(S,I,R) \in \mathbb{R}^3 : S + I + R = 1\Big\}.$$

The basic reproduction number of model (1.4) is expressed by $R_0 = \frac{\beta}{\mu+\gamma}$. To simplify our analysis, we can ignore the R equation since the first two equations in (1.4) do not contain R. Once behaviors of $(S(t), I(t))$ are known, those of $R(t)$ can be readily obtained from $R = 1 - (I + S)$. For this reason, we can consider the following equivalent system:

$$\begin{aligned} S'(t) &= \mu - \beta SI - \mu S, \\ I'(t) &= \beta SI - \gamma I - \mu I, \end{aligned} \tag{1.5}$$

with the feasible region is

$$\Pi_{SI} = \Big\{(S,I) \in \mathbb{R}^2 : S + I \leq 1\Big\}.$$

In general, the long-term behaviour of the epidemic is established by analyzing the equilibriums of its model, or the states in which the solution does not change over time. To find equilibria of (1.5), we set $S' = I' = 0$ and obtain a system of algebraic equations

$$\begin{aligned} 0 &= \mu - \beta SI - \mu S, \\ 0 &= \beta SI - \gamma I - \mu I. \end{aligned} \tag{1.6}$$

Solving these equations, we obtain two possible equilibria: $E_0 = (1, 0)$, the disease-free equilibrium, and $E^* = (S^*, I^*)$, the endemic equilibrium, where

$$S^* = \frac{\gamma + \mu}{\beta}, \qquad I^* = \frac{[\beta - (\mu + \gamma)]\mu}{(\gamma + \mu)\beta}.$$

More precisely, system (1.5) has two possible equilibria. If $R_0 \leq 1$, then $E_0 = (1, 0)$ is the only equilibrium in Π_{SI}. If $R_0 > 1$, then both E_0 and the endemic equilibrium E^* exist in Π_{SI}.

1.4.3 The SEIR epidemic model

Many infectious diseases involve an exposed phase after the infection is transmitted to a susceptible person, but before that person becomes symptomatic and infectious . To account for the latent period, we add an exposed compartment E, characterized by a mean duration of $\frac{1}{\alpha}$, thereby extending the classical epidemic model to the $SEIR$ framework (1.4), we obtain the following diagram:

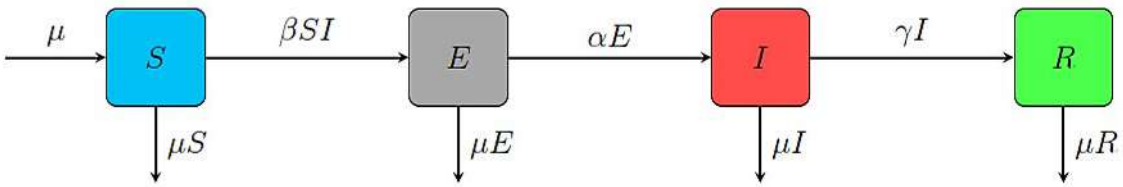

Figure 1.5: Transfer diagram for a SEIR epidemic model.

and we have

$$\begin{aligned} S'(t) &= \mu - \beta SI - \mu S, \\ E'(t) &= \beta SI - \alpha E - \mu E, \\ I'(t) &= \alpha E - \gamma I - \mu I, \\ R'(t) &= \gamma I - \mu R. \end{aligned} \tag{1.7}$$

For the SEIR model (1.7), the basic reproduction number is given by

$$R_0 = \beta . \frac{\alpha}{\alpha + \mu} . \frac{1}{\mu + \gamma},$$

which can be interpreted as

average number of effective contacts of a single infectious host	$\cdot$	probability of a newly infected host surviving the latent period	$\cdot$	mean infectious period	.

It is important to note that the mean infectious period, given by $\frac{1}{\gamma+\mu}$, represents the average time an individual remains both alive and infectious. Additionally, observe that in this case, the basic reproduction number R_0 does not explicitly depend on the initial number of susceptible individuals. This is because the total population $R + I + S + E = N$ is normalized to 1 in the model. As models become more intricate, deriving R_0 directly from the transmission diagram can become challenging. In such cases, alternative methods are used, most of which rely on stability analysis of the disease-free equilibrium[113].

1.5 Key concepts in epidemiologic dynamics

In general, infectious diseases spread through direct contact between susceptible and infected individuals. Let N denote the total population size, and let $Q(N)$ represent the number of individuals an infective comes into contact with per unit time. Some fundamental concepts are outlined below [78]:

1. Let p_0 be the probability that a single contact results in transmission. Then, the product $p_0Q(N)$ is referred to as the adequate contact rate, quantifying the infectivity of an individual. This rate depends on factors such as the pathogen's virulence and environmental conditions.

2. The fraction $\frac{S}{N}$ represents the probability that a contact involves a susceptible individual.

3. Consequently, $Q(N)\frac{S}{N}$ gives the expected number of contacts an infective makes with susceptible individuals per unit time. Note that not every such contact results in transmission.

4. The product $p_0Q(N)\frac{S}{N}$ represents the mean adequate contact rate between an infected individual and susceptibles. This is also referred to as the infection rate.

5. The total number of new infections per unit time is therefore $p_0Q(N)\frac{SI}{N}$, which is termed the incidence rate of the disease.

If we define $\Theta(t) = p_0Q(N)\frac{I}{N}$, then the incidence can be expressed as $\Theta(t)S$. The function $\Theta(t)$ is known as the force of infection. Furthermore, $\frac{I}{N}$ represents the proportion of the population that is currently infected, i.e., the prevalence of the disease. The absolute number of infected individuals, denoted $I(t)$, is also referred to as the prevalence.

There are two commonly used forms of incidence in epidemiological modeling:

If $Q(N) = \kappa N$, i.e., contact rate is proportional to population size with per capita contact rate κ, the incidence becomes $\beta S(t)I(t)$, and the force of infection is $\Theta(t) = \beta I$, where $\beta = p_0\kappa$ is known as the transmission coefficient. This form is called bilinear incidence or simple mass-action incidence.

If $Q(N) = \kappa$, i.e., the contact rate is constant regardless of population size, then the incidence becomes $\beta\frac{SI}{N}$, and the force of infection is $\Theta(t) = \beta\frac{I}{N}$, again with $\beta = p_0\kappa$. This is known as standard incidence.

1.6 Stochastic models

Deterministic models provide useful insights by modelling real-world occurrences, although they may inadequately represent the stochastic behaviours intrinsic to particular processes. In situations with tiny populations, the intrinsic randomness of virus propagation indicates that deterministic models may not consistently yield correct representations. Consequently, stochastic models are essential in disease transmission modelling. Stochastic epidemic modelling originated in the 1920s and 1930s, initiated by the seminal contributions of Kermack and McKendrick, who introduced deterministic compartmental models [53, 54, 55]. Their research provided a foundation for the advancement of stochastic epidemic models. In 1928 and 1931, R. Frost, and Greenwood introduced discrete-time stochastic models that advanced generation by generation of infectives

[22]. The Reed-Frost model, albeit unpublished at the time, was presented in lectures in 1928. Bartlett has made substantial contributions to the development of stochastic epidemic models. Bartlett's research, commencing in the late 1940s, highlighted the intrinsic randomness in the dynamics of infectious diseases. This was especially pertinent in small groups where random variations could significantly influence the progression of the disease. He augmented the deterministic models of Kermack and McKendrick by incorporating random factors essential to the transmission process [11]. Kendall made significant contributions during this period. His research on branching processesstochastic processes in which one person can produce numerous offspringhas significant implications for disease transmission, as one diseased individual can infect several others [52]. Bailey's book [10] provides a comprehensive examination of both deterministic and stochastic epidemic models, as well as instructions on parameter estimation. Disease outbreaks typically originate from a limited number of patients; thus, it is essential to integrate stochasticity into deterministic compartmental models. Various types of noise can be included into deterministic dynamics depending on the circumstances.

Recent advancements in epidemic modelling have included the incorporation of several noise types, such as Gaussian, Lévy, and telegraph noise. The parameters of epidemic models are often influenced by environmental white noise, resulting from a constant intake of tiny fluctuations. Understanding the influence of this noise on the models' behaviour is crucial. Stochastic differential equation models have gained prominence in this area, providing a more accurate representation of disease dynamics compared to deterministic models [130]. This phenomena has been extensively examined by several scholars [36, 46].

Continuous-time white noise process with finite-variance increments, exemplified by Brownian motion, exhibit continuous sample trajectories. This trait may be unnecessarily constraining if epidemic transmission rates can fluctuate suddenly, for instance, due to super-spreading events where a limited number of sick persons can transmit the disease to a substantial number of others, resulting in a rapid increase in cases. To accommodate jumps that signify sudden changes or shocks in sample pathways, a common method is to extend Gaussian processes to Lévy processes. Lévy processes possess stationary independent increments; nonetheless, in contrast to Gaussian processes, their sample paths may exhibit leaps [110, 135].

A further possible application lies in simulating the impact of stochastic events, such as meteorological fluctuations or natural calamities, on disease transmission. These occurrences can induce sudden changes in disease dynamics that are effectively represented by Lévy noise [29, 74].

1.7 Optimal control in epidemiology

The principal objective of epidemic modelling is to design effective control techniques to mitigate or eradicate the effects of a disease. This aim was already apparent in Bernoullis seminal research on smallpox [12], in which he employed epidemic models to demonstrate that injection with material from moderately afflicted persons may diminish mortality and ultimately augment Frances population. A comparable viewpoint was subsequently embraced by VanderPlank [114, 115], who delineated the notions of monocyclic (primary inoculum) and polycyclic (primary and secondary inoculum) infections. He established two basic plant disease models to illustrate various pathogen kinds, facilitating the quantification of essential factors to forecast disease advancement and determine efficient control strategies. His research further elucidated the notion of horizontal and vertical resistance, illustrating that the intentional amalgamation of diverse plant species could diminish both the primary and secondary inoculum. Strategies to prevent and control infectious diseases encompass vaccination, medical treatment, isolation, quarantine, and prophylactic measures.

Vaccination is a major public health achievement, leading to the eradication of smallpox and near-eradication of polio. Table 1.1 presents the decline in disease burden in the United States due to widespread vaccination efforts. However, vaccines do not provide complete protection, as pathogens can mutate, and immune responses may vary. The level of protection a vaccine provides is known as its efficacy.

Table 1.1: Achievements of vaccination in the US [82].

Disease	Baseline years	Cases	Cases in 1998	Decrease %
Smallpox	1900-1904	48,164	0	100
Diphtheria	1920-1922	175,885	1	100
Pertussis	1922-1925	147,271	6,279	95.7
Tetanus	1922-1926	1,314	34	97.4
Poliomyelitis	1951-1954	16,316	0	100
Measles	1958-1962	503,282	89	100

1.8 Structure of thesis

This thesis aims to comprehensively examine diverse stochastic epidemic models using theoretical and numerical analysis. The thesis is organised as follows:

In chapter 2 introduces several mathematical terminologies and theorems that will be used in the thesis.

In **chapter 3** a mathematical study to control the spread of the COVID-19 epidemic by applying external control measures. We formulat a COVID-19 epidemic model with perturbation by white noise. We considered that the model consists of four categories are susceptible-vaccinated-infected-recovered. We show that the model is well posed, we give sufficient conditions for the extinction and the existence of a unique stationary distribution and we explore V -geometric ergodicity of the model. For the control model, we discussed both the stochastic and deterministic model using the techniques of optimal control theory. Real-world data from Algeria are used to parameterize the model, ensuring its relevance and applicability to practical satiation. Using numerical simulation, the analytical results have been shown.

Next, in **chapter 4** focuses on how a new Hepatitis B virus (**HBV**) model behaves over a long period of time. We show that the model is well-defined by proving that there is a solution that exists globally and is positive. We have found conditions that are enough for extinction and the presence of a unique stationary distribution and, we conducted numerical simulation to back up our findings.

Furthermore, In **chapter 5**, we consider a time delayed stochastic SIR epidemic model with Crowley-Martin incidence rate and Holling Type II treatment rate. We prove that the positive global solution exists and is unique. Then, we provide sufficient condition for the extinction of the disease, the persistent in mean and a suitable Lyapunov function is constructed to show the existence of a unique stationary distribution . At least the numerical simulation is provided to bolster our theoretical results.

Finally, in **chapter 6** we analyze the long-term behavior of a developed stochastic model for Tungiasis epidemic. The proposed model categorizes the population into three groups: susceptible individuals, educated individuals, and infected individuals. We establish the well-posedness of the system. We derive sufficient conditions under which the disease either dies out or continues to persist within the population. To illustrate our theoretical findings, we perform numerical simulations that illustrate and support the analytical results, providing deeper insight into the dynamics of Tungiasis under stochastic influences.

Chapter 2

Mathematical Tools

This chapter aims to introduce the theory of Itô SDEs, SDEs with Lévy processes, and optimal control theory. This chapter primarily addresses stochastic processes, Brownian motion, stochastic integration, SDE, stationary distribution and the Pontryagin maximum principle. This chapter's content primarily derives from [31, 45, 50, 65, 79, 81, 95, 96, 136].

2.1 Basic Notions of Probability Theory

Probability theory is a field of mathematics focused on describing and analyzing systems whose outcomes are governed by chance. The complete collection of all possible outcomes referred to as elementary events is represented by a set Ω, with individual outcomes denoted by $\omega \in \Omega$. However, not every element in Ω is necessarily observable or of practical interest. Instead, we focus on a collection $\mathcal{F}$ of subsets of Ω that includes the events we can observe or are interested in studying. This collection $\mathcal{F}$ often satisfies the properties of a sigma-algebra, allowing the rigorous development of probability measures.

Definition 2.1. Let Ω be a set. A sigma-algebra $\mathcal{F}$ on Ω is a family $\mathcal{F}$ of subsets of Ω satisfying the following:

- $\emptyset \in \mathcal{F}$;
- $A \in \mathcal{F} \Rightarrow A^C \in \mathcal{F}$, where $A^C = \Omega \setminus A$;
- $B_1, B_2, B_3, \ldots \in \mathcal{F} \Rightarrow B := \bigcup_{m=1}^{\infty} B_m \in \mathcal{F}$.

The pair $(\Omega, \mathcal{F})$ is called a measurable space. The elements of $\mathcal{F}$ are henceforth called $\mathcal{F}$-measurable sets. If F is a family of subsets of Ω, then there exists the smallest sigma-algebra

$\sigma(F)$ on Ω containing F. This set $\sigma(F)$ is the sigma-algebra generated by F. If $\Omega = \mathbb{R}^n$ and F is a family of open sets in $\mathbb{R}^n$, then $\mathcal{B}^n = \sigma(F)$ is the Borel sigma-algebra, and the elements of $\mathcal{B}^n$ are Borel sets.

Definition 2.2. A probability measure $\mathbb{P}$ on a measurable space $(\Omega, \mathcal{F})$ is a function $\mathbb{P} : \mathcal{F} \to [0,1]$ such that:

- $\mathbb{P}(\emptyset) = 0, \quad \mathbb{P}(\Omega) = 1;$
- If $B_1, B_2, B_3, \ldots \in \mathcal{F}$ and $\{B_m\}_{m=1}^{\infty}$ are pairwise disjoint (i.e. $B_m \cap B_k = \emptyset$ if $m \neq k$), then

$$\mathbb{P}\left(\bigcup_{m=1}^{\infty} B_m\right) = \sum_{m=1}^{\infty} \mathbb{P}(B_m).$$

The triplet $(\Omega, \mathcal{F}, \mathbb{P})$ is a probability space.

Definition 2.3. Let $(\Omega, \mathcal{F}, \mathbb{P})$ be a probability space. A function $\mathcal{X} : \Omega \to \mathbb{R}^n$ is said to be $\mathcal{F}$-measurable if

$$\mathcal{X}^{-1}(U) := \{\omega \in \Omega : \mathcal{X}(\omega) \in \mathcal{O}\} \in \mathcal{F}$$

for every open set $\mathcal{O} \subset \mathbb{R}^n$ (or for every Borel set $\mathcal{O} \subset \mathbb{R}^n$).

A function $\mathcal{X}(\omega) = (\mathcal{X}_1(\omega), \mathcal{X}_2(\omega), \ldots, \mathcal{X}_n(\omega))^T$ taking values in $\mathbb{R}^n$ is said to be $\mathcal{F}$-measurable if all components $\mathcal{X}_i$ are $\mathcal{F}$-measurable. Similarly, a matrix-valued function $Y(\omega) = (\mathcal{X}_{mk}(\omega))_{1 \leq m,k \leq n}$ is $\mathcal{F}$-measurable if all elements $\mathcal{X}_{mk}$ are $\mathcal{F}$-measurable. The indicator function $\mathbf{1}_B$ of a set $B \subset \Omega$ is $\mathcal{F}$-measurable if and only if $B \in \mathcal{F}$.

Definition 2.4. A random variable Y is an $\mathcal{F}$-measurable function $Y : \Omega \to \mathbb{R}^n$. Every random variable Y induces a probability measure μ_Y on $\mathbb{R}^n$, defined by

$$\mu_Y(A) = \mathbb{P}(Y^{-1}(A)),$$

where μ_Y is called the distribution of Y. If

$$\int_{\Omega} Y(\omega) d\mathbb{P}(\omega) < \infty,$$

then the number

$$\mathbb{E}[Y] := \int_{\Omega} Y(\omega) d\mathbb{P}(\omega) = \int_{\mathbb{R}^n} y d\mu_Y(y)$$

is called the expectation of Y.

2.2 Stochastic process

The purpose of the theory of stochastic processes is to study random phenomena that evolve over time.

Definition 2.5. Let $(\Omega, \mathcal{F}, \mathbb{P})$ be a probability space, a filtration $\{\mathcal{F}_t\}_{t\geq 0}$ is an increasing sequence of sub-σ-algebras of $\mathcal{F}$, where $\mathcal{F}_t \subset \mathcal{F}_s \subset \mathcal{F}$ for all $0 \leq t < s < 1$. Then the filtration is said to be right continuous if $\mathcal{F}_t = \bigcap_{s>t} \mathcal{F}_s$ for all $t > 0$.
A set $B \in \Omega$ is said to be $\mathbb{P}$-null if there exists a set $A \in \mathcal{F}$ such that $B \subset A$ and $\mathbb{P}(A) = 0$.
When the probability space is complete, the filtration is said to satisfy the usual conditions if it is right continuous and $\mathcal{F}_0$ contains all $\mathbb{P}$-null sets.

Definition 2.6. A *stochastic process* is a family of $\mathbb{R}^n$-valued random variables $\{Y_t\}_{t\in D}$ with *index set* D and *set space* $\mathbb{R}^n$. The index set D is usually $\mathbb{R}_+$, but it may also be an interval $[a,b]$, the nonnegative integers or even subsets of $\mathbb{R}^n$. Note that for each fixed $t \in D$ we have a random variable

$$\Omega \ni \omega \to Y_t(\omega) \in \mathbb{R}^n.$$

On the other hand, for each fixed $\omega \in \Omega$ we have a function

$$D \ni t \to Y_t(\omega) \in \mathbb{R}^n,$$

which is called a *sample path* of the process, and we shall write $Y_\cdot(\omega)$ for the path.

Similarly, in the discret case, one can define stochastic processes matrix. A stochastic process $\{Y_t\}_{t\geq 0}$ is often denoted as $\{Y_t\}$, Y_t or $Y(t)$.

An $\mathbb{R}^n$-valued stochastic process $\{Y_t\}_{t\geq 0}$ is said to be *continuous* (resp. *left continuous, right continuous*) if for almost all $\omega \in \Omega$ function $Y_t(\omega)$ is continuous (resp. *left continuous, right continuous*) on $t \geq 0$. It is said to be *integrable* if for every $t \geq 0$, Y_t is an integrable random variable. It is said to be $\{\mathcal{F}_t\}$-*adapted* if for every t, Y_t is $\mathcal{F}_t$-measurable. A real-valued stochastic process $\{Z_t\}_{t\geq 0}$ is called an *increasing process* if for almost all $\omega \in \Omega$, $Z_t(\omega)$ is non-negative increasing right continuous on $t \geq 0$.

Definition 2.7. A random variable $\tau : \Omega \to [0, \infty]$ (it may take the value ∞) is called an $\{\mathcal{F}_t\}$-*stopping time* if $\{\omega : \tau(\omega) \leq t\} \in \mathcal{F}_t$ for any $t \geq 0$.

Definition 2.8. An $\mathbb{R}^n$-valued $\{\mathcal{F}_t\}$-adapted integrable process $\{\mathcal{M}_t\}_{t\geq 0}$ is called a *martingale with respect to* $\{\mathcal{F}_t\}$ if

$$\mathbb{E}(\mathcal{M}_t|\mathcal{F}_s) = \mathcal{M}_s, \quad \text{for all } 0 \leq s < t < \infty. \ a.s.$$

Definition 2.9. A stochastic process $Y = \{Y_t\}_{t\geq 0}$ is called *square-integrable* if $\mathbb{E}|Y_t|^2 < \infty$ for every $t \geq 0$. If $\mathcal{M} = \{\mathcal{M}_t\}_{t\geq 0}$ is a real-valued square-integrable continuous martingale, then there exists a unique continuous integrable adapted increasing process denoted by $\{\langle \mathcal{M}, \mathcal{M}\rangle_t\}$ such that $\{\mathcal{M}_t^2 - \langle \mathcal{M}, \mathcal{M}\rangle_t\}$ is a continuous martingale vanishing at $t = 0$. The process $\{\langle \mathcal{M}, \mathcal{M}\rangle_t\}$ is called the *quadratic variation* of $\mathcal{M}$.

Definition 2.10. A right continuous adapted process $\mathcal{M} = \{\mathcal{M}_t\}_{t\geq 0}$ is called a *local martingale* if there exists a nondecreasing sequence $\{\tau_m\}_{m\geq 1}$ of stopping times with $\tau_m \uparrow \infty$ a.s. such that $\{\mathcal{M}_{\tau_m \wedge t} - \mathcal{M}_0\}_{t\geq 0}$ is a martingale.

While every martingale is a local martingale, the opposite is not true.

Lemma 2.1. *(Strong Law of larg number [79]). Let $\mathcal{M} = \{\mathcal{M}_t\}_{t\geq 0}$ be a real-value continuous local martingale vanishing at $t = 0$ then*

$$\lim_{t\to\infty} \langle \mathcal{M},\mathcal{M}\rangle_t = \infty \ \ a.s. \ \Rightarrow \lim_{t\to\infty} \frac{\mathcal{M}_t}{\langle \mathcal{M},\mathcal{M}\rangle_t} = 0 \ a.s.$$

And also

$$\lim_{t\to\infty} \sup \frac{\langle \mathcal{M},\mathcal{M}\rangle_t}{t} < \infty \ \ a.s. \ \Rightarrow \lim_{t\to\infty} \frac{\mathcal{M}_t}{t} = 0 \ \ a.s.$$

2.3 Brownian motion

In 1827, biologist Robert Brown examined pollen grains suspended in water using a microscope. He observed that the grains displayed incessant movement, although he could not ascertain the underlying reason of this motion. This occurrence subsequently became recognized as Brownian Motion.

Definition 2.11. Let $(\Omega, \mathcal{F}, \mathbb{P})$ be a probability space with a filtration $\{\mathcal{F}_t\}_{t\geq 0}$. A stochastic process $\{\mathcal{W}_t\}_{t\geq 0}$ is called a standard one-dimensional Brownian motion is a real-valued continuous $\{\mathcal{F}_t\}$-adapted process such that:

- $\mathbb{P}\{\omega : \mathcal{W}(0,\omega) = 0\} = 1$.
- For any $0 \leq s < t$, the random variable $\mathcal{W}(t) - \mathcal{W}(s)$ is normally distributed with mean 0 and variance $t - s$, i.e. for any $a < b$,

$$\mathbb{P}\{a \leq \mathcal{W}(t) - \mathcal{W}(s) \leq b\} = \frac{1}{\sqrt{2\pi(t-s)}} \int_a^b e^{\frac{-x^2}{2(t-s)}} dx.$$

- $\mathcal{W}(t,\omega)$ has independent increments, *i.e.*, for any $0 \leq t_1 < t_2 < ... < t_n$, the random variables

$$\mathcal{W}(t_1), \mathcal{W}(t_2) - \mathcal{W}(t_1), ..., \mathcal{W}(t_n) - \mathcal{W}(t_{n-1}),$$

are independent.

Brownian motion has many properties, here are a few:

(i) $\mathcal{W}_t$ is a continuous martingale of square-integrable type and its quadratic variation is $\langle \mathcal{W}, \mathcal{W} \rangle_t = t$ for all $t \geq 0$.

(ii) According to the law of large numbers, we have:

$$\lim_{t \to +\infty} \frac{\mathcal{W}_t}{t} = 0 \quad a.s.$$

(iii) For every $\omega \in \Omega$, the trajectory $\omega \to \mathcal{W}_t(\omega)$ is not differentiable.

Now let us define a multi-dimensional Brownian motion.

Definition 2.12. An d-dimensional process $\mathcal{W}_t = \{(\mathcal{W}_t^1, \mathcal{W}_t^2, ..., \mathcal{W}_t^d)\}_{t \geq 0}$ is called an d-dimensional Brownian motion if every $\{\mathcal{W}_t^k\}$ is a one-dimensional Brownian motion, and $\{\mathcal{W}_t^1\}$,...,$\{\mathcal{W}_t^d\}$ are independent.

2.4 Itô integral

This part will present the formulation of the Itô stochastic integral and some related properties. This integral was initially described by K. Itô in 1949.
We now define the stochastic integral

$$\int_0^t g(t) d\mathcal{W}_s$$

with respect to an m-dimensional Brownian motion $\{\mathcal{W}_t\}$ for a class of $n \times m$-matrix-valued stochastic processes $\{g(t)\}$. Since for almost all $\omega \in \Omega$, the Brownian sample path $\mathcal{W}.(\omega)$ is nowhere differentiable, the integral cannot be defined in an ordinary way. However, we can define the integral for a large class of stochastic processes by making use of the stochastic nature of Brownian motion.

Let $(\Omega, \mathcal{F}, \mathbb{P})$ be a complete probability space with a filtration $\{\mathcal{F}_t\}_{t \geq 0}$ satisfying the usual conditions. Let $\mathcal{W} = \{\mathcal{W}_t\}_{t \geq 0}$ be a one-dimensional Brownian motion defined on the probability space adapted to the filtration.

Definition 2.13. A real-valued stochastic process $h = \{h(t)\}_{a\geq t\geq b}$ is called a simple process if there exists a partition $a = t_0 < t_1 < ... < t_n = b$ of $[a, b]$, and bounded random variables ζ_j, $0 \leq j \leq n-1$ such that ζ_j is $\mathcal{F}_{t_j}$-measurable and

$$h(t) = \zeta_0 I_{[t_0,t_1]}(t) + \sum_{j=1}^{n-1} \zeta_j I_{(t_j,t_{j+1}]}. \tag{2.1}$$

Denote by $\mathcal{M}_0([a, b], \mathbb{R})$ the family of all such processes .

Definition 2.14. For a simple process h with the form of 2.1 in $\mathcal{M}_0([a, b], \mathbb{R})$, define

$$\int_a^b h(t)d\mathcal{W}_t = \sum_{j=0}^{n-1} \zeta_j(\mathcal{W}_{t_{j+1}} - \mathcal{W}_{t_j}), \tag{2.2}$$

and call it the stochastic integral of g with respect to the Brownian motion $\{\mathcal{W}(t)\}$ or the Itô integral.

We now extend the integral definition from simple processes to processes in $\mathcal{M}^2([a, b], \mathbb{R})$.

Definition 2.15. Let $g \in \mathcal{M}^2([a, b], \mathbb{R})$. The Itô integral of g w.r.t. $\{\mathcal{W}_t\}$ is defined by

$$\int_a^b g(t)d\mathcal{W}_t = \lim_{n\to+\infty} \int_a^b h_n(t)d\mathcal{W}_t \ \text{ in } \ L^2(\Omega,\mathbb{R}),$$

where h_n is a sequence of simple processes such that

$$\lim_{n\to+\infty} \int_a^b |g(t) - h_n(t)|dt = 0.$$

Some properties of the stochastic integral are summarised below:

Theorem 2.1. *[79] Let $g_1, g_2 \in \mathcal{M}^2([a,b];\mathbb{R})$, and let α_1, α_2 be two real numbers. Then*

- $\int_a^b g(t)d\mathcal{W}_t$ *is $\mathcal{F}_b$- measurable.*
- $\mathbb{E}\int_a^b g(t)d\mathcal{W}_t = 0.$
- $\mathbb{E}\Big(\int_a^b g(t)d\mathcal{W}_t\Big)^2 = \mathbb{E}\int_a^b |g(t)|^2dt.$
- $\int_a^b \big[\alpha_1 g_1(t) + \alpha_2 g_2(t)\big]d\mathcal{W}_t = \alpha\int_a^b g_1(t)d\mathcal{W}_t + \alpha_2\int_a^b g_2(t)d\mathcal{W}_t.$

We now define the Itô formula, which is the fundamental tool of stochastic calculus. For example, the classical integral $\int_0^t \mathcal{W}_s d\mathcal{W}_s$ was problematic because it didn't have a proper mathematical meaning, as the trajectories of stochastic processes are not differentiable. Itô provided an alternative definition of the stochastic integral that helps us better address the differentiability issues of stochastic processes.

Definition 2.16. (Itô Process in One Dimension). Let $\mathcal{W}_t$ be a one-dimensional Brownian motion on $(\Omega, \mathcal{F}, \mathbb{P})$. A one-dimensional Itô process (or stochastic integral) is a stochastic process Y_t on $(\Omega, \mathcal{F}, \mathbb{P})$ of the form

$$Y_t = Y_0 + \int_0^t F(s,\omega)ds + \int_0^t G(s,\omega)d\mathcal{W}_s, \tag{2.3}$$

where $F \in \mathcal{L}^1(\mathbb{R}_+;\mathbb{R})$ and $G \in \mathcal{L}^2(\mathbb{R}_+;\mathbb{R})$.

An Y_t of the form 2.3 can sometimes be written in this shorter form:

$$dY_t = F\,dt + G\,d\mathcal{W}_t.$$

Theorem 2.2. *(Itô's Formula in One Dimension [79, 81]). Let Y_t be a stochastic process satisfying*

$$dY_t = F\,dt + G\,d\mathcal{W}_t,$$

and let $Q(t,x) \in C^2(\mathbb{R}_+ \times \mathbb{R})$, meaning twice continuously differentiable on $\mathbb{R}_+ \times \mathbb{R}$. Then $Z_t = Q(t, Y_t)$ is also a stochastic process and

$$dZ_t = \frac{\partial Q}{\partial t}(t,Y_t)dt + \frac{\partial Q}{\partial x}(t,Y_t)d\mathcal{W}_t + \frac{1}{2}\frac{\partial^2 Q}{\partial x^2}(t,Y_t)(d\mathcal{W}_t)^2,$$

where $(d\mathcal{W}_t)^2 = (d\mathcal{W}_t) \times (d\mathcal{W}_t)$ is calculated according to the rules:

$$dt \times dt = dt \times d\mathcal{W}_t = d\mathcal{W}_t \times dt = 0 \quad \text{and} \quad d\mathcal{W}_t \times d\mathcal{W}_t = dt.$$

Example 2.1. Let's consider again $I = \int_0^t \mathcal{W}_s d\mathcal{W}_s$.
Set $Y_t = \mathcal{W}_t$ and $Q(t,x) = \frac{1}{2}x^2$. We have $Z_t = Q(t,\mathcal{W}_t) = \frac{1}{2}\mathcal{W}_t^2$ and by Itô's formula,

$$\begin{aligned} dZ_t &= \frac{\partial Q}{\partial t}dt + \frac{\partial Q}{\partial x}d\mathcal{W}_t + \frac{1}{2}\frac{\partial^2 Q}{\partial x^2}(d\mathcal{W}_t)^2, \\ &= \mathcal{W}_t d\mathcal{W}_t + \frac{1}{2}(d\mathcal{W}_t)^2 = \mathcal{W}_t d\mathcal{W}_t + \frac{1}{2}dt. \end{aligned}$$

Therefore,

$$\begin{aligned} d\left(\frac{1}{2}\mathcal{W}_t^2\right) = \mathcal{W}_t d\mathcal{W}_t + \frac{1}{2}dt \Rightarrow \int_0^t d\left(\frac{1}{2}\mathcal{W}_s^2\right) &= \int_0^t \mathcal{W}_s d\mathcal{W}_s + \frac{1}{2}\int_0^t ds, \\ \Rightarrow \frac{1}{2}\mathcal{W}_t^2 &= \int_0^t \mathcal{W}_s d\mathcal{W}_s + \frac{1}{2}t, \\ \Rightarrow \int_0^t \mathcal{W}_s d\mathcal{W}_s &= \frac{1}{2}\mathcal{W}_t^2 - \frac{1}{2}t. \end{aligned}$$

We now extend Itô's formula to multiple dimensions. Let $B(t,\omega) = (\mathcal{W}_1(t,\omega), \ldots, \mathcal{W}_m(t,\omega))$ be an m-dimensional Brownian motion. If for $1 \leq i \leq n$ and $1 \leq j \leq m$, $F_i(t,\omega)$ and $G_{ij}(t,\omega)$ satisfy the conditions of the one-dimensional Itô's formula definition, then we have the following system:

$$\begin{cases} dY_1 = F_1 dt + G_{11} dB_1 + \cdots + G_{1m} d\mathcal{W}_m, \\ \vdots \\ dY_n = F_n dt + G_{n1} d\mathcal{W}_1 + \cdots + v_{nm} d\mathcal{W}_m. \end{cases}$$

Using simple matrix notation, we can write:

$$dY_t = F\, dt + G\, d\mathcal{W}_t,$$

where

$$Y_t = \begin{pmatrix} Y_1(t) \\ \vdots \\ Y_n(t) \end{pmatrix}, \quad F = \begin{pmatrix} F_1 \\ \vdots \\ F_n \end{pmatrix}, \quad G = \begin{pmatrix} G_{11} & \cdots & G_{1m} \\ \vdots & \ddots & \vdots \\ G_{n1} & \cdots & G_{nm} \end{pmatrix}, \quad d\mathcal{W}(t) = \begin{pmatrix} d\mathcal{W}_1(t) \\ \vdots \\ d\mathcal{W}_m(t) \end{pmatrix}.$$

The process Y_t is called an n-dimensional Itô process.

Theorem 2.3. *(Itô's Formula in Multiple Dimensions [79, 81]). Let*

$$dY_t = F\, dt + G\, d\mathcal{W}_t$$

an n-dimensional Itô process as defined above. Let $Q(t,x) = (Q_1(t,x), \ldots, Q_p(t,x)) \in C^2(\mathbb{R}_+ \times \mathbb{R}^n, \mathbb{R}^p)$. Then the process $Z(t,\omega) = Q(t, Y(t))$ is also an Itô process whose k^{th} component is given by

$$dZ_k = \frac{\partial Q_k}{\partial t}(t,Y)dt + \sum_{i=1}^{n} \frac{\partial Q_k}{\partial x_i}(t,Y)dY_i + \frac{1}{2}\sum_{i,j=1}^{n} \frac{\partial^2 Q_k}{\partial x_i \partial x_j}(t,Y)dY_i dY_j,$$

with the multiplication rules:

$$d\mathcal{W}_i \times d\mathcal{W}_j = \delta_{ij} dt, \quad d\mathcal{W}_i \times dt = dt \times d\mathcal{W}_i = dt \times dt = 0.$$

For example:

$$dY_i(t)dY_j(t) = \sum_{k=1}^{m} G_{ik}(t)G_{jk}(t)dt.$$

Moreover, the formula can be written in matrix form as:

$$dZ_t = \frac{\partial Q}{\partial t}dt + \frac{\partial Q}{\partial x}dY_t + \frac{1}{2}dY_t^T \frac{\partial^2 Q}{\partial x^2} dY_t.$$

Note that if $Y(t)$ were continuous and differentiable in t , the term $\frac{1}{2}dY_t^T\frac{\partial^2 Q}{\partial x^2}dY_t$ would vanish. For example, consider $Z_t = Y_1(t)Y_2(t)$. Using both previous formulas, we have:

$$\begin{aligned} d(Y_1(t)Y_2(t)) &= Y_1(t)dY_2(t) + Y_2(t)dY_1(t) + dY_1(t)dY_2(t), \\ &= Y_1(t)dY_2(t) + Y_2(t)dY_1(t) + \sum_{k=1}^{m} G_{1k}(t)G_{2k}(t)dt. \end{aligned}$$

2.5 Stationary Distribution

This section will present a renowned finding by Hasminskii regarding the determination of the stationary distribution of a SDE. Firstly, we delineate the concept of "stationary". A stochastic process $\{Y(t)\}, (-\infty < t < \infty)$ with values in $\mathbb{R}^d$ is said to be stationary if for every finite sequence of numbers $t_1, ..., t_n$, the joint distribution of the random variables $Y(t_1+h), ..., Y(t_n+h)$ is independent of h. i.e. the joint probability distribution does not change when shifted in time. The notion of a stationary distribution is both important and indispensable in the study of SDEs. Let $Y(t)$ be a regular time-homogeneous Markov.
A process in $\mathbb{R}^d$ described by the SDE in the following form

$$dY(t) = b(Y)dt + \sum_{r=1}^{k} \sigma_r(Y)d\mathcal{W}_r(t).$$

Then a *diffusion matrix* is defined by

$$A(y) = (a_{ij}(y)), \quad a_{ij} = \sum_{r=1}^{k} \sigma_r^i(y)\sigma_r^j(y).$$

Khaminskii [39] then gives two conditions for the existence and uniqueness of a stationary distribution of the process $Y(t)$. So if there exists an open domain $U \subset \mathbb{R}^d$ with regular boundary, such that

(a) In the domain U and some neighbourhood thereof, the smallest eigenvalue of the diffusion matrix $A(y)$ is bounded away from zero.

(b) If $y \in \mathbb{R}^d \setminus U$, the mean time τ at which a path issuing from x reaches the set U is finite, and $\sup_{y\in K} \mathbb{E}(\tau) < \infty$ for every compact subset $K \subset \mathbb{R}^d$.

Then $Y(t)$ has a unique stationary distribution μ. If $g(y)$ is an integrable function with respect to μ, then

$$\mathbb{P}\left\{\lim_{T\to\infty} \frac{1}{T}\int_0^T g(Y_y(t))dt = \int_{\mathbb{R}^d} g(y)\mu(dx)\right\} = 1, \quad \forall\, y \in \mathbb{R}^d.$$

Remark 2.1. To prove (a), it is sufficient to prove that there exists a positive constant M such that

$$\sum_{i,j=1}^{k} a_{ij}\theta_i\theta_j \geq M|\theta|^2 \; x \in U, \; \theta \in D,$$

(see [34, 107]). To show (b), it is sufficient to prove that there exists a non-negative C^2-function V and a neighborhood U such that, LV is negative for any $\mathbb{R}^d_+ \setminus U$. [134]

2.6 Basic Definition and Results on Lévy Processes

Definition 2.17. A $\mathcal{F}_t$-adapted process $\{\eta(t)\}_{t\geq 0} = \{\eta_t\}_{t\geq 0} \subset \mathbb{R}$ with $\eta_0 = 0$ a.s. is a Lévy process if η_t is continuous in probability and its increments are *independent and stationary.*

Theorem 2.4. *[96] Let $\{\eta_t\}$ be a Lévy process. Then η_t has a càdlàg version (right-continuous with left limits) which is also a Lévy process.*

Given this result, we will now assume that the Lévy processes we use are càdlàg.
The jump of η_t for $t \geq 0$ is defined as

$$\Delta\eta_t = \eta_t - \eta_{t-}.$$

Let $\mathbb{B}_0$ be the family of Borel sets $U \subset \mathbb{R}$ whose closure, not containing 0, is denoted by $\overline{U}$. For any $U \in \mathbb{B}_0$, we define

$$N(t,U) = N(t,U,\omega) = \sum_{s:0<s\leq t} 1_U(\Delta\eta_s).$$

In other words, $N(t,U)$ is the number of jumps of size $\Delta\eta_s \in U$ that occur before or at time t. We call $N(t,U)$ the Poisson random measure (or jump measure) of $\eta(.)$.
Given that every Brownian motion $\{\mathcal{W}_t\}_{t\geq 0}$ has independent and stationary increments, it follows that $\mathcal{W}_t$ is a Lévy process. Let us note other important examples:

Example 2.2. (Poisson process). The Poisson process $\pi(t)$ with intensity $\lambda > 0$ is a Lévy process with values in $\mathbb{N} \cup \{0\}$ such that

$$P(\pi(t) = n) = \frac{(\lambda t)^n}{n!}e^{-\lambda t}, \quad n = 0, 1, 2, \ldots$$

Example 2.3. (Compound Poisson Process). Let $X(n)$, $n \in \mathbb{N}$ be a sequence of independent and identically distributed real random variables with common distribution $\mu_{X(1)} = \mu_X$, and let

$\pi(t)$ be a Poisson process with intensity λ, independent of all the $X(n)$. The compound Poisson process $Y(t)$ is defined by

$$Y(t) = X(1) + \cdots + X(\pi(t)), \quad t \geq 0.$$

An increment of this process is given by

$$Y(s) - Y(t) = \sum_{k=\pi(t)+1}^{\pi(s)} X(k), \quad s > t.$$

This is independent of $X(1), \ldots, X(\pi(t))$, and this distribution depends only on the difference $(s-t)$ and the distribution of $X(1)$. Therefore, $Y(t)$ is a Lévy process.

To find the Lévy measure ν of $Y(t)$, we note that if $U \in \mathcal{B}_0$ then

$$\begin{aligned}\nu(U) &= \mathbb{E}[N(1,U)] = \mathbb{E}\left[\sum_{s:\,0<s\leq T} \mathbf{1}_U(\Delta Y(s))\right], \\ &= \mathbb{E}[(\text{number of jumps}) \times \mathbf{1}_U(\text{jump})] = \mathbb{E}[\pi(1)\mathbf{1}_U(X)] = \lambda\mu_X(U),\end{aligned}$$

by independence. We conclude that $\nu = \lambda_{\mu X}$.

This shows that a Lévy process can be represented by a compound Poisson process if and only if its Lévy measure is finite. However, note that there are many interesting Lévy processes η_t with an infinite Lévy measure ν, even when $\int_{|z|<1} \nu(dz) = \infty$. In general, it can be proven that for any fixed $r > 0$, the processes

$$M_t^{(k)} := \int_{\frac{1}{k}\leq|z|\leq r} z(N(t,dz) - t\nu(dz)), \quad k = 1, 2, \ldots$$

are martingales in $L^2(\mathbb{P})$ and they converge in $L^2(\mathbb{P})$ to a martingale denoted M_t and defined by

$$M_t = \int_{|z|<r} z(N(t,dz) - t\nu(dz)).$$

We have the following result:

Theorem 2.5. *(Itô-Lévy Decomposition [45, 101]). Let $\{\eta_t\}$ be a Lévy process. Then η_t has the decomposition*

$$\eta_t = \alpha t + \sigma\mathcal{W}(t) + \int_{|z|<r} z\overline{N}(t,dz) + \int_{|z|\geq r} zN(t,dz),$$

for constants $\alpha \in \mathbb{R}$, $\sigma \in \mathbb{R}$, $r \in [0,\infty]$. Here,

$$\overline{N}(dt,dz) = N(dt,dz) - \nu(dz)dt$$

is the compensated Poisson random measure of $\eta(\cdot)$*, and* $\mathcal{W}(t)$ *is a Brownian motion independent of* $\overline{N}(dt, dz)$*.*

For each $A \in \mathcal{B}_0$*, the process* $M_t := \overline{N}(t, A)$ *is a martingale.*

If $\alpha = 0$ *and* $r = \infty$*, then* η_t *is a Lévy martingale.*

In the case where $r = 1$*, if for all* $t \geq 0$ *we have* $E[\eta_t] < \infty$*, then*

$$\int_{|z|\geq 1} |z|\nu(dz) < \infty,$$

and consequently, in the case where $r = \infty$*, we write*

$$\eta_t = \alpha t + \sigma\mathcal{W}(t) + \int_{\mathbb{R}} z\overline{N}(t, dz).$$

Theorem 2.6. *(Itô-Lévy Formula in Dimension 1 [96]) Suppose that* $X(t) \in \mathbb{R}$ *is an Itô-Lévy process of the form*

$$dX(t) = \alpha(t,\omega)dt + \beta(t,\omega)d\mathcal{W}(t) + \int_{\mathbb{R}} \gamma(t, z, \omega)\tilde{N}(dt, dz),$$

where

$$\tilde{N}(dt, dz) = \begin{cases} N(dt, dz) - \nu(dz)dt & \text{if } |z| < r, \\ N(dt, dz) & \text{if } |z| \geq r, \end{cases}$$

for any $r \in [0, \infty]$*.*

Let $f \in C^2(\mathbb{R}^2)$ *and define* $Y(t) = f(t, X(t))$*. Then* $Y(t)$ *is also an Itô-Lévy process and*

$$\begin{aligned} dY(t) =& \frac{\partial f}{\partial t}(t, X(t))dt + \frac{\partial f}{\partial x}(t, X(t))\left[\alpha(t,\omega)dt + \beta(t,\omega)d\mathcal{W}(t)\right] \\ &+ \frac{1}{2}\beta^2(t,\omega)\frac{\partial^2 f}{\partial x^2}(t, X(t))dt \\ &+ \int_{|z|<r}\left[f(t, X(t^-) + \gamma(t,z)) - f(t, X(t^-)) - \frac{\partial f}{\partial x}(t, X(t^-))\gamma(t,z)\right]\nu(dz)dt \\ &+ \int_{\mathbb{R}}\left[f(t, X(t^-) + \gamma(t,z)) - f(t, X(t^-))\right]\tilde{N}(dt, dz). \end{aligned}$$

Note that:

$$\text{If } r = 0, \text{ then } \tilde{N} = N \text{ everywhere.}$$

$$\text{If } r = \infty, \text{ then } \tilde{N} = \overline{N} \text{ everywhere.}$$

Example 2.4. (Geometric Lévy Process) Consider the following SDE:

$$dX(t) = X(t^-)\left[\alpha dt + \beta d\mathcal{W}(t) + \int_{\mathbb{R}} \gamma(t, z)\tilde{N}(dt, dz)\right],$$

where α, β are constants and $\gamma(t, z) > -1$. To find the solution $X(t)$ of this equation, we rewrite it as:

$$\frac{dX(t)}{X(t^-)} = \alpha dt + \beta d\mathcal{W}(t) + \int_{\mathbb{R}} \gamma(t,z)\tilde{N}(dt,dz).$$

Now, define

$$Y(t) = \ln(X(t)).$$

Applying Itô's formula, we obtain

$$\begin{aligned} dY(t) &= \frac{X(t)}{X(t)}\left[\alpha dt + \beta d\mathcal{W}(t)\right] - \frac{1}{2}\beta^2 X^{-2}(t)X^2(t)dt \\ &\quad + \int_{|z|<r}\left[\ln(X(t^-)+\gamma(t,z)X(t^-)) - \ln(X(t^-)) - X^{-1}(t^-)\gamma(t,z)X(t^-)\right]\nu(dz)dt \\ &\quad + \int_{\mathbb{R}}\left[\ln(X(t^-)+\gamma(t,z)X(t^-)) - \ln(X(t^-))\right]\tilde{N}(dt,dz), \\ &= \left(\alpha - \frac{1}{2}\beta^2\right)dt + \beta d\mathcal{W}(t) + \int_{|z|<r}\left[\ln(1+\gamma(t,z)) - \gamma(t,z)\right]\nu(dz)dt \\ &\quad + \int_{\mathbb{R}}\ln(1+\gamma(t,z))\tilde{N}(dt,dz). \end{aligned}$$

Therefore, integrating between 0 and t, we have

$$\begin{aligned} Y(t) &= Y(0) + \left(\alpha - \frac{1}{2}\beta^2\right)t + \beta\mathcal{W}(t) \\ &\quad + \int_0^t\int_{|z|<r}\left[\ln(1+\gamma(s,z)) - \gamma(s,z)\right]\nu(dz)ds \\ &\quad + \int_0^t\int_{\mathbb{R}}\ln(1+\gamma(s,z))\tilde{N}(ds,dz), \end{aligned}$$

which gives the solution

$$\begin{aligned} X(t) &= X(0)\exp\left[\left(\alpha - \frac{1}{2}\beta^2\right)t + \beta\mathcal{W}(t)\right. \\ &\quad + \int_0^t\int_{|z|<r}\left(\ln(1+\gamma(s,z)) - \gamma(s,z)\right)\nu(dz)ds \\ &\quad \left. + \int_0^t\int_{\mathbb{R}}\ln(1+\gamma(s,z))\tilde{N}(ds,dz)\right]. \end{aligned}$$

By analogy with the diffusion case ($N = 0$), we call this process $X(t)$ a geometric Lévy process. It is often used as a model for stock prices.

We now introduce the multidimensional variant of the Itô-Lévy theorem.

Theorem 2.7. *(Multidimensional Itô-Lévy Formula [136]) Let $X(t) \in \mathbb{R}^n$ be an Itô-Lévy process satisfying*

$$dX(t) = \alpha(t,\omega)dt + \sigma(t,\omega)d\mathcal{W}(t) + \int_{\mathbb{R}^l}\gamma(t,z,\omega)\tilde{N}(dt,dz),$$

where: $\alpha : [0,T] \times \Omega \to \mathbb{R}^n$, $\sigma : [0,T] \times \Omega \to \mathbb{R}^{n\times m}$, $\gamma : [0,T] \times \mathbb{R}^l \times \Omega \to \mathbb{R}^{n\times l}$ *are adapted processes such that the integrals exist, and* $\mathcal{W}(t)$ *is an m-dimensional Brownian motion and*

$$\begin{aligned}\tilde{N}(dt,dz)^T &= \left(\tilde{N}_1(dt,dz_1),\ldots,\tilde{N}_l(dt,dz_l)\right),\\ &= \left(N_1(dt,dz_1) - 1_{|z_1|<r_1}\lambda_1(dz_1)dt,\ldots,N_l(dt,dz_l) - 1_{|z_l|<r_l}\lambda_l(dz_l)dt\right),\end{aligned}$$

where $\{N_l\}$ *are independent Poisson processes, and* λ_j *are Lévy measures coming from the independent one-dimensional Lévy processes* $\eta_1,\ldots,\eta_l$.
Note that each column $\gamma^{(k)}$ *of the* $n \times l$ *matrix* $\gamma = (\gamma_{ij})$ *depends on* z *only through its* k*-th coordinate* z_k*, i.e.,*

$$\gamma^{(k)}(t,z,\omega) = \gamma^{(k)}(t,z_k,\omega), \quad z = (z_1,\ldots,z_l) \in \mathbb{R}^l, \quad k = 1,2,\ldots,l.$$

When we write out the i*-th component of* $dX(t)$ *explicitly, we obtain*

$$dX_i(t) = \alpha_i(t,\omega)dt + \sum_{j=1}^{m}\sigma_{ij}(t,\omega)d\mathcal{W}_j(t) + \sum_{j=1}^{l}\int_{\mathbb{R}}\gamma_{ij}(t,z_j,\omega)\tilde{N}_j(dt,dz_j), \quad 1 \le i \le n.$$

Let $f \in C^{1,2}([0,T]\times\mathbb{R}^n;\mathbb{R})$. *Define* $Y(t) = f(t,X(t))$. *Then*

$$\begin{aligned}dY(t) = {}& \frac{\partial f}{\partial t}dt + \sum_{i=1}^{n}\frac{\partial f}{\partial x_i}\left(\alpha_i dt + \sum_{j=1}^{m}\sigma_{ij}d\mathcal{W}_j(t)\right) + \frac{1}{2}\sum_{i,j=1}^{n}(\sigma\sigma^T)_{ij}\frac{\partial^2 f}{\partial x_i\partial x_j}dt\\ &+ \sum_{k=1}^{l}\int_{|z_k|<r_k}\left[f(t,X(t^-)+\gamma^{(k)}(t,z_k)) - f(t,X(t^-)) - \sum_{i=1}^{n}\gamma_i^{(k)}\frac{\partial f}{\partial x_i}(t,X(t^-))\right]\lambda_k(dz_k)dt\\ &+ \sum_{k=1}^{l}\int_{\mathbb{R}}\left[f(t,X(t^-)+\gamma^{(k)}(t,z_k)) - f(t,X(t^-))\right]\tilde{N}_k(dt,dz_k),\end{aligned}$$

where $\gamma^{(k)} \in \mathbb{R}^n$ *is the* k*-th column of the* $n \times l$ *matrix* $\gamma = (\gamma_{ik})$, *and* $\gamma_i^{(k)} = \gamma_{ik}$ *is the* i*-th coordinate of* $\gamma^{(k)}$.

2.7 Optimal control theory

Optimal control refers to the method of identifying the best control and state paths for a dynamic system over a specific time interval to maximize or minimize a given objective, cost functional, or performance index.

The optimal control has its roots in the calculus of variations. The earliest formal developments in this field date back to the 17th century, when J. Bernoulli posed the famous Brachistochrone problem to renowned mathematicians of the time-including Leibniz, Newton, J. Bernoulli, L'Hôpital, and v. Tschirnhaus. The challenge was to determine the curve along which a particle,

influenced solely by gravity, travels from point "A" to point "B" in the shortest possible time within a vertical plane.

The expansion of the calculus of variations into optimal control theory was largely driven by military needs and experienced significant growth after 1950. A major breakthrough came L.S. Pontryagin (1908-1988) and his collaborators-who formulated and proved the Pontryagins Maximum Principle [95]. Today, this principle is a cornerstone in the study of optimization problems involving differential equations, providing essential conditions for optimality.

At present, optimal control theory is a vast field encompassing multiple methodologies. It enables the manipulation of control variables within a system to fulfill a desired objective, where the system itself may be modeled by ODE, PDE, SDE...

2.7.1 Optimal control problem

A standard optimal control problem involves defining a performance index or cost functional $\mathfrak{J}(\mathfrak{x}(t), \mathfrak{u}(t))$, a set of state variables $\mathfrak{x}(t) \in X$, and a set of control variables $\mathfrak{u}(t) \in \Omega$, all defined over the time interval $t_0 \leq t \leq t_f$. The primary objective is to determine a piecewise continuous control function $\mathfrak{u}(t)$ and its corresponding state trajectory $\mathfrak{x}(t)$ that maximize the given objective functional. The structure and development of this part are largely based on the work of Lenhart and Workman [65].

Definition 2.18. An optimal control problem is in the form

$$\begin{aligned} \max_{\mathfrak{u}} \quad & \mathfrak{J}(\mathfrak{x}(t), \mathfrak{u}(t)) = \int_{t_0}^{t_f} \mathfrak{f}(t, \mathfrak{x}(t), \mathfrak{u}(t))dt, \\ \text{s.t.} \quad & \dot{\mathfrak{x}}(t) = \mathfrak{g}(t, \mathfrak{x}(t), u(t)), \\ & \mathfrak{x}(t_0) = \mathfrak{x}_0. \end{aligned} \tag{2.4}$$

$\mathfrak{x}(t_f)$ could be free, which means that the value of $\mathfrak{x}(t_f)$ is unrestricted, or could be fixed, i.e., $\mathfrak{x}(t_f) = \mathfrak{x}_f$.

In our context, the functions $\mathfrak{f}$ and $\mathfrak{g}$ are assumed to be continuously differentiable with respect to all three of their arguments. We also consider the control set Ω to be Lebesgue measurable. Consequently, since the controls are taken to be piecewise continuous, the corresponding state trajectories will be piecewise differentiable.

We have concentrated on identifying the function's maximum value. We can alternate between maximization and minimization by merely negating the cost functional:

$$\min\{\mathfrak{j}\} = -\max\{-\mathfrak{j}\}.$$

2.7.2 Pontryagins Maximum Principle (PMP)

The requisite first-order requirements for determining the best control were formulated by Pontryagin and his collaborators. This outcome is regarded as one of the most significant achievements in Mathematics throughout the 20th century.

Pontryagin proposed the concept of adjoint functions to augment the differential equation within the objective functional. Adjoint functions serve a role analogous to Lagrange multipliers in multivariate calculus, which incorporate constraints into the function of multiple variables intended for maximization or minimization.

Definition 2.19. Let the previous optimal control problem considered in (2.4). The function

$$\mathfrak{H}(t, \mathfrak{x}(t), \mathfrak{u}(t), \lambda(t)) = \mathfrak{f}(t, \mathfrak{x}(t), \mathfrak{u}(t)) + \lambda(t)\mathfrak{g}(t, \mathfrak{x}(t), \mathfrak{u}(t)) \tag{2.5}$$

is called Hamiltonian function and λ is the adjoint variable.

Theorem 2.8. *(Pontryagins Maximum Principle [65]). If $\mathfrak{u}^*(t)$ and $\mathfrak{x}^*(t)$ are optimal for problem (2.4), then there exists a piecewise differentiable adjoint variable $\lambda(t)$ such that*

$$\mathfrak{H}(t, \mathfrak{x}^*(t), \mathfrak{u}(t), \lambda(t)) \leq \mathfrak{H}(t, \mathfrak{x}^*(t), \mathfrak{u}^*(t), \lambda(t)) \tag{2.6}$$

for all controls $\mathfrak{u}$ at each time t, where $\mathfrak{H}$ is the Hamiltonian previously defined and

$$\lambda'(t) = -\frac{\partial \mathfrak{H}(t, \mathfrak{x}^*(t), \mathfrak{u}^*(t), \lambda(t))}{\partial \mathfrak{x}}, \tag{2.7}$$

$$\lambda(t_f) = 0. \tag{2.8}$$

Remark 2.2. The last condition, $\lambda(t_f) = 0$, called transversality condition, is only used when the optimal control problem does not have terminal value in the state variable, i.e., $\mathfrak{x}(t_f)$ is free.

This principle transforms the task of identifying a control that maximizes the objective functional-subject to the state ODE and initial condition-into the problem of pointwise optimization of the Hamiltonian. As a result, with the adjoint equation and the Hamiltonian in place, we obtain:

$$0 = \frac{\partial \mathfrak{H}}{\partial \mathfrak{u}} \tag{2.9}$$

at $\mathfrak{u}^*$ for each t, namely, the Hamiltonian has a critical point, usually this condition is called optimality condition. Thus to find the necessary conditions, we do not need to calculate the integral in the objective functional, we need just utilize the Hamiltonian.

2.7.3 Optimal control with payoff terms

In certain instances, it is essential to not only maximize (or minimize) terms across the entire time period but also to maximize (or minimize) a function value at a single moment in time, particularly toward the conclusion of the time interval. In certain scenarios, the objective function must consider the value of the state at the terminal time, such as the count of infected individuals after the conclusion of an epidemic model [65].

Definition 2.20. An optimal control problem with payoff term is in the form

$$\begin{aligned} \max_{\mathfrak{u}} \quad & \mathfrak{J}(\mathfrak{x}(t), \mathfrak{u}(t)) = \phi(\mathfrak{x}(t_f)) + \int_{t_0}^{t_f} \mathfrak{f}(t, x(t), \mathfrak{u}(t))dt, \\ \text{s.t.} \quad & \dot{\mathfrak{x}}(t) = \mathfrak{g}(t, \mathfrak{x}(t), \mathfrak{u}(t)), \\ & \mathfrak{x}(t_0) = \mathfrak{x}_0, \end{aligned} \tag{2.10}$$

where $\phi(\mathfrak{x}(t_f))$ is a goal w.r.t. the final position or population level $\mathfrak{x}(t_f)$. The term $\phi(\mathfrak{x}(t_f))$ is called payoff.

Utilizing the PMP, requisite conditions can be formulated for this issue.

Proposition 2.1. If $\mathfrak{u}^*(t)$ *and* $\mathfrak{x}^*(t)$ are optimal for problem (2.10), then there exists a piecewise differentiable adjoint variable $\lambda(t)$ such that

$$\mathfrak{H}(t, \mathfrak{x}^*(t), \mathfrak{u}(t), \lambda(t)) \leq \mathfrak{H}(t, \mathfrak{x}^*(t), \mathfrak{u}^*(t), \lambda(t)) \tag{2.11}$$

for any controls $\mathfrak{u}$ at each time t, *where* $\mathfrak{H}$ is the Hamiltonian previously defined and

$$\lambda'(t) = -\frac{\partial \mathfrak{H}(t, \mathfrak{x}^*(t), \mathfrak{u}^*(t), \lambda(t))}{\partial \mathfrak{x}} \quad \text{(adjoint condition)}, \tag{2.12}$$

$$\frac{\partial \mathfrak{H}}{\partial \mathfrak{u}} = 0 \quad \text{(optimality condition)}, \tag{2.13}$$

$$\lambda(t_f) = \phi'(\mathfrak{x}(t_f)) \quad \text{(transversality condition)}. \tag{2.14}$$

Numerous problems necessitate bounds on the control to achieve a realistic solution. For example, the amount of drugs in the organism must be non-negative and it is necessary to impose a limit. For the last example, despite being simplistic, it makes more sense to constrain the control as $0 \leq \mathfrak{u} \leq 1$.

2.7.4 Optimal control with bounded controls

Definition 2.21. An optimal control with bounded control can be written in the form

$$\max_{\mathfrak{u}} \quad \mathfrak{J}(\mathfrak{x}(t), \mathfrak{u}(t)) = \int_{t_0}^{t_f} \mathfrak{f}(t, \mathfrak{x}(t), \mathfrak{u}(t))dt, \tag{2.15}$$

s.t.

$$\begin{aligned}\dot{\mathfrak{x}}(t) &= \mathfrak{g}(t, \mathfrak{x}(t), \mathfrak{u}(t)),\\ \mathfrak{x}(t_0) &= \mathfrak{x}_0,\\ \mathfrak{a} \leq \mathfrak{u}(t) &\leq \mathfrak{b},\end{aligned}$$

where $\mathfrak{a}, \mathfrak{b}$ are constants and $\mathfrak{a} < \mathfrak{b}$.

To solve problems with bounds on the control, it is essential to formulate alternative necessary conditions.

Proposition 2.2. If $\mathfrak{u}^*(t)$ and $\mathfrak{x}^*(t)$ are optimal for problem (2.15), then there exists a piecewise differentiable adjoint variable $\lambda(t)$ such that

$$\mathfrak{H}(t, \mathfrak{x}^*(t), \mathfrak{u}(t), \lambda(t)) \leq \mathfrak{H}(t, \mathfrak{x}^*(t), \mathfrak{u}^*(t), \lambda(t)) \tag{2.16}$$

for all controls $\mathfrak{u}$, where $\mathfrak{H}$ is the Hamiltonian previously defined and

$$\begin{aligned}\lambda'(t) &= -\frac{\partial \mathfrak{H}(t, \mathfrak{x}^*(t), \mathfrak{u}^*(t), \lambda(t))}{\partial \mathfrak{x}},\\ \lambda(t_f) &= 0.\end{aligned}$$

By an adaptation of the PMP, the optimal control must satisfy:

$$\mathfrak{u}^* = \begin{cases} \mathfrak{a}, & \text{if } \frac{\partial \mathfrak{H}}{\partial \mathfrak{u}} < 0,\\ \mathfrak{a} \leq \tilde{\mathfrak{u}} \leq \mathfrak{b}, & \text{if } \frac{\partial \mathfrak{H}}{\partial \mathfrak{u}} = 0,\\ \mathfrak{b}, & \text{if } \frac{\partial \mathfrak{H}}{\partial \mathfrak{u}} > 0,\end{cases}$$

i.e., the maximization is over all admissible controls, and $\tilde{\mathfrak{u}}$ is obtained by the expression $\frac{\partial \mathfrak{H}}{\partial \mathfrak{u}} = 0$. In particular, the optimal control $\mathfrak{u}^*$ maximizes $\mathfrak{H}$ pointwise with respect to $\mathfrak{a} \leq \mathfrak{u} \leq \mathfrak{b}$.

In the case of a minimization problem, $\mathfrak{u}^*$ is selected to minimize the Hamiltonian $\mathfrak{H}$ pointwise. As a result, $<$ and $>$ in the first and third lines of the optimality conditions are reversed.

Remark 2.3. In certain software packages, explicit characterizations for control bounds may not be provided. In such cases, and when supported by the implementation, the optimal control $\tilde{\mathfrak{u}}$ can be expressed in a compact form as being bounded between $\mathfrak{a}$ and $\mathfrak{b}$, without the need for truncation.

$$\mathfrak{u}^*(t) = \min\{\mathfrak{a}, \max\{\mathfrak{b}, \tilde{\mathfrak{u}}\}\}. \tag{2.17}$$

We have completed the introduction of the mathematical tools that will be utilized subsequently. In the subsequent four chapters, we will develop various stochastic epidemic models. Each chapter will provide a general introduction to the model. Several prior studies will be referenced to elucidate the purpose and inspiration of our research. Subsequently, we shall demonstrate some aspects of the model, encompassing the criteria for extinction and persistence. Furthermore, computer simulation will be employed to substantiate our theory.

Unless stated otherwise, throughout this thesis we consider $(\Omega, \mathcal{F}, \{\mathcal{F}_t\}_{t\geq 0}, \mathbb{P})$ to be a complete probability space equipped with a filtration $\{\mathcal{F}_t\}_{t\geq 0}$ that satisfies the usual conditions.

Chapter 3

Optimal Control analysis of Stochastic COVID-19 Infection Model

In this chapter a mathematical study to control the spread of the COVID-19 epidemic by applying external control measures. We formulat a COVID-19 epidemic model with perturbation by white noise. We considered that the model consists of four categories are susceptible-vaccinated-infected-recovered. We show that the model is well posed, we give sufficient conditions for the extinction and the existence of a unique stationary distribution. We explore V -geometric ergodicity of the model. For the control model, we discussed both the stochastic and deterministic model using the techniques of optimal control theory. Real-world data from Algeria are used to parameterize the model, ensuring its relevance and applicability to practical satiation. Using numerical simulation, the analytical results have been shown.

3.1 Introduction

Modeling and simulation are the major instruments for making decisions when it comes to controlling epidemics [15, 17]. In any case, each epidemic is unique in terms of its biological traits, which force the dynamical models outlining their processes of transmission to be tailored to each individual case in order to deal with real-world circumstances [99].The highly infectious Coronavirus disease, which emerged in China in December 2019, rapidly spread across the globe, posing a significant threat to global health [117]. The COVID-19 pandemic triggered an unprecedented international health crisis, leading to immense human suffering and widespread social disruption. In response, various measures were undertaken to curb the virus's spread, including non-pharmaceutical interventions, mass vaccination campaigns, and other public health strategies.

Mathematical modeling of epidemics refers to the use of mathematical frameworks to describe the transmission dynamics of diseases within a population. These models are valuable tools for evaluating the effectiveness of public health interventions and predicting the course of an epidemic. They provide powerful insights into the mechanisms of disease spread and assist in the development of effective control strategies.

Numerous deterministic epidemic models have been explored in earlier research [1, 5, 93]. However, SDE models are often considered more effective for simulating biological phenomena, as they incorporate a higher degree of realism. Unlike deterministic models, which yield a single predicted trajectory, stochastic models can be run multiple times to generate a distribution of potential outcomes, offering richer and more practical insights [7, 8]. Since the transmission of infectious diseases is inherently random, it is crucial to incorporate environmental noise into models to reflect real-world fluctuations. Various forms of environmental noise-such as white noise [80], Lévy noise [103], and colored noise [60]-enhance the accuracy and utility of epidemic models in different ways. Specifically, white noise captures random, uncorrelated variations in disease transmission, addressing uncertainties linked to factors like human behavior and contact patterns. It is commonly added to deterministic frameworks to introduce randomness and improve predictive accuracy. In recent studies, white noise has been widely employed in epidemic modeling to better capture stochastic effects and improve our understanding of disease dynamics [6, 72, 97]. The application of optimal control theory in epidemiology plays a crucial role in devising effective strategies for disease prevention and mitigation. Numerous studies have employed this theory to enhance the management of epidemic outbreaks through various epidemiological models. For instance, in [1], the authors developed a deterministic SEIQR-type optimal control model to address the spread of COVID-19 in Nigeria. A novel stochastic optimal control model for hepatitis C was investigated in [66]. In [38], fractional optimal control was applied to analyze the COVID-19 epidemic in Algeria. Additionally, [93] presented a study on the spread of COVID-19 in Indonesia, incorporating the impact of vaccination using real-world data.

This chapter is devoted to developing both stochastic and deterministic optimal control frameworks for modeling and managing the dynamics of the COVID-19 epidemic. By combining mathematical modeling with optimization techniques, we aim to design strategies that effectively reduce the transmission of the virus, while accounting for constraints such as limited resources and societal priorities. The study begins with the formulation of a compartmental model for COVID-19 that incorporates random perturbations through white noise, thereby capturing the inherent uncertainties and stochastic fluctuations observed in real-world epidemic scenarios. This stochastic formulation provides a more realistic representation of the epidemics dynamics. Our objective is

to deepen the understanding of the pandemic's progression and to determine optimal interventions. We evaluate the impact of key control measures-including vaccination, social distancing, and treatment-on reducing infection rates and preventing future outbreaks. These effects are illustrated through graphical representations. To enhance the models relevance, we calibrate it using actual epidemiological data reported in Algeria over a defined time period. Model parameters are estimated using statistical methods that ensure the best fit to observed data, thereby increasing the accuracy and reliability of the framework. The effectiveness of the proposed control strategies is further examined through numerical simulations, which support the analytical findings. The results underscore the potential of various interventions to manage the spread of COVID-19. This knowledge serves as a valuable tool for policymakers and public health officials, assisting them in making informed decisions on the deployment of interventions, resource distribution, and the overall optimization of public health strategies.

Motivated by the above, as well as by works [3, 93]. We develop a stochastic mathematical model to describe the transmission dynamics of the COVID-19 epidemic. The total population, denoted by $N(t)$, is divided into four compartments: $S(t)$ for susceptible, $V(t)$ for vaccinated, $I(t)$ for infected, and $R(t)$ for recovered at any time $t > 0$, with the relation $R + S + I + V = N$. The model is based on several assumptions that reflect key characteristics of COVID-19: all model parameters are non-negative; susceptible individuals can receive vaccinations; infected individuals are capable of transmitting the virus to both susceptible and vaccinated individuals; and individuals who recover from the infection gain temporary immunity.

Assuming that white noise is proportional to the population compartments is a common and effective technique for modeling stochastic fluctuations in population dynamics [6, 72, 97, 118]. This method reflects the idea that larger population groups experience more significant random variations.

Given that the white noise terms are directly proportional to S, V, I, and R, we derive the following stochastic model:

$$\begin{aligned}
dS(t) &= \Big[-\beta\frac{S(t)I(t)}{N} - (k+\delta)S(t) + \Delta + \mu R(t)\Big]dt + \rho_1 S(t)dW_1(t),\\
dV(t) &= \Big[-\delta V(t) - (1-\tau)\beta\frac{V(t)I(t)}{N} + kS(t)\Big]dt + \rho_2 V(t)dW_2(t),\\
dI(t) &= \Big[-(\alpha+\delta+\delta_0)I(t) + \frac{\beta S(t)I(t)}{N} + (1-\tau)\frac{\beta V(t)I(t)}{N}\Big]dt + \rho_3 I(t)dW_3(t),\\
dR(t) &= \Big[-(\delta+\mu)R(t) + \alpha I(t)\Big]dt + \rho_4 R(t)dW_4(t),
\end{aligned} \tag{3.1}$$

with

$$X(0) = (S(0),V(0),I(0),R(0)) \in \mathbb{R}_+,$$

where W_1, W_2, W_3 and W_4 are independently Brownian motion. ρ_1, ρ_2, ρ_3 and ρ_4 are the thew white noise intensity.

If we put $\rho_j = 0,\ j = 1,2,3,4$. As a result, the deterministic counterpart of model (3.1) is given by the following system:

$$\begin{aligned} dS(t) &= \Big[-(k+\delta)S(t) + \Delta - \beta\frac{S(t)I(t)}{N} + \mu R(t)\Big]dt, \\ dV(t) &= \Big[-\delta V(t) + kS(t) - (1-\tau)\beta\frac{V(t)I(t)}{N}\Big]dt, \\ dI(t) &= \Big[-(\alpha+\delta+\delta_0)I(t) + \beta\frac{S(t)I(t)}{N} + \beta(1-\tau)\frac{V(t)I(t)}{N}\Big]dt, \\ dR(t) &= \Big[-(\delta+\mu)R(t) + \alpha I(t)\Big]dt. \end{aligned} \tag{3.2}$$

Table 3.1 presents the definitions and values of the parameters embedded in the model.

Table 3.1: Parameter's bilogical description.

parameters	Description
Δ	natality rate.
k	vaccination rate.
β	contact frequency between infected and susceptible individuals.
τ	vaccine effectiveness rate.
μ	loss of natural immunity.
δ_0	mortality rate attributable to COVID-19 infection.
δ	natural mortality rate.
α	recovery rate.

The dynamics of the spread of the COVID-19 epidemic for model (3.2) can be complectly analyzed based on the threshold number which, with reference to [113] is given as follows

$$R_0^d = \frac{\beta\delta + (1-\tau)\beta k}{(k+\delta)(\alpha+\delta+\delta_0)}.$$

The region

$$\Pi_{SVIR} = \left\{(S,V,I,R) \in \mathbb{R}_+^4 : S+V+I+R \leq \frac{\Delta}{\delta}\right\}$$

is positively invariant w.r.t. model (3.2).

In the following we will conduct a qualitative study and dynamic analysis of compartmental model (3.1).

3.2 Qualitative Properties

3.2.1 Global Positive Solution: Existence and Uniqueness

In the following, we show that system (3.1) admits a unique positive solution. The solution of model (3.1) may explode in a finite time, since the coefficients dont satisfy the linear growth condition, even though they satisfy the locally Lipschitz condition. Khasminskii and Mao gave the Lyapunov function argument, which is a powerful test for non-explosion of solutions without the linear growth condition and referred to as the Khasminskii-Mao theorem [57, 79].

Theorem 3.1. *For all $X(0) \in \mathbb{R}^4_+$, a unique solution $X(t) = (S(t),V(t),I(t),R(t))$ of system (3.1) can be determined. Moreover, $X(t)$ will stay in $\mathbb{R}^4_+$ $\forall\, t \geq 0$ a.s.*

Proof. By using the Lyapunov analysis method [79], we can prove that the solution of system (3.1) is positive and global.

Coefficients of the model are localy lipshitz continous for all $X(0) \in \mathbb{R}^4_+$, there is a unique solution $X(t)$ on $t \in [0,\tau_e)$, where τ_e is the explosion time. To show that this solution is global, we must prove that $\tau_e = \infty$ $a.s$. Assume that we have a sufficiently large nonnegative number m such that $S(0)$, $V(0)$, $I(0)$ and $R(0)$ all lie within $[\frac{1}{m}, m]$. Define the following stopping time:

$$\tau_l = \inf\Big\{t \in [0,\tau_e) : \min\Big\{S(t),V(t),I(t),R(t)\Big\} \leq \frac{1}{l} \text{ Or } \max\Big\{S(t),V(t),I(t),R(t)\Big\} \geq l\Big\}, \forall l \geq m. \tag{3.3}$$

We set $\inf \varnothing = \infty$ where $\varnothing$ is the empty set. Clearly τ_l is increasing. Set $\tau_\infty = \lim_{l\to\infty} \tau_l$, with $\tau_e \geq \tau_\infty$ $a.s$.

If we show that $\tau_\infty = \infty$ $a.s.$, then $\tau_e = \infty$ and $X(t) \in \mathbb{R}^4_+$ $a.s$ $\forall\, t \geq 0$. Next, we are going to prove that $\tau_\infty = \infty$, the proof goes by contradiction. we assume that $\tau_\infty < \infty$, then there exists $\varepsilon \in]0,1[$ and $0 < T$ satisfying $\varepsilon \leq \mathbb{P}\{\tau_\infty \leq T\}$. Therefore there is an integer $k_1 \geq m$, such that

$$\mathbb{P}\{\tau_l \leq T\} \geq \varepsilon, \forall l \geq k_1. \tag{3.4}$$

Define a C^2-function $\Sigma : \mathbb{R}^4_+ \to \mathbb{R}_+$:

$$\Sigma(X) = R + V + S + I - 4 - (\ln V + \ln R + \ln S + \ln I).$$

The nonnegativity of Σ can be seen from this function $\mathfrak{F}(x^*) = x^* - 1 - \ln x^* \geq 0,\ \forall x^* > 0$.

Using Itô formula gives

$$
\begin{aligned}
d\Sigma(X) =&\Big(1-\frac{1}{V}\Big)dV+\frac{1}{2V^2}(dV)^2+\Big(1-\frac{1}{S}\Big)dS+\frac{1}{2S^2}(dS)^2+\Big(1-\frac{1}{I}\Big)dI+\frac{1}{2I^2}(dI)^2\\
&+\Big(1-\frac{1}{R}\Big)dR+\frac{1}{2R^2}(dR)^2,\\
=&\Big(1-\frac{1}{S}\Big)\Big(\Big[\Delta-\beta\frac{S(t)I(t)}{N}+\mu R(t)-(k+\delta)S(t)\Big]dt+\rho_1 S(t)dW_1(t)\Big)\\
&+\frac{1}{2S^2}\Big(\Big[\Delta-\beta\frac{S(t)I(t)}{N}+\mu R(t)-(k+\delta)S(t)\Big]dt+\rho_1 S(t)dW_1(t)\Big)^2\\
&+\Big(1-\frac{1}{V}\Big)\Big(\Big[kS(t)-(1-\tau)\beta\frac{V(t)I(t)}{N}-\delta V(t)\Big]dt+\rho_2 V(t)dW_2(t)\Big)\\
&+\frac{1}{2V^2}\Big(\Big[kS(t)-\beta(1-\tau)\frac{V(t)I(t)}{N}-\delta V(t)\Big]dt+\rho_2 V(t)dW_2(t)\Big)^2\\
&+\Big(1-\frac{1}{I}\Big)\Big(\Big[\beta\frac{S(t)I(t)}{N}+\beta(1-\tau)\frac{V(t)I(t)}{N}-(\alpha+\delta+\delta_0)I(t)\Big]dt+\rho_3 I(t)dW_3(t)\Big)\\
&+\frac{1}{2I^2}\Big(\Big[\beta\frac{S(t)I(t)}{N}+\beta(1-\tau)\frac{V(t)I(t)}{N}-(\alpha+\delta+\delta_0)I(t)\Big]dt+\rho_3 I(t)dW_3(t)\Big)^2\\
&+\Big(1-\frac{1}{R}\Big)\Big(\Big[\alpha I(t)-(\delta+\mu)R(t)\Big]dt+\rho_4 R(t)dW_4(t)\Big)\\
&+\frac{1}{2R^2}\Big(\Big[\alpha I(t)-(\delta+\mu)R(t)\Big]dt+\rho_4 R(t)dW_4(t)\Big)^2,\\
=&L\Sigma(X)dt+\rho_1(S(t)-1)dW_1(t)+\rho_2(V(t)-1)dW_2(t)+\rho_3(I(t)-1)dW_3(t)\\
&+\rho_4(R(t)-1)dW_4(t),
\end{aligned}
$$

where $L\Sigma:\ \mathbb{R}^4_+\to\mathbb{R}_+$ is given by

$$
\begin{aligned}
L\Sigma(X) =&\Delta-\delta(S+V+R+I)-\frac{\Delta}{S}+\beta\frac{I}{N}-\mu\frac{R}{S}-k\frac{S}{V}+\beta(1-\tau)\frac{I}{N}-\beta\frac{S}{N}-\delta_0 I\\
&-\beta(1-\tau)\frac{V}{N}-\alpha\frac{I}{R}+\mu+\alpha+4\delta+\delta_0+k+\frac{\rho_1^2+\rho_2^2+\rho_3^2+\rho_4^2}{2},\\
\le&\Delta+\beta+(1-\tau)\beta+4\mu+\alpha+\delta_0+k+\delta+\frac{\rho_1^2+\rho_2^2+\rho_3^2+\rho_4^2}{2}:=M.
\end{aligned}
$$

M is independent of t, S, I, V, and R.

$$
\Rightarrow\quad d\Sigma(X)\le Mdt+\rho_1(S-1)dW_1(t)+\rho_2(V-1)dW_2(t)+\rho_3(I-1)dW_3(t)+\rho_4(I-1)dW_4(t).
$$

Integration over $[0,\ \tau_l\wedge T]$ gives

$$
\begin{aligned}
\int_0^{\tau_l\wedge T}d\Sigma(X)\le&\int_0^{\tau_l\wedge T}Mdr+\int_0^{\tau_l\wedge T}\rho_1(S(r)-1)dW_1(r)+\int_0^{\tau_l\wedge T}\rho_2(V(r)-1)dW_2(r)\\
&+\int_0^{\tau_l\wedge T}\rho_3(I(r)-1)dW_3(r)+\int_0^{\tau_l\wedge T}\rho_4(R(r)-1)dW_4(r).
\end{aligned}
$$

Taking expectation, We obtain

$$\mathbb{E}\Big[\Sigma\big(X(\tau_l \wedge T)\big)\Big] \leq \Sigma\big(X(0)\big) + \mathbb{E}\Big[\int_0^{\tau_l \wedge T} M dr\Big],$$
$$\leq \Sigma\big(X(0)\big) + MT.$$

Let $\Gamma_l = \{\tau_l \leq T\}\ \forall\ l \geq k_1$ and by (3.4) we have $\mathbb{P}(\Gamma_l) \geq \varepsilon$. It is worth noticing that for every ω in Γ_l, we can find at least one $S(\tau_l,\omega)$, $V(\tau_l,\omega)$, $I(\tau_l,\omega)$, and $R(\tau_l \wedge T)$ that are equal to l or $\frac{1}{l}$, hence

$$\Sigma\big(X(\tau_l,\omega)\big) \geq \mathfrak{F}(l) \wedge \mathfrak{F}(\frac{1}{l}),$$

therefore

$$\begin{aligned}
\Sigma\big(X(0)\big) + MT &\geq \mathbb{E}\Big[1_{\Gamma_l}(\omega)\Sigma\big(X(\tau_l \wedge T)\big)\Big], \\
&= \mathbb{E}\Big[1_{\Gamma_l}(\omega)\Sigma\big(X(\tau_l,\omega)\big)\Big], \\
&\geq \mathbb{E}\Big[1_{\Gamma_l}(\omega)\mathfrak{F}(l) \wedge \mathfrak{F}(\frac{1}{l})\Big], \\
&\geq \mathbb{E}\Big[1_{\Gamma_l}(\omega)\Big]\mathfrak{F}(l) \wedge \mathfrak{F}(\frac{1}{l}), \\
&\geq \varepsilon\mathfrak{F}(l) \wedge \mathfrak{F}(\frac{1}{l}).
\end{aligned}$$

$\mathbf{1}_{\Gamma_l(\omega)}$ is the indicator function of Γ_l.
When $l \to \infty$, then $\infty > \Sigma\big(X(0)\big) + MT = \infty$ is a contradiction, hence $\tau_\infty = \infty\ a.s.$ □

3.2.2 Stochastic permanence and ultimate boundedness

In this section, we study the stochastic permanence of model (3.1). First we present the following definitions

Definition 3.1. [69, 70] The SDE (3.1) is said to be stochastically ultimately bounded, if $\forall$ $\epsilon \in (0,1)$, there is a positive constant κ_ε, such that $\forall\ X(0) \in \mathbb{R}^4_+$, the solution $X(t)$ of model (3.1) has the property that

$$\limsup_{t\to+\infty} \mathbb{P}\{\|X(t)\| > \kappa_\varepsilon\} < \varepsilon.$$

Definition 3.2. [69, 70] The solution $X(t)$ of model (3.1) is said to be stochastically permanent if $\forall\ \epsilon \in (0,1)$, there exist positive constants σ_ε, η_ε with any initial value $X(0) \in \mathbb{R}^4_+$ such that

$$\liminf_{t\to+\infty} \mathbb{P}\{\|X(t)\| \leq \sigma_\varepsilon\} \geq 1-\varepsilon, \qquad \liminf_{t\to+\infty} \mathbb{P}\{\|X(t)\| \geq \eta_\varepsilon\} \geq 1-\varepsilon.$$

It is obvious that if the SDE is stochastically permanent, it must be stochastically ultimately bounded.

Remark 3.1. In [16, 71], the authors gave a new definition for stochastically permanent: Let $X(t) = (X_1(t),...,X_4(t))^T$ be the solution of a stochastic system with initial value $X(0) \in \mathbb{R}^d_+$. For any $0 < \varepsilon < 1$, if there exists a positive constant θ_ε such that for all $j = 1, \cdots, 4$,

$$\liminf_{t\to+\infty} \mathbb{P}\{X_j(t) \geq \theta_\varepsilon\} \geq 1 - \varepsilon,$$

then the stochastic model (3.1) is said to be stochastically persistent; if there exists a positive constant χ_ε such that for all $j = 1, \cdots, 4$,

$$\liminf_{t\to+\infty} \mathbb{P}\{X_j(t) \leq \chi_\varepsilon\} \geq 1 - \varepsilon,$$

then the stochastic model (3.1) is said to be stochastically bounded from above. If the stochastic system is both stochastically persistent and stochastically bounded from above, then it is said to be stochastically permanent.

Remark 3.2. [16] It is important to highlight that, according to Def.3.2, stochastic permanence implies that the total population-represented by the sum of all subpopulations in the system-remains bounded below by a positive value and above by a finite constant, with probability arbitrarily close to 1. Moreover, as indicated in Remark 3.1, this concept also ensures that each individual subpopulation stays within positive and bounded limits. In this study, we adopt Def.3.2 as our formal criterion for stochastic permanence.

Theorem 3.2. *The system (3.1) is stochastically ultimate bounded, moreover is stochastically permanent.*

Proof. Let $X_0 \in \mathbb{R}^4_+$, by summing up the equations in (3.1), we obtain, $\quad \forall\, t \geq 0$

$$dN(t) = (\Delta - \delta N(t) - \delta_0 I(t))\, dt + \rho_1 S(t)\, dW_1(t) + \rho_2 V(t)\, dW_2(t) + \rho_3 I(t)\, dW_3(t) + \rho_4 R(t)\, dW_4(t).$$

Define a C^2 function $\Upsilon : \mathbb{R}_+ \to [1, \infty)$ by $\Upsilon(n) = n + \frac{1}{n}$, the Itô's formula shows that

$$\begin{aligned} d\Upsilon(N(t)) = L\Upsilon(N(t))\, dt + \left(1 - \frac{1}{N(t)^2}\right) \big[&\rho_1 S(t)\, dW_1(t) + \rho_2 V(t)\, dW_2(t) + \rho_3 I(t)\, dW_3(t) \\ &+ \rho_4 R(t)\, dW_4(t)\big], \end{aligned}$$

where $L\Upsilon(N)$ is given by

$$\begin{aligned}
L\Upsilon(N) &= (\Delta - \delta N - \delta_0 I) - \frac{\Lambda - \delta N - \delta_0 I}{N^2} + \frac{1}{N^3}(\rho_1^2 S^2 + \rho_2^2 V^2 + \rho_3^2 I^2 + \rho_4^2 R^2), \\
&\leq (\Delta - \delta N) - \frac{\Lambda}{N^2} + \frac{\delta + \delta_0}{N} + \frac{1}{N}\sum_{i=1}^{4}\rho_i^2, \\
&\leq -\delta\left(N + \frac{1}{N}\right) + \Delta + \frac{1}{N}\left(2\delta + \delta_0 + \sum_{i=1}^{4}\rho_i^2\right) - \frac{\Lambda}{N^2}, \\
&\leq -\delta\Upsilon(N) - \left(\frac{\sqrt{\Delta}}{N} - \frac{1}{2\sqrt{\Delta}}\left(2\delta + \delta_0 + \sum_{i=1}^{4}\rho_i^2\right)\right)^2 + \Delta + \frac{1}{4\Delta}\left(2\delta + \delta_0 + \sum_{i=1}^{4}\rho_i^2\right)^2, \\
&= -\delta\Upsilon(N) + C,
\end{aligned}$$

where $C = \Delta + \frac{1}{4\Delta}\left(2\delta + \delta_0 + \sum_{i=1}^{4}\rho_i^2\right)^2$.
Using the integration by parts formula to $e^{\delta t}\Upsilon(N(t))$ yields

$$\begin{aligned}
d(e^{\delta t}\Upsilon(N(t))) &= \delta e^{\delta t}\Upsilon(N(t))\,dt + e^{\delta t}\,d\Upsilon(N(t)), \\
&\leq \delta e^{\delta t}\Upsilon(N(t))\,dt + e^{\delta t}\left[(-\delta\Upsilon(N(t)) + C)\,dt + \left(1 - \frac{1}{N(t)^2}\right)\left[\sum_{i=1}^{4}\rho_i X_i(t)\,dW_i(t)\right]\right], \\
&= Ce^{\delta t}dt + e^{\delta t}\left(1 - \frac{1}{N(t)^2}\right)\left[\sum_{i=1}^{4}\rho_i X_i(t)\,dW_i(t)\right].
\end{aligned}$$

By integrating from 0 to $t \wedge \tau_l$ (τ_l is given in (3.3)), and then taking the expectation on both sides of this inequality, we get for all $t \geq 0$ and $l \geq m$

$$\mathbb{E}\left[e^{\delta(t\wedge\tau_l)}\Upsilon(N(t\wedge\tau_l))\right] \leq \Upsilon(N(0)) + \mathbb{E}\left[\int_0^{t\wedge\tau_l} Ce^{\delta s}ds\right] \leq \Upsilon(N(0)) + \frac{C}{\delta}(e^{\delta t} - 1).$$

Letting $\tau_l \to \infty$

$$\mathbb{E}\left[\Upsilon(N(t))\right] \leq \Upsilon(N(0)) \times e^{-\delta t} + \frac{C}{\delta}(1 - e^{-\delta t}) \leq \Upsilon(N(0)) \times e^{-\delta t} + \frac{C}{\delta}.$$

Let $\varepsilon > 0$, and take $\sigma_\varepsilon = \frac{C}{\varepsilon\delta}$, by using Chebyshevs inequality , we get

$$\mathbb{P}\left(\Upsilon(N(t)) > \sigma_\varepsilon\right) \leq \frac{1}{\sigma_\varepsilon} \times \mathbb{E}[\Upsilon(N(t))] \leq \frac{1}{\sigma_\varepsilon}\left(\Upsilon(N(0)) \times e^{-\delta t}\right) + \varepsilon,$$

then

$$\mathbb{P}\left(N(t) + \frac{1}{N(t)} \leq \sigma_\varepsilon\right) \geq 1 - \varepsilon - \frac{1}{\sigma_\varepsilon}\left(\Upsilon(N(0)) \times e^{-\delta t}\right),$$

therefore

$$\mathbb{P}\left(\frac{1}{\sigma_\varepsilon} \leq N(t) \leq \sigma_\varepsilon\right) \geq \mathbb{P}\left(N(t) + \frac{1}{N(t)} \leq \sigma_\varepsilon\right) \geq 1 - \varepsilon - \frac{1}{\sigma_\varepsilon}\left(\Upsilon(N(0)) \times e^{-\delta t}\right),$$

noting that

$$\frac{1}{4}N \leq \|X\| \leq N,$$

we obtain

$$1-\varepsilon-\frac{1}{\sigma_\varepsilon}\left(\widetilde{V}(N(0))\times e^{-\delta t}\right)\leq\mathbb{P}\left(\frac{1}{\sigma_\varepsilon}\leq N(t)\leq\sigma_\varepsilon\right)\leq\mathbb{P}\left(\frac{1}{2\sigma_\varepsilon}\leq\|X(t,X_0)\|\leq\sigma_\varepsilon\right),$$

then

$$\liminf_{t\to\infty}\mathbb{P}\left(\eta_\varepsilon\leq\|X(t,X_0)\|\leq\sigma_\varepsilon\right)\geq 1-\varepsilon,$$

where $\eta_\varepsilon=\frac{1}{2\sigma_\varepsilon}$.

The proof is end. □

3.2.3 V-geometric ergodic

Lemma 3.1. *[83, 84] Assume that the following Assumptions hold:*

(A1) For a compact set $K_1\subset\mathbb{R}^4_+$, there exist $T,\zeta>0$ and a probability measure μ on $\mathbb{R}^4_+$ with $\mu(K_1)>0$ such that

$$P_T(X_0,A)\geq\zeta\mu(A),\quad\forall X_0\in K_1,\ \forall A\in\mathcal{B}(\mathbb{R}^4_+).$$

(A2) There is a function $U:\mathbb{R}^4_+\to[1,\infty)$ with $\lim_{|X(t)|\to\infty}U(X)=\infty$ and real numbers $b_1,b_2\in(0,\infty)$ such that

$$LU(X)\leq b_1-b_2U(X).$$

Then the Markov process $X(t)$ is V-geometrically ergodic: there exists a unique stationary distribution π such that, for some constants $M,\lambda>0$,

$$|\mathbb{E}f(X(t))-\pi(f)|\leq MU(X_0)e^{-\lambda t},\quad\forall X_0\in\mathbb{R}^4_+,$$

for all measurable function $f\in\mathcal{G}:=\left\{\text{measurable } f:\mathbb{R}^4_+\to\mathbb{R}^4 \text{ with } |f(X)|\leq U(X)\right\}$.

Theorem 3.3. *Markov process $X(t)$ of model (3.1) with $X_0\in\mathbb{R}^4_+$ is V-geometrically ergodic.*

Proof. We define for $X(t)\in\mathbb{R}^4_+$:

$$\Upsilon_*(X(t))=N+\frac{1}{N}.$$

It follows that $\Upsilon_*(X(t))\to\infty$ as $|X(t)|\to\infty$. By Itô's formula, we have

$$\begin{aligned}L\Upsilon_*(X(t))&=\Delta-\delta N-\delta_0 I-\frac{\Delta-\delta N-(\delta_0)I}{N^2}+\frac{\rho_1^2S^2+\rho_2^2V^2+\rho_3^2I^2+\rho_4^2R^2}{N^3},\\&\leq C-\delta\Upsilon_*(X).\end{aligned}$$

Thus (A2) in Lemma 3.1 holds.

As model (3.1) satisfies the condition of uniform ellipticity, Proposition 11.1 in [9] confirms the existence of a function

$$p:\mathbb{R}_+\times\mathbb{R}^4_+\times\mathbb{R}^4_+\to\mathbb{R}^*_+$$

such that p is jointly continuous, $p_t(X_0, Y)$ is strictly positive for all (t, X_0, Y), and such that for all measure sets A

$$P_t(X_0, A) = \int_A p_t(X_0, Y)dY.$$

It follows that for any $\omega > 0$, there exists a positive constant $q = q_{\omega,t} > 0$ so that $\inf\{p_t(X_0, Y) : X_0, Y \in \mathbb{R}^4_+, \|X_0\|, \|Y\| \leq \omega\} \geq q$. Assumption 1 follows immediately from this, since for any measurable set A

$$P_t(x, A) = \int_A p_t(X_0, Y)dY \geq q\,\lambda^*(A \cap \mathcal{B}_\omega(0)) = q\,\lambda^*(\mathcal{B}_\omega(0))\mu(A),$$

where λ^* is Lebesgue measure and $\mu(A) = \lambda^*(A \cap \mathcal{B}_\omega(0))/\lambda^*(\mathcal{B}_\omega(0))$. Thus (A1) in Lemma 3.1 holds.

This proof is finish. □

3.2.4 Extinction of the infection

The objective of this section is to determine sufficient conditions under which the disease will be eradicated from the system described by model (3.1). This is a fundamental problem in the field of epidemiology.

To proceed, we define a threshold parameter

$$R_0 = \frac{\beta + \beta(1-\tau)}{(\delta + \alpha + \delta_0 + \frac{\rho_3^2}{2})}.$$

Theorem 3.4. *$X(t)$ be a solution of the model (3.1) with $X(0) \in \mathbb{R}^4$, if $R_0 < 1$, then $\limsup_{t\to\infty} \frac{\ln I(t)}{t} < 0$ a.s., namely, $I(t) \longrightarrow 0$ exponentially a.s.*

Proof. Make use of Itô formula we have

$$d\ln I(t) = \Big[\beta\frac{S(t)}{N} + (1-\tau)\beta\frac{V(t)}{N} - (\alpha + \delta + \delta_0 + \frac{\rho_3^2}{2})\Big]dt + \rho_3 dW_3(t). \tag{3.5}$$

Integrating over $[0, t]$ and then with the division with t yields

$$\frac{\ln I(t)}{t} = \frac{\beta}{t}\int_0^t \frac{S(r)}{N}dr + \frac{\beta(1-\tau)}{t}\int_0^t \frac{V(r)}{N}dr - (\alpha + \delta + \delta_0 + \frac{\rho_3^2}{2}) + \frac{\rho_3}{t}\int_0^t dW_3(r) + \frac{\ln I(0)}{t},$$

$$\leq \beta(1 + (1-\tau))(\alpha + \delta + \delta_0 + \frac{\varrho_3^2}{2}) + \frac{\rho_3}{t}\int_0^t dW_3(r) + \frac{\ln I(0)}{t},$$

$$\Rightarrow \quad \frac{\ln I(t)}{t} \leq (\alpha + \delta + \delta_0 + \frac{\rho_3^2}{2})(R_0 - 1) + \frac{\rho_3}{t}\int_0^t dW_3(r) + \frac{\ln I(0)}{t}. \tag{3.6}$$

Moreover $\frac{1}{t}\int_0^t dW_3(r)$ is a continuous local martingale. By lemma 2.1, we obtain

$$\lim_{t\to\infty}\frac{1}{t}\int_0^t dW_3(r)=0 \quad a.s.$$

Taking $\limsup_{t\to\infty}$ of (3.6) and if $R_0<1$ we get

$$\limsup_{t\to\infty}\frac{\ln I(t)}{t}\leq(\alpha+\delta+\delta_0+\frac{\rho_3^2}{2})(R_0-1)<0,$$

which imply $\lim_{t\to\infty} I(t)=0 \quad a.s.$ □

3.2.5 Stationary distribution

Understanding the conditions under which a disease persists or dies out is a central problem in epidemiology. In this section, we aim to demonstrate that the system described by model (3.1) admits a stationary distribution under certain specified conditions.

Theorem 3.5. *If*

$$\bar{R}_0:=\frac{\delta k\beta(1-\tau)}{(\delta+k+\frac{\rho_1^2}{2})(\delta+\frac{\rho_2^2}{2})(\delta_0+\alpha+\delta+\frac{\rho_3^2}{2})}>1,$$

then, the solution of system (3.1) has a unique stationary distribution $\pi(.)$, and it is ergodic.

Proof. To establish Theorem 3.5 , it is sufficient to verify that the conditions stated in Remark 2.1 are satisfied.

First we examine condition (b) by constructing a non-negative C^2-function $\chi:\mathbb{R}_+^4\longrightarrow\mathbb{R}_+$.

We define

$$\Upsilon_1(X)=-w_1\ln S-w_2\ln V-w_3\ln I+R+S+I+V,$$

$\omega_1,\omega_2,\omega_3>0$ we will define later.

Applying Itô formula we get

$$\begin{aligned}
L(R+I+S+V)&=\Delta-\delta(R+I+V+S)-\delta_0 I,\\
L(-\ln S)&=-\frac{\Delta}{S}+\frac{\beta I}{N}-\frac{\mu R}{S}+\frac{\rho_1^2}{2}+k+\delta,\\
L(-\ln V)&=-\frac{kS}{V}+\frac{(1-\tau)\beta I}{N}+\delta+\frac{\rho_2^2}{2},\\
L(-\ln I)&=-\frac{\beta S}{N}-\frac{(1-\tau)\beta V}{N}+\alpha+\delta_0+\delta+\frac{\rho_3^2}{2}.
\end{aligned}$$

Consequently,

$$\begin{aligned}
L\Upsilon_1=&\Delta-\delta(S+V+I+R)-\delta_0 I-\frac{w_1\Delta}{S}+\frac{w_1\beta I}{N}-\frac{w_1\mu R}{S}+w_1(\frac{\rho_1^2}{2}+k+\delta)\\
&-\frac{w_2kS}{V}+\frac{w_2(1-\tau)\beta I}{N}+w_2(\delta+\frac{\rho_2^2}{2})-\frac{w_3\beta S}{N}-\frac{w_3(1-\tau)\beta V}{N}+w_3(\alpha+\delta_0+\delta+\frac{\rho_3^2}{2}),
\end{aligned}$$

using the inequality $\sqrt[4]{e_1e_2e_3e_4} \leq \frac{1}{4}(e_1+e_3+e_2+e_4) \quad e_1, e_3e_2, e_4 > 0$, we obtain

$$\begin{aligned}
L\Upsilon_1 \leq & -4\sqrt[4]{\delta N \frac{w_1\Delta}{S}\frac{w_2kS}{V}\frac{w_3(1-\tau)\beta V}{N}} + \Delta - \delta_0 I + \frac{w_1\beta I}{N} - \frac{w_1\mu R}{S} + w_1(\frac{\rho_1^2}{2}+k+\delta) \\
& + \frac{w_2(1-\tau)\beta I}{N} + w_2(\delta+\frac{\rho_2^2}{2}) - \frac{w_3\beta S}{N} + w_3(\alpha+\delta_0+\delta+\frac{\rho_3^2}{2}), \\
= & -4\sqrt[4]{\delta w_1\Delta w_2 k w_3(1-\tau)\beta} + \Delta - \delta_0 I + \frac{w_1\beta I}{N} - \frac{w_1\mu R}{S} + w_1(\frac{\rho_1^2}{2}+k+\delta) + \frac{w_2(1-\tau)\beta I}{N} \\
& + w_2(\delta+\frac{\rho_2^2}{2}) - \frac{w_3\beta S}{N} + w_3(\alpha+\delta_0+\delta+\frac{\rho_3^2}{2}).
\end{aligned}$$

Let's put

$$\Delta = w_1(\delta+k+\frac{\rho_1^2}{2}) = w_2(\delta+\frac{\rho_2^2}{2}) = w_3(\delta_0+\alpha+\delta+\frac{\rho_3^2}{2}),$$

then

$$w_1 = \frac{\Delta}{(\delta+k+\frac{\rho_1^2}{2})}, \quad w_2 = \frac{\Delta}{(\delta+\frac{\rho_2^2}{2})}, \quad w_3 = \frac{\Delta}{(\delta_0+\alpha+\delta+\frac{\rho_3^2}{2})}.$$

As a result

$$\begin{aligned}
L\Upsilon_1 \leq & -4\sqrt[4]{\frac{\delta k\beta(1-\tau)\Delta^4}{(\delta+k+\frac{\rho_1^2}{2})(\delta+\frac{\rho_2^2}{2})(\delta_0+\alpha+\delta+\frac{\rho_3^2}{2})}} + 4\Delta - \delta_0 I + \frac{w_1\beta I}{N} - \frac{w_1\mu R}{S} + \frac{w_2(1-\tau)\beta I}{N} \\
& - \frac{w_3\beta S}{N}, \\
\leq & -4\Delta\Big(\sqrt[4]{\frac{\delta k\beta(1-\tau)}{(\delta+k+\frac{\rho_1^2}{2})(\delta+\frac{\rho_2^2}{2})(\delta_0+\alpha+\delta+\frac{\rho_3^2}{2})}} - 1\Big) + \frac{w_1\beta I}{N} + \frac{w_2(1-\tau)\beta I}{N} - \frac{w_3\beta S}{N}, \\
= & -4\Delta\big[(R_0^s)^{\frac{1}{4}} - 1\big] + \frac{w_1\beta I}{N} + \frac{w_2(1-\tau)\beta I}{N} - \frac{w_3\beta S}{N}.
\end{aligned}$$

We define

$$\Upsilon_2(X) = w_4\big(V+R+I+S-w_1\ln V - w_2\ln S - w_3\ln I\big) + S + R + I + V - \ln V - \ln S - \ln R.$$

Obviously

$$\liminf_{q\to+\infty, X\in\mathbb{R}_+^4\setminus U_q} \Upsilon_2(X) = +\infty,$$

where $U_q =]\frac{1}{q}, q[^3$.

In contrast,

$$\frac{\partial\Upsilon_2(X)}{\partial S} = w_4 + 1 - \frac{w_4w_1+1}{S}, \qquad \frac{\partial\Upsilon_2(X)}{\partial V} = w_4 + 1 - \frac{w_4w_2+1}{V},$$

$$\frac{\partial\Upsilon_2(X)}{\partial I} = w_4 + 1 - \frac{w_4w_3}{I} \qquad \frac{\partial\Upsilon_2(X)}{\partial R} = w_4 + 1 - \frac{1}{R},$$

the function Υ_2 have unique stagnation point $X_* = \Big(\frac{w_4w_1+1}{w_4+1}, \frac{w_4w_2+1}{w_4+1}, \frac{w_4w_3}{w_4+1}, \frac{1}{w_4+1}\Big)$.
The Hessian matrix of Υ_2 at X_* is given by

$$\begin{bmatrix} \frac{w_4w_1+1}{S_*^2} & 0 & 0 & \\ 0 & \frac{w_4w_2+1}{V_*^2} & 0 & \\ 0 & 0 & \frac{w_4w_3}{I_*^2} & \\ 0 & 0 & 0 & \frac{1}{R_*^2} \end{bmatrix}.$$

The Hessian matrix is positive definite and Υ_2 is continous function then we can say that Υ_2 has a unique minimum $X_* = (S_*,V_*,I_*,R_*) \in \mathbb{R}^4_+$.
Let

$$\chi(X) = \Upsilon_2(X) - \Upsilon_2(X_*).$$

Applying Itô formula we obtain

$$\begin{aligned} L\chi(X) &= L\Upsilon_2(X) \\ &\leq w_4\Big[-4\Delta\big[(R_0^s)^{\frac{1}{4}}-1\big] + \frac{w_1\beta I}{N} + \frac{w_2(1-\tau)\beta I}{N} - \frac{w_3\beta S}{N}\Big] + \Delta - \delta N - \frac{\Delta}{S} \\ &- \frac{\alpha I}{R} + \frac{\beta I}{N} - \frac{\mu R}{S} + \frac{\rho_1^2}{2} + k + 2\delta + \mu + \frac{\rho_4^2}{2} - \frac{kS}{V} + \frac{(1-\tau)\beta I}{N} + \delta + \frac{\rho_2^2}{2}, \\ &= -4w_4\Delta\big[(R_0^s)^{\frac{1}{4}}-1\big] + \frac{w_4w_1\beta I}{N} + \frac{w_4w_2(1-\tau)\beta I}{N} - \frac{w_4w_3\beta S}{N} + \Delta - \delta N \\ &- \frac{\Delta}{S} - \frac{\alpha I}{R} + \frac{\beta I}{N} - \frac{\mu R}{S} + \frac{\rho_1^2}{2} + k + 2\delta + \mu + \frac{\rho_4^2}{2} - \frac{kS}{V} + \frac{(1-\tau)\beta I}{N} + \delta + \frac{\rho_2^2}{2}, \end{aligned}$$

w_4 is a positive number that satisfies:

$$-4w_4\Delta\big[(R_0^s)^{\frac{1}{4}}-1\big] + \mathbf{W} < -1,$$

where

$$\mathbf{W} = \Delta + (1-\tau)\beta + \beta + k + 3\delta + \mu + \frac{\rho_4^2+\rho_2^2+\rho_1^2}{2}.$$

Let $\varepsilon_l > 0, l = 1,2,...,8$, we state a bounded closed set

$$U = \Big\{X \in \mathbb{R}^4_+ : \varepsilon_1 \leq S \leq \frac{1}{\varepsilon_2}, \varepsilon_3 \leq V \leq \frac{1}{\varepsilon_4}, \varepsilon_5 \leq I \leq \frac{1}{\varepsilon_6}, \varepsilon_7 \leq R \leq \frac{1}{\varepsilon_8}\Big\}.$$

Suitable small positive constants ε_l can be chosen to satisfy the following conditions

- $\mathbf{E} - \dfrac{\Delta}{\varepsilon_1} < 0,$
- $\mathbf{E} - \dfrac{k}{\varepsilon_1} < 0,$

- $-4w_4\Delta\left[(R_0^s)^{\frac{1}{4}}-1\right]+\dfrac{[w_1+w_2(1-\tau)]w_4\beta\varepsilon_3}{N}+\mathbf{W}<0,$
- $\mathbf{E}-\dfrac{\alpha}{\varepsilon_5}<0,$
- $\mathbf{E}-\dfrac{\delta}{\varepsilon_2}<0,$
- $\mathbf{E}-\dfrac{\delta}{\varepsilon_4}<0,$
- $\mathbf{E}-\dfrac{\delta}{\varepsilon_6}<0,$
- $\mathbf{E}-\dfrac{\delta}{\varepsilon_8}<0,$

where

$$\mathbf{E}=w_4w_1\beta+w_4w_2(1-\tau)\beta+(1-\tau)\beta+\beta+\Delta+k+3\delta+\mu+\frac{\rho_4^2+\rho_2^2+\rho_1^2}{2}.$$

Next, we show that $L\chi<0$ on $\mathbb{R}^4_+\setminus U$, $\mathbb{R}^4_+\setminus U=\bigcup_{j=1}^{8}U_j$ where

$$U_1=\left\{X\in\mathbb{R}^4_+,0<S<\varepsilon_1\right\},\quad U_2=\left\{X\in\mathbb{R}^4_+,0<V<\varepsilon_3,S>\varepsilon_1\right\},$$
$$U_3=\left\{X\in\mathbb{R}^4_+,0<I<\varepsilon_5\right\},\quad U_4=\left\{X\in\mathbb{R}^4_+,0<R<\varepsilon_7,I>\varepsilon_5\right\},$$
$$U_5=\left\{X\in\mathbb{R}^4_+,S>\frac{1}{\varepsilon_2}\right\},\quad U_6=\left\{X\in\mathbb{R}^4_+,V>\frac{1}{\varepsilon_4}\right\},$$
$$U_7=\left\{X\in\mathbb{R}^4_+,I>\frac{1}{\varepsilon_6}\right\},\quad U_8=\left\{X\in\mathbb{R}^4_+,R>\frac{1}{\varepsilon_8}\right\}.$$

Case 1. let $X\in U_1$

$$\begin{aligned}L\chi(X)\leq&-4w_4\Delta\left[(R_0^s)^{\frac{1}{4}}-1\right]+\frac{w_4w_1\beta I}{N}+\frac{w_4w_2(1-\tau)\beta I}{N}-\frac{w_4w_3\beta S}{N}+\Delta-\delta N\\&-\frac{\Delta}{S}-\frac{\alpha I}{R}+\frac{\beta I}{N}-\frac{\mu R}{S}+\frac{\rho_1^2}{2}+k+2\delta+\mu+\frac{\rho_4^2}{2}-\frac{kS}{V}+\frac{(1-\tau)\beta I}{N}+\delta+\frac{\rho_2^2}{2},\\\leq&w_4w_1\beta+w_4w_2(1-\tau)\beta+\Delta+\beta+(1-\tau)\beta+\frac{\rho_1^2}{2}+k+3\delta+\mu+\frac{\rho_4^2}{2}+\frac{\rho_2^2}{2}-\frac{\Delta}{S},\\\leq&\mathbf{E}-\frac{\Delta}{\varepsilon_1}<0.\end{aligned}$$

Case 2. let $X \in U_2$

$$\begin{aligned}
L\chi(X) \leq & -4w_4\Delta\left[(R_0^s)^{\frac{1}{4}}-1\right]+\frac{w_4w_1\beta I}{N}+\frac{w_4w_2(1-\tau)\beta I}{N}-\frac{w_4w_3\beta S}{N}+\Delta-\delta N \\
& -\frac{\Delta}{S}-\frac{\alpha I}{R}+\frac{\beta I}{N}-\frac{\mu R}{S}+\frac{\rho_1^2}{2}+k+2\delta+\mu+\frac{\rho_4^2}{2}-\frac{kS}{V}+\frac{(1-\tau)\beta I}{N}+\delta+\frac{\rho_2^2}{2}, \\
\leq & w_4w_1\beta+w_4w_2(1-\tau)\beta+\Delta+(1-\tau)\beta+\beta+k+3\delta+\mu+\frac{\rho_4^2+\rho_2^2+\rho_1^2}{2}-k\frac{S}{V}, \\
\leq & w_4w_1\beta+w_4w_2(1-\tau)\beta+\beta+(1-\tau)\beta+\Delta+k+3\delta+\mu+\frac{\rho_4^2+\rho_2^2+\rho_1^2}{2}-k\frac{\varepsilon_1}{\varepsilon_3}.
\end{aligned}$$

We put $\varepsilon_3=\varepsilon_1^2$,

$$\leq \mathbf{E}-\frac{k}{\varepsilon_1}<0.$$

Case 3. let $X \in U_3$

$$\begin{aligned}
L\chi(X) \leq & -4w_4\Delta\left[(R_0^s)^{\frac{1}{4}}-1\right]+\frac{w_4w_1\beta I}{N}+\frac{w_4w_2(1-\tau)\beta I}{N}-\frac{w_4w_3\beta S}{N}+\Delta-\delta N \\
& -\frac{\Delta}{S}-\frac{\alpha I}{R}+\frac{\beta I}{N}-\frac{\mu R}{S}+\frac{\rho_1^2}{2}+k+2\delta+\mu+\frac{\rho_4^2}{2}-\frac{kS}{V}+\frac{(1-\tau)\beta I}{N}+\delta+\frac{\rho_2^2}{2}, \\
\leq & -4w_4\Delta\left[(R_0^s)^{\frac{1}{4}}-1\right]+\frac{[w_1+w_2(1-\tau)]w_4\beta\varepsilon_3}{N}+\Delta+(1-\tau)\beta+\beta+k+3\delta \\
& +\mu+\frac{\rho_4^2+\rho_2^2+\rho_1^2}{2}, \\
\leq & -4w_4\Delta\left[(R_0^s)^{\frac{1}{4}}-1\right]+\frac{[w_1+w_2(1-\tau)]w_4\beta\varepsilon_3}{N}+\mathbf{W}<0.
\end{aligned}$$

Case 4. let $X \in U_4$

$$\begin{aligned}
L\chi(X) \leq & -4w_4\Delta\left[(R_0^s)^{\frac{1}{4}}-1\right]+\frac{w_4w_1\beta I}{N}+\frac{w_4w_2(1-\tau)\beta I}{N}-\frac{w_4w_3\beta S}{N}+\Delta-\delta N \\
& -\frac{\Delta}{S}-\frac{\alpha I}{R}+\frac{\beta I}{N}-\frac{\mu R}{S}+\frac{\rho_1^2}{2}+k+2\delta+\mu+\frac{\rho_4^2}{2}-\frac{kS}{V}+\frac{(1-\tau)\beta I}{N}+\delta+\frac{\rho_2^2}{2}, \\
\leq & w_4w_1\beta+w_4w_2(1-\tau)\beta+\Delta+(1-\tau)\beta+\beta+k+3\delta+\mu+\frac{\rho_1^2+\rho_2^2+\rho_4^2}{2}-\alpha\frac{I}{R}, \\
\leq & w_4w_1\beta+w_4w_2(1-\tau)\beta+\Delta+(1-\tau)\beta+\beta+k+3\delta+\mu+\frac{\rho_1^2+\rho_2^2+\rho_4^2}{2}-\alpha\frac{\varepsilon_7}{\varepsilon_5},
\end{aligned}$$

let $\varepsilon_7=\varepsilon_5^2$,

$$\leq \mathbf{E}-\frac{\alpha}{\varepsilon_5}<0.$$

Case 5. let $X \in U_5$

$$\begin{aligned}
L\chi(X) \leq & -4w_4\Delta\left[(R_0^s)^{\frac{1}{4}} - 1\right] + \frac{w_4w_1\beta I}{N} + \frac{w_4w_2(1-\tau)\beta I}{N} - \frac{w_4w_3\beta S}{N} + \Delta - \delta N \\
& - \frac{\Delta}{S} - \frac{\alpha I}{R} + \frac{\beta I}{N} - \frac{\mu R}{S} + \frac{\rho_1^2}{2} + k + 2\delta + \mu + \frac{\rho_4^2}{2} - \frac{kS}{V} + \frac{(1-\tau)\beta I}{N} + \delta + \frac{\rho_2^2}{2}, \\
\leq & w_4w_1\beta + w_4w_2\beta(1-\tau) + \Delta + (1-\tau)\beta + \beta + k + 3\delta + \mu + \frac{\rho_1^2+\rho_2^2+\rho_4^2}{2} - \delta S, \\
\leq & \mathbf{E} - \frac{\delta}{\varepsilon_2} < 0.
\end{aligned}$$

Case 6. let $X \in U_6$

$$\begin{aligned}
L\chi(X) \leq & -4w_4\Delta\left[(R_0^s)^{\frac{1}{4}} - 1\right] + \frac{w_4w_1\beta I}{N} + \frac{w_4w_2(1-\tau)\beta I}{N} - \frac{w_4w_3\beta S}{N} + \Delta - \delta N \\
& - \frac{\Delta}{S} - \frac{\alpha I}{R} + \frac{\beta I}{N} - \frac{\mu R}{S} + \frac{\rho_1^2}{2} + k + 2\delta + \mu + \frac{\rho_4^2}{2} - \frac{kS}{V} + \frac{(1-\tau)\beta I}{N} + \delta + \frac{\rho_2^2}{2}, \\
\leq & w_4w_1\beta + w_4w_2\beta(1-\tau) + \Delta + (1-\tau)\beta + \beta + k + 3\delta + \mu + \frac{\rho_1^2+\rho_2^2+\rho_4^2}{2} - \delta V, \\
\leq & \mathbf{E} - \frac{\delta}{\varepsilon_4} < 0.
\end{aligned}$$

Case 7. let $X \in U_7$

$$\begin{aligned}
L\chi(X) \leq & -4w_4\Delta\left[(R_0^s)^{\frac{1}{4}} - 1\right] + \frac{w_4w_1\beta I}{N} + \frac{w_4w_2(1-\tau)\beta I}{N} - \frac{w_4w_3\beta S}{N} + \Delta - \delta N \\
& - \frac{\Delta}{S} - \frac{\alpha I}{R} + \frac{\beta I}{N} - \frac{\mu R}{S} + \frac{\rho_1^2}{2} + k + 2\delta + \mu + \frac{\rho_4^2}{2} - \frac{kS}{V} + \frac{(1-\tau)\beta I}{N} + \delta + \frac{\rho_2^2}{2}, \\
\leq & w_4w_1\beta + w_4w_2\beta(1-\tau) + \Delta + (1-\tau)\beta + \beta + k + 3\delta + \mu + \frac{\rho_1^2+\rho_2^2+\rho_4^2}{2} - \delta I, \\
\leq & \mathbf{E} - \frac{\delta}{\varepsilon_6} < 0.
\end{aligned}$$

Case 8. let $X \in U_8$

$$\begin{aligned}
L\chi(X) \leq & -4w_4\Delta\left[(R_0^s)^{\frac{1}{4}} - 1\right] + \frac{w_4w_1\beta I}{N} + \frac{w_4w_2(1-\tau)\beta I}{N} - \frac{w_4w_3\beta S}{N} + \Delta - \delta N \\
& - \frac{\Delta}{S} - \frac{\alpha I}{R} + \frac{\beta I}{N} - \frac{\mu R}{S} + \frac{\rho_1^2}{2} + k + 2\delta + \mu + \frac{\rho_4^2}{2} - \frac{kS}{V} + \frac{(1-\tau)\beta I}{N} + \delta + \frac{\rho_2^2}{2}, \\
\leq & w_4w_1\beta + w_4w_2\beta(1-\tau) + \Delta + (1-\tau)\beta + \beta + k + 3\delta + \mu + \frac{\rho_1^2+\rho_2^2+\rho_4^2}{2} - \delta R, \\
\leq & \mathbf{E} - \frac{\delta}{\varepsilon_8} < 0.
\end{aligned}$$

According to the above $L\chi < 0$ for all $X \in \mathbb{R}_+^4 \setminus U$ therefor, the condition (b) is satisfied.

Next, we present condition (a). The diffusion matrix corresponding to problem 3.1 is given by:

$$\begin{bmatrix}
\rho_1^2S^2 & 0 & 0 & 0 \\
0 & \rho_2^2V^2 & 0 & 0 \\
0 & 0 & \rho_3^2I^2 & 0 \\
0 & 0 & 0 & \rho_4^2R^2
\end{bmatrix},$$

and

$$\sum_{i,j=1}^{4} a_{ij}(X)\Theta_i\Theta_j = \rho_1^2 S^2\Theta_1^2 + \rho_2^2 V^2\Theta_2^2 + \rho_3^2 I^2\Theta_3^2 + \rho_4^2 R^2\Theta_4^2,$$

$$\geq m|\Theta|^2 \quad \text{for all} \quad X \in U,\ \Theta \in \mathbb{R}_+^4,$$

where $m = \min\{\rho_1^2 S^2, \rho_2^2 V^2, \rho_3^2 I^2, \rho_4^2 R^2\}$, hence, the condition (a) is verified.
Thus, the model (2.11) has a unique ergodic stationary distribution $\pi(\cdot)$. □

3.3 Formulation of stochastic optimal control

This section focuses on identifying optimal intervention strategies to minimize the spread of the disease using mathematical optimization techniques. The primary objective is to determine control measures that effectively reduce the overall impact of the epidemic while accounting for practical constraints. One widely used approach for achieving this is optimal control theory, which provides a systematic framework for designing and evaluating intervention strategies. To this end, the epidemic model is first formulated, and control variables are introduced to represent various possible interventions aimed at curbing disease transmission. These control variables may include measures such as social distancing, vaccination, quarantine, and treatment.
In this study, we introduce two control variables, $c_1(t)$ and $c_2(t)$, to analyze the proposed models (3.1) and (3.2).

- The control variable $c_1(t)$ represent COVID-19 time-dependent vaccine.
- The control variable $c_2(t)$ shows the time-dependent treatment effects.

Our objective is to reduce susceptible and infected persons and to maximize recovered persons at the lowest cost of control variants.

3.3.1 Analysis of deterministic optimal control problem

In this section, we proposed a control scheme that is deemed optimal if it minimizes the cost function

$$J_1(c_1,c_2) = \int_0^{T_e} \left[a_1 S + a_2 I + \frac{1}{2}(p_1 c_1^2(t) + p_2 c_2^2(t))\right] dt, \tag{3.7}$$

s.t.

$$\begin{aligned} dS(t) &= \Big[-(kc_1(t)+\delta)S(t) + \Delta - \beta\frac{S(t)I(t)}{N} + \mu R(t)\Big]dt, \\ dV(t) &= \Big[-(1-\tau)\beta\frac{V(t)I(t)}{N} + kc_1(t)S(t) - \delta V(t)\Big]dt, \\ dI(t) &= \Big[-(\alpha c_2+\delta+\delta_0)I(t) + \beta\frac{S(t)I(t)}{N} + \beta(1-\tau)\frac{V(t)I(t)}{N}\Big]dt, \\ dR(t) &= \Big[-(\delta+\mu)R(t) + \alpha c_2(t)I(t)\Big]dt, \end{aligned} \tag{3.8}$$

with

$$S(0) = S_0 > 0, I(0) = I_0 \geq 0, V(0) = V_0 \geq 0, R(0) = R_0 > 0. \tag{3.9}$$

In the cost function (3.7), the positive constants a_1 and a_2 serve as weighting factors to balance the sizes of the susceptible and infected populations, respectively. The positive coefficients p_1 and p_2 represent the costs associated with vaccination and treatment, and T_e denotes the final time. Based on the structure of cost function (3.7), our primary objective is to minimize both the number of susceptible and infected individuals, as well as the control costs c_1 and c_2. Therefore, we aim to determine the optimal control variables $(c_1^*, c_2^*) \in \Omega$ such that:

$$J_1(c_1^*,c_2^*) = \min_{\Omega} J_1(c_1,c_2), \tag{3.10}$$

subject to the system (3.8) with (3.9), where Ω is control admissible set

$$\Omega := \Big\{(c_1,c_2)|\ \ c_j : [0,T_e] \to [0,1] \text{ Lebesgue measurable, } j = 1,2.\Big\}.$$

Existence of optimal control problem

In what follows, we show that there is a solution of problem (3.7)-(3.9), and then we show the existence of optimal control variables.

The control variables c_1, c_2 are positive bounded Lebesgue mesurable and with positivity of initial value, positive bounded solution

Let

$$Z_t = AZ + G(Z)$$

where

$$Z = \begin{bmatrix} S(t) \\ V(t) \\ I(t) \\ R(t), \end{bmatrix}; \quad A = \begin{bmatrix} -(kc_1(t)+\delta) & 0 & 0 & \mu \\ kc_1(t) & -\delta & 0 & 0 \\ 0 & 0 & -(\alpha c_2(t)+\delta+\delta_0) & 0 \\ 0 & 0 & \alpha c_2(t) & -(\delta+\mu) \end{bmatrix};$$

$$G(Z) = \begin{bmatrix} \Delta - \beta\frac{S(t)I(t)}{N} \\ -\beta(1-\tau)\frac{V(t)I(t)}{N} \\ \beta\frac{S(t)I(t)}{N} + \beta(1-\tau)\frac{V(t)I(t)}{N} \\ 0 \end{bmatrix}.$$

$$\begin{aligned} G(Z_1) - G(Z_2) &\leq b_1|S_1 - S_2| + b_2|V_1 - V_2| + b_3|I_1 - I_2| + b_4|R_1 - R_2| \\ &\leq b\Big[|S_1 - S_2| + |V_1 - V_2| + |I_1 - I_2| + |R_1 - R_2|\Big], \end{aligned}$$

were $b = \max\{b_1,b_2,b_3,b_4\}$ is a positive constant which is independent of the state variables of the model.

$$|F(Z_1) - F(Z_2)| \leq 2M|Z_1 - Z_2|,$$

and $M = \max\{b,\|A\|\} < \infty$, then F is uniformly Lipshitz continuous. Since the control and state parameters are clearly positive, we conclude that a solution to system (3.8) exists.
Next, we establish the result that guarantees the existence of an optimal control that minimizes the cost function.

Theorem 3.6. *There is a control variable $c^* = (c_1^*,c_2^*) \in \Omega$ satisfying*

$$J_1(c_1^*,c_2^*) = \min_{\Omega} J_1(c_1,c_2), \quad \forall (S_0,V_0,I_0,R_0) \in \mathbb{R}_+^4.$$

Proof. To obtain the necessary result, we must verify that the conditions of Corollary (4.1) in [31] are satisfied.

- The set of admissible control and corresponding state variables is nonempty, because the solution of system exist.
- The set Ω is closed and convex and therefore, by definition Ω is closed. Let $u_1, u_2 \in \Omega$ and $0 \leq \lambda \leq 1$ such that $u_1 = (c_1,c_2)$ and $u_2 = (c_1',c_2')$. Hence, $\lambda u_1 + (1-\lambda)u_2 = (\lambda c_1 + (1-\lambda)c_1', \lambda c_2 + (1-\lambda)c_2') \in \Omega$. Thus Ω is convex.
- The optimal control system is bounded by a linear function of the state and control variables. In our case, the system is linear with respect to c_1 and c_2. Moreover, the solution is absolutely continuous, which implies that it remains bounded. Therefore, the required condition is satisfied.

- The integrand $\mathcal{L}_1$ of the cost function is strictly convex on Ω, since the Hessian matrix of $\mathcal{L}_1$ on Ω is given by

$$\begin{bmatrix} p_1 & 0 \\ 0 & p_2 \end{bmatrix},$$

is definite positive.

- There exist $m_1 > 0, m_2 > 0$ and $m_3 > 1$ such that

$$\mathcal{L}_1(c_1,c_2) \geq m_1|(c_1,c_2)|^{m_3} - m_2.$$

$$\begin{aligned} \mathcal{L}_1(c_1,c_2) &= a_1S + a_2I + \frac{1}{2}(p_1c_1^2(t) + p_2c_2^2(t), \\ &\geq \frac{1}{2}min\{p_1,p_2\}(c_1^2(t) + c_2^2(t)), \\ &\geq \frac{1}{2}min\{p_1,p_2\}(c_1^2(t) + c_2^2(t)) - 1, \\ &= \frac{1}{2}min\{p_1,p_2\}|(c_1,c_2)|^2 - 1. \end{aligned}$$

Let $m_1 = \frac{1}{2}min\{p_1,p_2\}$, $m_2 = 1$ and $m_3 = 2$.

Therefore, the above conditions ensure the existence of the optimal control (c_1^*, c_2^*). □

3.3.2 Characterization of an optimal control

This section explores the necessary optimality conditions and the characterization of the optimal control for our problem, using PMP 2.8. This principle shifts the problem (3.7)-(3.9) into a problem of minimizing point-wise a Hamiltonian $\mathcal{H}_1$ corresponds to the controls c_1, c_2. We define the Lagrangian $\mathcal{L}_1$ associated to the control problem (3.8)

$$\mathcal{L}_1(S,I,c_1,c_2) = a_1S + a_2I + \frac{1}{2}(b_1c_1^2(t) + b_2c_2^2(t)),$$

and the Hamiltonian function $\mathcal{H}_1$ is given by

$$\mathcal{H}_1(z,c,\gamma) = \gamma.\varphi(z,c) + \mathcal{L}_1(z,c),$$

where

$$z = (S,V,I,R),\ \gamma = (\gamma_1,\ \gamma_2,\gamma_3,\gamma_4),\ c = (c_1,c_2),\ \varphi = (\varphi_1,\varphi_2,\varphi_3,\varphi_4).$$

$$\begin{aligned} \varphi_1(z,c) &= \Delta - \beta\frac{S(t)I(t)}{N} + \mu R(t) - (kc_1(t) + \delta)S(t), \\ \varphi_2(z,c) &= kc_1(t)S(t) - (1-\tau)\beta\frac{V(t)I(t)}{N} - \delta V(t), \\ \varphi_3(z,c) &= \frac{S(t)I(t)}{N} + (1-\tau)\beta\frac{V(t)I(t)}{N} - (\alpha c_2 + \delta + \delta_0)I(t), \\ \varphi_4(z,c) &= \alpha c_2(t)I(t) - (\delta + \mu)R(t). \end{aligned}$$

So the Hamiltonian will have this forme

$$\begin{aligned}\mathcal{H}_1(z,c,\gamma) =& a_1 S + a_2 I + \frac{1}{2}(b_1 c_1^2(t) + b_2 c_2^2(t)) \\ &+ \gamma_1\big[\Delta - \beta\frac{S(t)I(t)}{N} + \mu R(t) - (kc_1(t) + \delta)S(t)\big] \\ &+ \gamma_2\big[kc_1(t)S(t) - (1-\tau)\beta\frac{V(t)I(t)}{N} - \delta V(t)\big] \\ &+ \gamma_3\big[\frac{S(t)I(t)}{N} + (1-\tau)\beta\frac{V(t)I(t)}{N} - (\alpha c_2 + \delta + \delta_0)I(t)\big] \\ &+ \gamma_4\big[\alpha c_2(t)I(t) - (\delta+\mu)R(t)\big].\end{aligned}$$

To find the characterization of $(c_1^*(t),c_2^*(t))$, we apply PMP wick states that if $(z^\star,c^\star)$ be an optimality solution of our control system, we can determine a non-trivial vector say γ such that

$$\begin{aligned}\frac{d\gamma(t)}{dt} &= -\frac{\partial \mathcal{H}_1}{\partial z}(z^\star(t),c^\star(t),\gamma(t)), \\ 0 &= \frac{\partial \mathcal{H}_1}{dc}(z^\star(t),c^\star(t),\gamma(t)),\end{aligned} \tag{3.11}$$

with

$$\gamma(T_e) = 0, \tag{3.12}$$

and

$$\mathcal{H}_1(z^\star(t),c^\star(t),\gamma(t)) = \min_{c\in\Omega}\mathcal{H}_1(z^\star(t),c(t),\gamma(t)). \tag{3.13}$$

Theorem 3.7. *Let $(S^\star V^\star I^\star R^\star)$ be the optimal solution associated to the optimal control $c_1^\star, c_2^\star$ of our problem, then $\exists\ \gamma_j(t) \neq 0$, for $j = 1...4$ that satisfies the following*

$$\begin{aligned}\gamma_1' &= \beta\frac{I}{N}\gamma_1 + kc_1\gamma_1 - a_1, \\ \gamma_2' &= (1-\tau)\beta\frac{I}{N}\gamma_2 + \delta\gamma_2, \\ \gamma_3' &= -\beta\frac{S}{N}\gamma_3 + (\tau-1)\beta\frac{V}{N}\gamma_3 + (\alpha c_2 + \delta + \delta_0)\gamma_3 - a_2, \\ \gamma_4' &= (\delta+\mu)\gamma_4,\end{aligned} \tag{3.14}$$

with

$$\gamma_j(T_e) = 0, \quad j = 1,...4, \tag{3.15}$$

and

$$\begin{aligned}c_1^* &= \min\Big\{\max\Big\{\frac{kS(\gamma_1-\gamma_2)}{a_3},0\Big\},1\Big\}, \\ c_2^* &= \min\Big\{\max\Big\{\frac{\alpha I(\gamma_3-\gamma_4)}{a_4},0\Big\},1\Big\}.\end{aligned} \tag{3.16}$$

Proof. Applying the adjoint system (3.11) of the PMP, it gives us the system (3.14), and the condition (3.15) is a direct result of terminal condition (3.12).
To obtain the formula of optimal control $c_1^\star$,$c_2^\star$ which is given by (3.16), we solve the following system

$$\begin{aligned}\frac{d\mathcal{H}_1}{dc_1} &= kS(\gamma_2-\gamma_1)+a_3c_1=0,\\ \frac{d\mathcal{H}_1}{dc_2} &= \alpha I(\gamma_4-\gamma_3)+a_4c_2=0.\end{aligned}$$

By considering the lower and upper limit of the controls. Thus, we obtain the result (3.16) □

Next, we will explore the control theory for the stochastic version of problem (3.2), applying the same intervention measures as previously described.

3.3.3 Stochastic optimal control strategy

In this section, we formulate and analyze the stochastic control version of model (3.1), using the same control function. The resulting stochastic control system is given as follows:

$$\begin{aligned}dS(t) &= \Big[\Delta-\beta\frac{S(t)I(t)}{N}+\mu R(t)-(kc_1(t)+\delta)S(t)\Big]dt+\rho_1S(t)dW_1(t),\\ dV(t) &= \Big[kc_1(t)S(t)-(1-\tau)\beta\frac{V(t)I(t)}{N}-\delta V(t)\Big]dt+\rho_2V(t)dW_2(t),\\ dI(t) &= \Big[\beta\frac{S(t)I(t)}{N}+(1-\tau)\beta\frac{V(t)I(t)}{N}-(\alpha c_2+\delta+\delta_0)I(t)\Big]dt+\rho_3I(t)dW_3(t),\\ dR(t) &= \Big[\alpha c_2(t)I(t)-(\delta+\mu)R(t)\Big]dt+\rho_4R(t)dW_4(t).\end{aligned} \tag{3.17}$$

To simplify writhen, we put

$$z(t)=(S(t),V(t),I(t),R(t)),\quad c=(c_1,c_2),\quad h=(h_1,h_2,h_3,h_4),\quad \sigma=(\sigma_1,\sigma_2,\sigma_3,\sigma_4),$$

then system (3.17) become

$$dz(t)=h(z,c)dt+\sigma(z)dW(t),$$

where

$$\begin{aligned}h_1(z(t),c(t)) &= \Delta-\beta\frac{S(t)I(t)}{N}+\mu R(t)-(kc_1(t)+\delta)S(t),\\ h_2(z(t),c(t)) &= kc_1(t)S(t)-(1-\tau)\beta\frac{V(t)I(t)}{N}-\delta V(t),\\ h_3(z(t),c(t)) &= \beta\frac{S(t)I(t)}{N}+(1-\tau)\beta\frac{V(t)I(t)}{N}-(\alpha c_2+\delta+\delta_0)I(t),\\ h_4(z(t),c(t)) &= \alpha c_2(t)I(t)-(\delta+\mu)R(t).\end{aligned}$$

And

$$\sigma_1 = \rho_1 S, \quad \sigma_2 = \rho_2 V, \quad \sigma_3 = \rho_3 I, \quad \sigma_4 = \rho_4 R.$$

The Cost function is given by

$$j_2(c) = \mathbb{E}\Big[\int_0^{T_e} \Big[a_1 S + a_2 I + \frac{1}{2}(a_3 c_1^2(t) + a_4 c_2^2(t))\Big] dt, + \frac{p_1}{2} S^2(T_e) + \frac{p_2}{2} V^2(T_e) + \frac{p_3}{2} I^2(T_e) + \frac{p_4}{2} R^2(T_e)\Big],$$

where $a_i, p_i \quad i = 1,...,4$ are non-negative real numbers.

Our objective is to determine optimal control $c^\star = (c_1^\star, c_2^\star)$, such that

$$j_2(c^\star) = \min_{c \in \Omega^*} j_2(c),$$

where

$$\Omega^* = \big\{c_j(t) : \quad c_j(t) \in [0, c_j^{max}], \forall c_j \in L^2[0, T_e], \quad j = 1,2\big\}.$$

We define the Hamiltonian function

$$\mathcal{H}_2(z, c, v, \eta) = \langle h(z, c), v\rangle + \langle \sigma(z), \eta\rangle + \mathcal{L}_2(z, c),$$

where $\langle .,. \rangle$ represent the inner product in Euclidean space and $v = (v_1, v_2, v_3, v_4)$ and $\eta = (\eta_1, \eta_2, \eta_3, \eta_4)$ represent the vectors adjoint respectively.

Then

$$\begin{aligned}
\mathcal{H}_2 =& a_1 S + a_2 I + \frac{1}{2}(a_3 c_1^2 + a_4 c_2^2) + v_1(\Delta - \beta \frac{SI}{N} + \mu R - (kc_1 + \delta) S) \\
&+ v_2(kc_1 S - (1 - \tau)\beta \frac{VI}{N} - \delta V) \\
&+ v_3(\beta \frac{SI}{N} + (1 - \tau)\beta \frac{VI}{N} - (\alpha c_2 + \delta + \delta_0) I) \\
&+ v_4(\alpha c_2 I - (\delta + \mu) R) + \eta_1 \rho_1 S + \eta_2 \rho_2 V + \eta_3 \rho_3 I + \eta_4 \rho_4 R.
\end{aligned}$$

The stochastic maximum principle ensures that the following condition is met:

$$\begin{aligned}
dz^\star(t) &= \frac{\partial \mathcal{H}_2(z^\star(t), c^\star(t), v, \eta)}{\partial v} dt + \sigma(z^\star) dW(t), \\
dv(t) &= -\frac{\partial \mathcal{H}_2(z^\star(t), c^\star(t), v, \eta)}{\partial z} dt + \eta dW(t), \\
\mathcal{H}_2(z^\star(t), c^\star(t), v, \eta) &= \min_{c \in \Omega^*} \mathcal{H}_2(z^\star(t), c(t), v, \eta),
\end{aligned}$$

with

$$z^\star(0) = (S_0, V_0, I_0, R_0), \quad v(T_e) = -\frac{\partial \theta(z(T_e))}{\partial z},$$

where

$$\theta = \frac{p_1}{2} S^2(T_e) + \frac{p_2}{2} V^2(T_e) + \frac{p_3}{2} I^2(T_e) + \frac{p_4}{2} R^2(T_e),$$

and $z^*(t)$ is the optimal trajectory of $z(t)$.

Theorem 3.8. *Our control problem has an OC as the following form*

$$(c_1^\star,c_2^\star) = \Big(\min\Big\{\max\Big\{\frac{kS(v_1-v_2)}{a_3},0\Big\},c_1^{max}\Big\}, \min\Big\{\max\Big\{\frac{\alpha I(v_3-v_4)}{a_4},0\Big\},c_2^{max}\Big\}\Big).$$

Proof. Applying the stochastic minimum principle, we get the adjoint system

$$\begin{aligned}
dv_1(t) &= (-a_1 + (v_1-v_3)\beta\frac{I(t)}{N} + (v_1-v_2)kc_1(t) + v_1\delta + \eta_1\rho_1)dt + \eta_1 dW_1,\\
dv_2(t) &= ((v_2-v_3)(1-\tau)\beta\frac{I(t)}{N} + v_2\delta + \eta_2\rho_2)dt + \eta_2 dW_2,\\
dv_3(t) &= (-a_2 + (v_1-v_3)\beta\frac{s(t)}{N} + (v_3-v_4)(\alpha c_2) + v_3(\delta+\delta_0))dt + \eta_3 dW_3,\\
dv_4(t) &= (-v_1\mu + v_4(\delta+\mu) + \eta_4\rho_4)dt + \eta_4 dW_4,
\end{aligned}$$

with

$$v_1(T_e) = -p_1S(T_e), v_2(T_e) = -p_2V(T_e), v_3(T_e) = -p_3I(T_e), v_4(T_e) = -p_4R(T_e),$$

and we have

$$\begin{aligned}
\frac{d\mathcal{H}_2}{dc_1} &= kS(v_2-v_1) + a_3c_1 = 0,\\
\frac{d\mathcal{H}_2}{dc_2} &= \alpha I(v_4-v_3) + a_4c_2 = 0.
\end{aligned}$$

Then

$$\begin{aligned}
c_1^\star(t) &= \frac{kS^\star(t)(v_1(t)-v_2(t))}{a_3},\\
c_2^\star(t) &= \frac{\alpha I^\star(t)(v_3(t)-v_4(t))}{a_4}.
\end{aligned}$$

From the upper and lower bounds of c_1,c_2, we obtain

$$\begin{aligned}
c_1^\star(t) &= \min\Big\{\max\Big\{\frac{kS^\star(t)(v_1(t)-v_2(t))}{a_3},0\Big\},1\Big\},\\
c_2^\star(t) &= \min\Big\{\max\Big\{\frac{\alpha I^\star(t)(v_3(t)-v_4(t))}{a_4},0\Big\},1\Big\}.
\end{aligned}$$

□

3.4 Numerical Simulations

3.4.1 Parameter Estimation

In this part, we outline the procedure used to estimate the model parameters through the nonlinear least-squares methoda widely used statistical technique for parameter estimation in mathematical

modeling. This method minimizes the sum of squared differences between observed data and model predictions, thereby ensuring the best possible fit to the data. Nonlinear least squares is particularly effective in regression analysis and curve fitting. To ensure accurate parameter estimation, we used a combination of previously established values and real-world COVID-19 case data. Some parameters were directly taken from reference [38], while the remaining ones were estimated by fitting the model to reported COVID-19 cases in Algeria from October 22 to March 14, 2022. The data were obtained from source [123].

The estimated parameter values are presented in Table 3.2, and the corresponding fitted curve is shown in Figure 3.1.

Table 3.2: Parameter's value.

parameters	value in days	references
Δ	1534	[38]
k	0.0100	fitting
β	0.2918	fitting
τ	0.5038	fitting
μ	0.0001	fitting
δ_0	0.0579	fitting
δ	$1/(77.5 * 365)$	[38]
α	0.1175	fitting

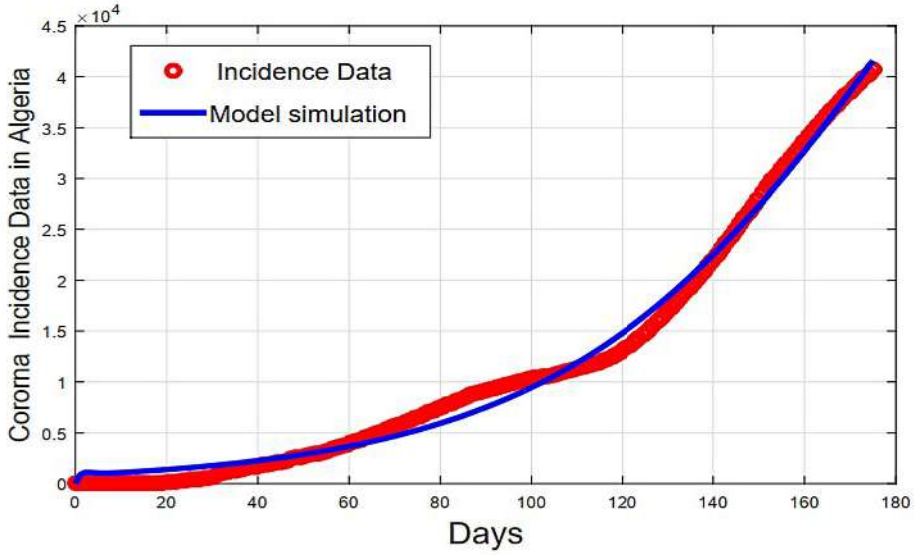

Figure 3.1: Cumulative COVID-19 case data in Algeria and corresponding predictions from the deterministic model.

3.4.2 Sensitivity analysis

Sensitivity analysis helps evaluate the impact of individual parameters on the behavior of the model, particularly by measuring how changes in parameter values affect the R_0 . This relationship is formulated as follows [100]:

$$\mathcal{S}_p = \frac{\partial R_0}{\partial p} . \frac{p}{R_0}.$$

We express the normalized sensitivity indices as follows:

$$\mathcal{S}_\beta = 1, \ \mathcal{S}_\alpha = \frac{-\alpha}{\alpha + \delta + \delta_0 + \frac{\eta_3^2}{2}}, \ \mathcal{S}_\delta = \frac{-\delta}{\alpha + \delta + \delta_0 + \frac{\eta_3^2}{2}}, \ \mathcal{S}_{\delta_0} = \frac{-\delta_0}{\alpha + \delta + \delta_0 + \frac{\eta_3^2}{2}},$$

$$\mathcal{S}_\tau = \frac{-\tau}{2 - \tau}, \ \mathcal{S}_{\rho_3} = \frac{-\rho_3^2}{\alpha + \delta + \delta_0 + \frac{\eta_3^2}{2}}.$$

As shown in Table 3.3 and Figure 3.2, model parameters with positive sensitivity indices indicate that increasing the corresponding parameter, while keeping the others constant, leads to an increase in the basic reproduction number R_0. This suggests that COVID-19 would spread more extensively within the population. In contrast, parameters with negative sensitivity indices are associated with a reduction in R_0, implying a decrease in the infection rate. Based on the sensitivity indices presented in Table 3.3, the most influential factor driving the spread of COVID-19 is the transmission rate β, which significantly contributes to the acceleration of disease transmission. On the other hand, the recovery rate α emerges as a key parameter in reducing disease prevalence. Therefore, to effectively control the spread of COVID-19, it is crucial to adopt strategies that aim to increase the recovery rate α while concurrently reducing the transmission rate β.

Table 3.3: The parameter sensitivity index of R_0.

Parameters	β	α	δ	δ_0	τ	ρ_3
Value	0.2918	0.1175	$1/(77.5 \times 365)$	0.0579	0.5038	0.3
Snsitivity index	1	-0.5330	-1.6037×10^{-4}	-0.2627	-0.3367	-0.4083

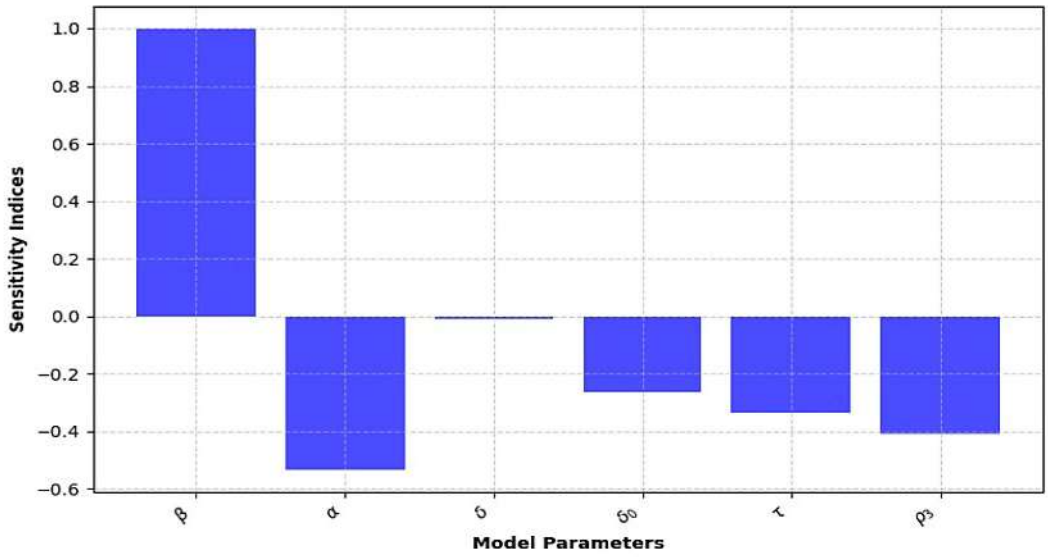

Figure 3.2: Results of the sensitivity analysis of R_0 for model (3.1).

3.4.3 Examples of numerical simulations

In order to validate the theoretical results, we carry out simulations using the stochastic **R-K4** method to discretize model (3.1), as shown below:

$$\begin{aligned}
S_{j+1} &= S_j + \left[\Delta - \beta\frac{S_jI_j}{N_j} + \mu R_j - (k+\delta)S_j\right]\Delta t + \rho_1 S_j\sqrt{\Delta t}B_{1_j} + \frac{\rho_1^2}{2}S_j(B_{1_j}-1)\Delta t,\\
V_{j+1} &= V_j + \left[kS_j - (1-\tau)\beta\frac{V_jI_j}{N_j} - \delta V_j\right]\Delta t + \rho_2 V_j\sqrt{\Delta t}B_{2_j} + \frac{\rho_2^2}{2}V_j(B_{2_j}-1)\Delta t,\\
I_{j+1} &= I_j + \left[\beta\frac{S_jI_j}{N_j} + (1-\tau)\beta\frac{V_jI_j}{N_j} - (\alpha+\delta+\delta_0)I_j\right]\Delta t + \rho_3 I_j\sqrt{\Delta t}B_{3_j} + \frac{\rho_3^2}{2}I_j(B_{3_j}-1)\Delta t,\\
R_{j+1} &= R_j + \left[\alpha I_j - (\delta+\mu)R_j\right]\Delta t + \rho_4 R_j\sqrt{\Delta t}B_{4_j} + \frac{\rho_4^2}{2}R_j(B_{4_j}-1)\Delta t,
\end{aligned} \tag{3.18}$$

where B_1, B_1, B_3 and B_4 are normally-distributed $\mathcal{N}(0,1)$ random variables and Δt is step size. Through several empirical examples, we aim to highlight the following key aspects:

- The qualitative behavior of system (3.1) when $R_0 < 1$.
- The existence of the stationary distribution for model (3.1) when $\bar{R}_0 > 1$.
- The influence of various control measures on the progression of COVID-19.

Numerical examples for extinction and stationary distribution

To verify extinction and the existence of a stationary distribution , we used the parameter values specified in the two examples. In Example 3.1, the chosen values are used to numerically illustrate Theorem 3.4, which states that the disease will almost surely die out if $R_0 < 1$. This is confirmed by Fig. 3.3, where the parameters satisfy the conditions of the theorem.
In Example 3.2, a different set of parameter values is used to demonstrate the outcome predicted by Theorem 3.5, where the condition $\bar{R}_0 > 1$ holds. The results are illustrated in Fig. 3.4.

Example 3.1. We assume that: $\Delta = 1530, k = 0.664$, $\beta = 0.451$, $\delta = 0.65$, $\mu = 0.01$, $\tau = 0.576, \alpha = 0.791$, $\delta_0 = 0.795$, $\rho_1 = 0.2, \rho_2 = 0.1, \rho_3 = 0.3, \rho_4 = 0.2$, and initial values $S(0) = 500, V(0) = 50, I(0) = 30, R(0) = 0$, we get $R_0 < 1$, then the epidemic will be extinct from the population.

Example 3.2. Let us take another parameter's values : $\Delta = 1530, k = 0.664$, $\beta = 0.451, \delta_0 = 0.127$, $\tau = 0.057$, $\alpha = 0.179$ $\mu = 0.01$, $\delta = 0.65$, and we reduce the noise intensity values: $\rho_1 = 0.1, \rho_2 = 0.1, \rho_3 = 0.1, \rho_4 = 0.1$, and the same initial values of example 3.1. Using these parameter values, we find that $\bar{R}_0 > 1$. According to Theorem 3.5, this implies that model (3.1) admits a unique stationary distribution. Biologically, this indicates that the disease will persist in the population and will not be eradicated naturally under the given conditions.

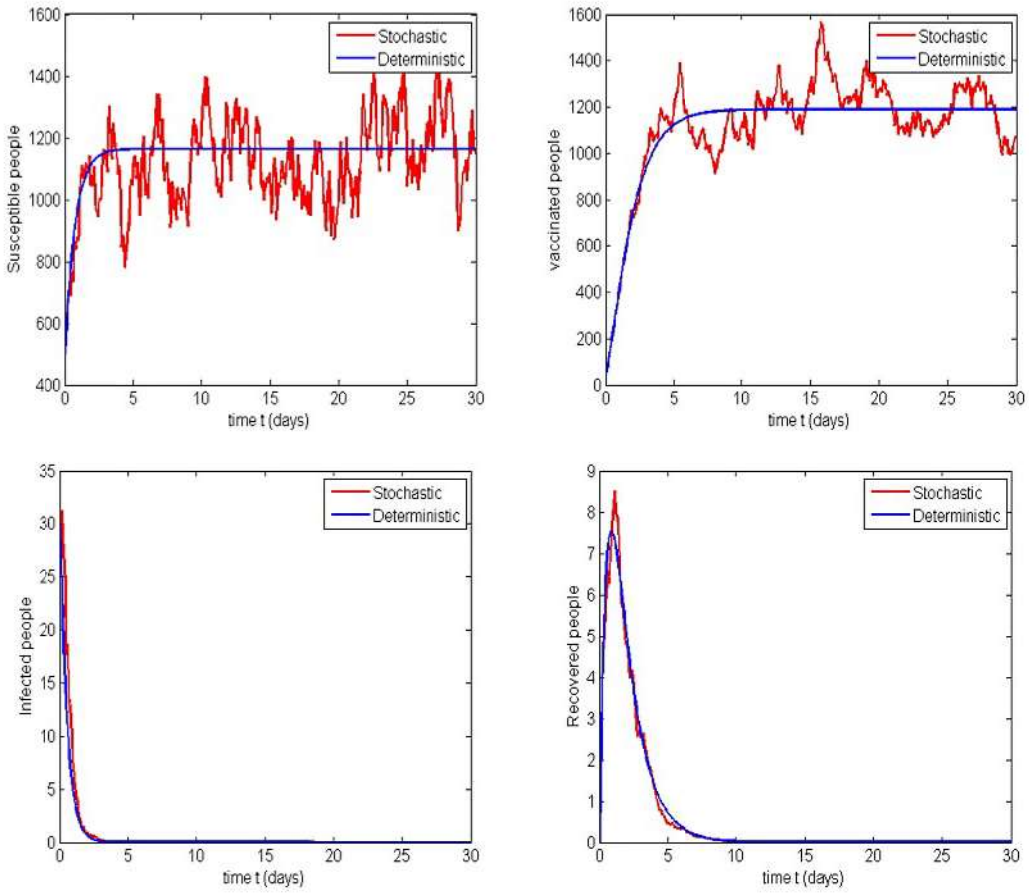

Figure 3.3: Comparative trajectories of the deterministic model (3.2) and stochastic model (3.1) based on the parameter values from Example 3.1.

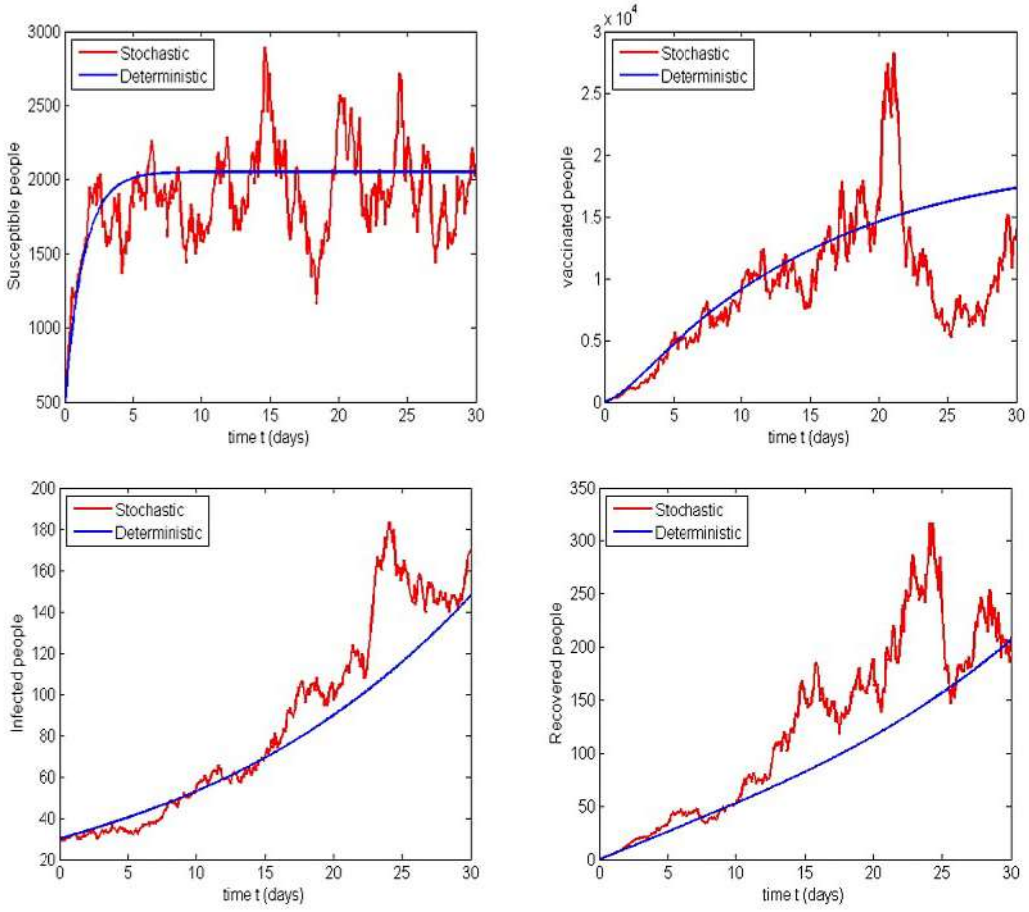

Figure 3.4: Comparative trajectories of the deterministic model (3.2) and stochastic model (3.1) based on the parameter values from Example 3.2.

By combining theoretical analysis with numerical simulations, we found that when $\bar{R}_0 > 1$, a smaller intensity of white noise allows model (3.1) to admit a unique ergodic stationary distribution. In contrast, when $R_0 < 1$, a higher level of white noise can lead to disease extinction. Compared to the deterministic model, the incorporation of white noise introduces significant effects on disease persistence and extinction, thereby enhancing the dynamic complexity and realism of the epidemic model.

Numerical example on control strategies of COVID-19

In this section, we present the theoretical results obtained by applying optimal control theory to our model. To solve the control problem numerically, we employ the R-K4 method. Specifically, we discretize the state equations, the associated adjoint systems, and the control variables, incorporating both the control characterizations and the necessary subsidiary conditions.

The parameters listed in Table 3.2 were used to perform simulations both with and without the

implementation of control measures. The corresponding results are presented in Figures 3.5 and 3.6.

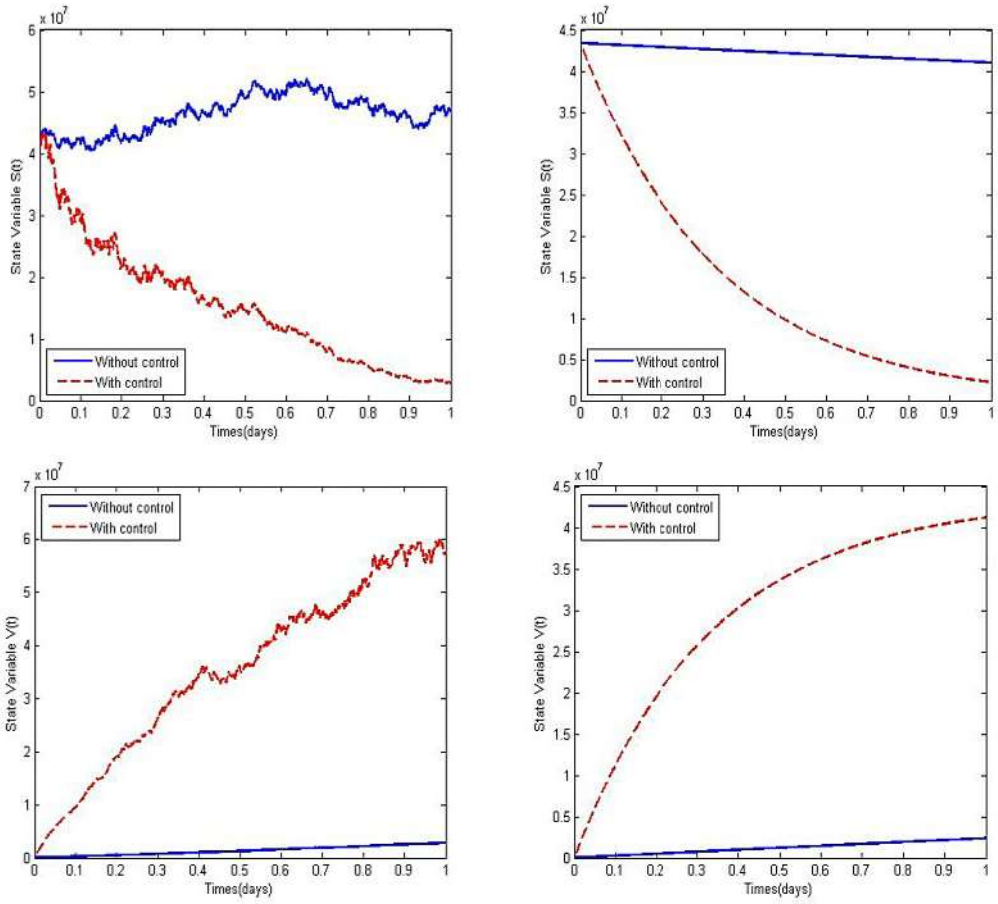

Figure 3.5: Comparative simulations of deterministic and stochastic models showing the evolution of S and V compartments, under scenarios with and without optimal control.

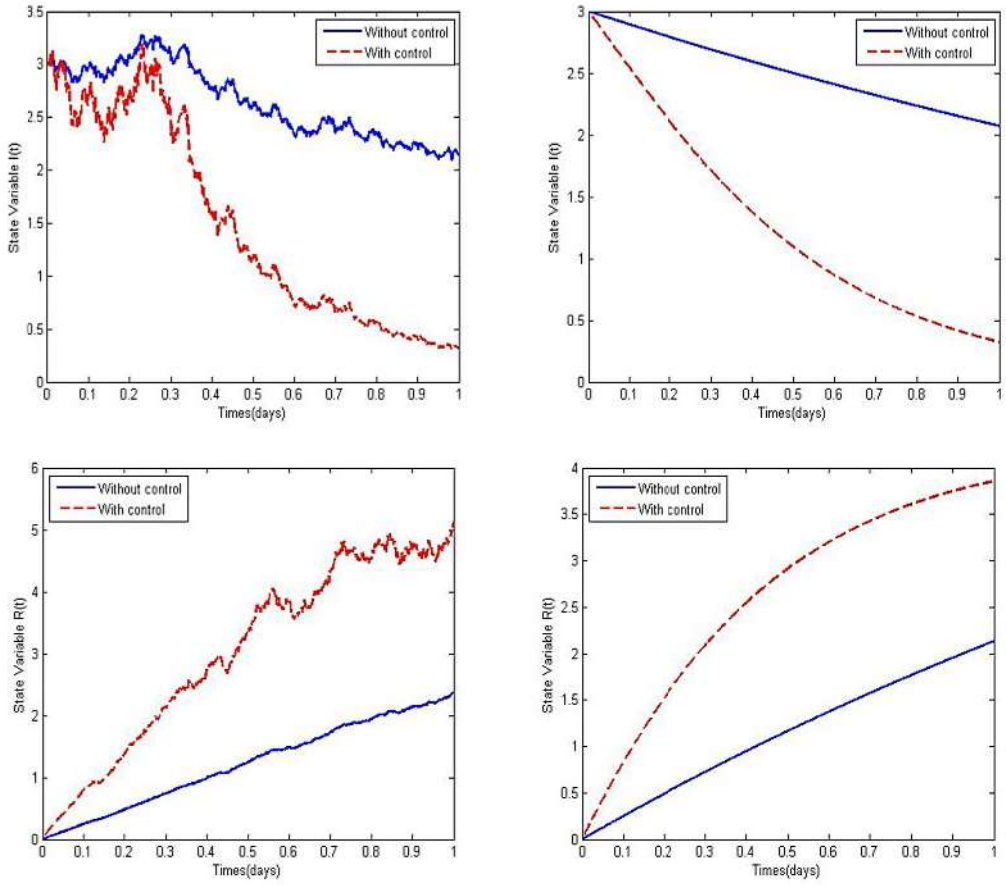

Figure 3.6: Analysis of deterministic versus stochastic simulations of I and R trajectories, under scenarios with and without optimal control.

Figures 3.5 and 3.6 present simulations of the deterministic and stochastic models that describe the dynamics of the S, V, I, and R compartments, respectively, under scenarios both with and without optimal control strategies (c_1^* and c_2^*). The inclusion of vaccination and treatment controls results in a noticeable decrease in the S and I populations, accompanied by an increase in the V and R groups. This outcome reflects the effect of vaccination in transferring individuals from the susceptible to the vaccinated class. At the same time, treatment accelerates recovery, thereby reducing the number of infected individuals and increasing the recovered population.
Based on the obtained results, it is evident that both treatment and vaccination controls play critical roles in shaping public health strategies for mitigating the impact of COVID-19. Treatment controlwhich includes the use of antiviral medications and supportive carehelps to reduce disease severity and shorten recovery time, thereby alleviating the burden on healthcare systems. Vaccination control, in turn, reduces the number of S, lowers transmission rates, and prevents severe cases, thereby contributing to herd immunity and promoting long-term epidemic control.

Effective public health policy must integrate both strategies: promoting widespread vaccination coverage while ensuring access to timely and effective treatment, especially in the face of emerging variants and for the protection of high-risk populations. A well-balanced approach combining vaccination and treatment is essential for sustainable epidemic management and preparedness for future pandemics.

3.5 Conclusion

This chapter presents a comprehensive mathematical framework for the optimal control of COVID-19 in a stochastic setting, utilizing a robust computational modeling approach. By incorporating stochastic dynamics, empirical data, and advanced optimization techniques, the proposed methodology provides a powerful tool for modeling, analyzing, and mitigating the spread of COVID-19. The stochastic model is rigorously examined from a theoretical perspective, and the analytical results are validated through numerical simulations based on estimated parameters. Furthermore, a stochastic optimal control model is developed by introducing time-dependent control variables to facilitate effective mitigation strategies for future outbreaks. The necessary conditions for optimality and the corresponding solutions of the stochastic control system are derived and discussed in detail. The insights obtained from this study offer significant value to policymakers and public health authorities, enabling the formulation of data-driven strategies to limit virus transmission, protect public health, and enhance societal resilience.

Chapter 4

On the dynamic behavior of a novel stochastic **HBV** model with logistic growth and saturated incidence

This chapter focuses on how a new Hepatitis B virus (**HBV**) model behaves over a long period of time. We show that the model is well-defined by proving that there is a solution that exists globally and is positive. We have found conditions that are enough for extinction and the presence of a unique stationary distribution. Finally, we conducted numerical simulation to back up our findings.

4.1 Introduction

Hepatitis B is a global health concern, affecting a substantial portion of the population worldwide. According to the **WHO**, over two billion people have been infected with the **HBV** at some point in their lives. Among them, 350 million suffer from chronic, lifelong infections [122]. An estimated 25-40% of those with chronic **HBV** may eventually develop serious liver conditions, including cirrhosis or primary hepatocellular carcinoma [91]. **HBV** carrier rates vary significantly worldwide, ranging from 0.1% to 20% in different regions [64]. Chronic **HBV** infection is more likely to develop when initial exposure to the virus occurs at a young age, often due to insufficient immune response to clear the virus [89]. **HBV** is extremely infectious, spreading through contact with blood or bodily fluids, and is 50-100 times more transmissible than **HIV**. While **HBV** can be managed with therapies like interferon or lamivudine, these treatments are costly and often out of reach in low-income areas where the virus is most widespread. Understanding **HBV** and

its mechanisms is essential for developing affordable vaccines and treatments for the countries most affected by this virus. Mathematical modeling of **HBV** dynamics plays a crucial role in understanding the infection, immune response, and treatment strategies. It offers insights into virus-host interactions, the effectiveness of antiviral drugs, and the possible outcomes of both chronic and acute infections. Many of models have been proposed to comprehend the dynamics of **HBV** [42, 68, 88, 90, 108, 112, 124]. In the study of virus infection dynamics, the basic virus infection model (**BVIM**), which was first presented by Nowak et al. in [90, 91], is one of the most used models. The **BVIM** is expressed as

$$\begin{aligned} \mathcal{H}' &= \Gamma - \mu_0 \mathcal{H} - \beta \mathcal{V} \mathcal{H}, \\ \mathcal{I}' &= -\mu_1 \mathcal{I} + \beta \mathcal{V} \mathcal{H}, \\ \mathcal{V}' &= -\mu_2 \mathcal{V} + \varphi \mathcal{I}, \end{aligned} \tag{4.1}$$

where $\mathcal{H}$ is uninfected cells, $\mathcal{I}$ is infected cells and free virus $\mathcal{V}$, the parameters are shown in table 4.1.

In [88], Min et al. extended the model (4.1) to include a standard incidence function and get the following amended basic **HBV** virus model

$$\begin{aligned} \mathcal{H}' &= \Gamma - \frac{\beta \mathcal{V} \mathcal{H}}{\mathcal{I} + \mathcal{H}} - \mu_0 \mathcal{H}, \\ \mathcal{I}' &= -\mu_1 \mathcal{I} + \frac{\beta \mathcal{V} \mathcal{H}}{\mathcal{I} + \mathcal{H}}, \\ \mathcal{V}' &= \varphi \mathcal{I} - \mu_2 \mathcal{V}. \end{aligned} \tag{4.2}$$

Drawing on the finding in [91] and accounting for the regenerative capacity of hypatocytes, Lie et al. [68] devloped a **HBV** model incorporating logistic growth as follows

$$\begin{aligned} \mathcal{H}' &= \eta_1 \mathcal{H}\big(1 - \frac{\mathcal{H} + \mathcal{I}}{N}\big) - \mu_0 \mathcal{H} - \beta \mathcal{V} \mathcal{H}, \\ \mathcal{I}' &= -\mu_1 \mathcal{I} + \beta \mathcal{V} \mathcal{H}, \\ \mathcal{V}' &= \varphi \mathcal{I} - \mu_2 \mathcal{V}. \end{aligned} \tag{4.3}$$

Furthermore, as suggested in [112], patial differential equation **HBV** model was devloped and examined in [108] by assuming logistic proliferation for both infected and uninfected hepatocytes and use the standard incidence function. In particular,

$$\begin{aligned} \frac{\partial \mathcal{H}}{\partial t} &= \Gamma - \mu_0 \mathcal{H}(t) + \eta_1 \mathcal{H}\big(1 - \frac{\mathcal{I} + \mathcal{H}}{N}\big) - \frac{\beta \mathcal{H} \mathcal{V}}{\mathcal{I} + \mathcal{H}}, \\ \frac{\partial \mathcal{I}}{\partial t} &= -\mu_1 \mathcal{I} + \frac{\beta \mathcal{H} \mathcal{V}}{\mathcal{H} + \mathcal{I}} + \eta_2 \mathcal{I}\big(1 - \frac{\mathcal{H} + \mathcal{I}}{N}\big), \\ \frac{\partial \mathcal{V}}{\partial t} &= \Delta \mathcal{V}(t,x) + \varphi \mathcal{I} - \mu_2 \mathcal{V} - \frac{\beta \delta \mathcal{H} \mathcal{V}}{\mathcal{H} + \mathcal{I}}. \end{aligned} \tag{4.4}$$

In most viral infection models, the infection rate is typically assumed to be bilinear, depending on both the concentration of free virus $\mathcal{V}$ and uninfected cells $\mathcal{H}$. However, experiments reported introduced in [28] have demonstrated that, for microparasitic infections, the infection rate increases with the dose of the parasite and generally exhibits a sigmoidal pattern. Therefore, it is reasonable to model the **HBV** infection rate with a saturation response [25, 105, 126].

It is important to recognize that various random disturbances can occur within the host during the **HBV** infection process, including fluctuations in temperature, mood, and other physiological rhythms. These factors may influence the dynamics of **HBV** infection. Consequently, alongside traditional ordinary differential equation models like model (4.1), there has been increasing focus on stochastic differential equations, which incorporate white noise process to account for these random variations [42, 76, 120, 124]. For example in [42] Hui and Nie extended model (4.2) to include stochastic perturbation, also in [124] a stochastic version of model (4.3) was analyzed.

Motivated by what mentioned above and Considering that white noise is directly proportional to $\mathcal{V}$,$\mathcal{H}$,$\mathcal{I}$, in this chapter we discussed the following **HBV** model:

$$\begin{aligned} d\mathcal{H} &= \Big[\Gamma - \frac{\beta\mathcal{H}\mathcal{V}}{1+\alpha\mathcal{V}} - \mu_0\mathcal{H} + \eta_1\mathcal{H}\big(1 - \frac{\mathcal{I}+\mathcal{H}}{N}\big)\Big]dt + \xi_1\mathcal{H}d\mathcal{B}_1, \\ d\mathcal{I} &= \Big[-\mu_1\mathcal{I} + \frac{\beta\mathcal{V}\mathcal{H}}{1+\alpha\mathcal{V}} + \eta_2\mathcal{I}\big(1 - \frac{\mathcal{I}+\mathcal{H}}{N}\big)\Big]dt + \xi_2\mathcal{I}d\mathcal{B}_2, \\ d\mathcal{V} &= \Big[\varphi\mathcal{I} - \mu_2\mathcal{V} - \frac{\beta\delta\mathcal{H}\mathcal{V}}{1+\alpha\mathcal{V}}\Big]dt + \xi_3\mathcal{V}d\mathcal{B}_3, \end{aligned} \tag{4.5}$$

with

$$\mathcal{X}(0) = (\mathcal{H}(0),\mathcal{I}(0),\mathcal{V}(0)) \in \mathbb{R}^3_+,$$

where $\mathcal{B}_1$,$\mathcal{B}_2$,$\mathcal{B}_3$ are Brownian motion independent defined on $(\Omega,\mathcal{F},\{\mathcal{F}_t\}_{t\geq 0},\mathbb{P})$. The parameters ξ_1,ξ_2,ξ_3 are the level of white noise intensity.

If we put $\xi_j = 0,\ j = 1,2,3.$, the following deterministic version of model (4.5) will result:

$$\begin{aligned} \mathcal{H}' &= \Gamma - \frac{\beta\mathcal{V}\mathcal{H}}{1+\alpha\mathcal{V}} - \mu_0\mathcal{H} + \eta_1\mathcal{H}\big(1 - \frac{\mathcal{I}+\mathcal{H}}{N}\big), \\ \mathcal{I}' &= -\mu_1\mathcal{I} + \frac{\beta\mathcal{V}\mathcal{H}}{1+\alpha\mathcal{V}} + \eta_2\mathcal{I}\big(1 - \frac{\mathcal{I}+\mathcal{H}}{N}\big), \\ \mathcal{V}' &= \varphi\mathcal{I} - \mu_2\mathcal{V} - \frac{\beta\delta\mathcal{H}\mathcal{V}}{1+\alpha\mathcal{V}}. \end{aligned} \tag{4.6}$$

If $\eta_1 > \mu_0$, the **HBV**-free equilibrium of model (4.6) is $P_0 = (\lambda,0,0)$ with $\lambda = \frac{N}{2\eta_1}\Big([\eta_1 - \mu_0] + \sqrt{(\eta_1-\mu_0)^2 + \frac{4\Gamma\eta_1}{N}}\Big)$.

The dynamics of the spread of **HBV** model (4.6) can be completly analyzed based on the basic

reproduction number which the approach described in [113] can compute. It is given as follows

$$R_0^d = \frac{\beta\varphi}{(\frac{\mu_2}{\lambda} + \beta\delta)(\mu_1 + \eta_2(\frac{\lambda}{N} - 1))}.$$

The model's parameters are presented in the following table

Table 4.1: Parameter description.

parameters	Meaning
Γ	Rate at which healthy hepatocytes are produced.
β	The rate at which infections spread.
μ_0	The pace at which healthy hepatocytes die.
μ_1	Death rate of cells infected with **HBV**.
μ_2	**HBV** virions' rate of decay.
N	Carrying capacity of healthy cells.
δ	Adjustment parameter.
α	Saturation incidence coefficient.
η_1	Maximum development rate of healthy hepatocytes per person.
η_2	Maximum development rate of infected hepatocytes per person.
φ	Replication rate of **HBV** virions generated by cells infected with **HBV**.

4.2 Global Positive Solution: Existence and Uniqueness

To explore the dynamic behavior of model (4.5), we start by establishing the existence of a global positive solution. We put $\mathcal{X}(t) = (\mathcal{H}(t),\mathcal{I}(t),\mathcal{V}(t))$.

Theorem 4.1. *For all $\mathcal{X}(0) \in \mathbb{R}^3_+$, there is a unique solution $\mathcal{X}(t)$ of system (4.5) . Morever, $\mathcal{X}(t)$ will remain in $\mathbb{R}^3_+$, $\forall\ t \geq 0$ a.s.*

Proof. For the prove, we use the same approach using the following Lyapunov function:

$$\Lambda : \mathbb{R}^3_+ \to \mathbb{R}_+, \quad \text{where}$$

$$\Lambda(\mathcal{X}) = -(\ln \mathcal{H} + \ln \mathcal{V} + \ln \mathcal{I}) + \mathcal{H} + \mathcal{I} + \mathcal{V} - 3.$$

Applyin the Itô formula, we get

$$
\begin{aligned}
d\Lambda(\mathcal{X}) =&\Big(1-\frac{1}{\mathcal{H}}\Big)d\mathcal{H}+\frac{1}{2\mathcal{H}^2}(d\mathcal{H})^2+\Big(1-\frac{1}{\mathcal{I}}\Big)d\mathcal{I}+\frac{1}{2\mathcal{I}^2}(d\mathcal{I})^2+\Big(1-\frac{1}{\mathcal{V}}\Big)d\mathcal{V}+\frac{1}{2\mathcal{V}^2}(d\mathcal{V})^2,\\
=&\Big(1-\frac{1}{\mathcal{H}}\Big)\Big(\Big[\Gamma-\frac{\beta\mathcal{H}(t)\mathcal{V}(t)}{1+\alpha\mathcal{V}(t)}-\mu_0\mathcal{H}(t)+\eta_1\mathcal{H}(t)\big(1-\frac{\mathcal{I}(t)+\mathcal{H}(t)}{N}\big)\Big]dt+\xi_1\mathcal{H}(t)d\mathcal{B}_1(t)\Big)\\
&+\frac{1}{2\mathcal{H}^2}\Big(\Big[\Gamma-\frac{\beta\mathcal{H}(t)\mathcal{V}(t)}{1+\alpha\mathcal{V}(t)}-\mu_0\mathcal{H}(t)+\eta_1\mathcal{H}(t)\big(1-\frac{\mathcal{I}(t)+\mathcal{H}(t)}{N}\big)\Big]dt+\xi_1\mathcal{H}(t)d\mathcal{B}_1(t)\Big)^2\\
&+\Big(1-\frac{1}{\mathcal{I}}\Big)\Big(\Big[\frac{\beta\mathcal{H}(t)\mathcal{V}(t)}{1+\alpha\mathcal{V}(t)}+\eta_2\mathcal{I}(t)\big(1-\frac{\mathcal{I}(t)+\mathcal{H}(t)}{N}\big)-\mu_1\mathcal{I}(t)\Big]dt+\xi_2\mathcal{I}(t)d\mathcal{B}_2(t)\Big)\\
&+\frac{1}{2\mathcal{I}^2}\Big(\Big[\frac{\beta\mathcal{H}(t)\mathcal{V}(t)}{1+\alpha\mathcal{V}(t)}+\eta_2\mathcal{I}(t)\big(1-\frac{\mathcal{I}(t)+\mathcal{H}(t)}{N}\big)-\mu_1\mathcal{I}(t)\Big]dt+\xi_2\mathcal{I}(t)d\mathcal{B}_2(t)\Big)^2\\
&+\Big(1-\frac{1}{\mathcal{V}}\Big)\Big(\Big[\varphi\mathcal{I}(t)-\mu_2\mathcal{V}(t)-\frac{\beta\delta\mathcal{H}(t)\mathcal{V}(t)}{1+\alpha\mathcal{V}(t)}\Big]dt+\xi_3\mathcal{V}(t)d\mathcal{B}_3(t)\Big)\\
&+\frac{1}{2\mathcal{V}^2}\Big(\Big[\varphi\mathcal{I}(t)-\mu_2\mathcal{V}(t)-\frac{\beta\delta\mathcal{H}(t)\mathcal{V}(t)}{1+\alpha\mathcal{V}(t)}\Big]dt+\xi_3\mathcal{V}(t)d\mathcal{B}_3(t)\Big)^2,\\
=&L\Lambda(\mathcal{X})dt+\xi_3(\mathcal{V}(t)-1)d\mathcal{B}_3(t)+\xi_2(\mathcal{I}(t)-1)d\mathcal{B}_2(t)+\xi_1(\mathcal{H}(t)-1)d\mathcal{B}_1(t),
\end{aligned}
$$

where $L\Lambda:\ \mathbb{R}^3_+\to\mathbb{R}_+$ is defined by

$$
\begin{aligned}
L\Lambda(\mathcal{X}) =&\Big(1-\frac{1}{\mathcal{H}}\Big)\Big(\Gamma-\frac{\beta\mathcal{H}(t)\mathcal{V}(t)}{1+\alpha\mathcal{V}(t)}-\mu_0\mathcal{H}(t)+\eta_1\mathcal{H}(t)\big(1-\frac{\mathcal{I}(t)+\mathcal{H}(t)}{N}\big)\Big)+\frac{\xi_1^2}{2}\\
&+\Big(1-\frac{1}{\mathcal{I}}\Big)\Big(\frac{\beta\mathcal{H}(t)\mathcal{V}(t)}{1+\alpha\mathcal{V}(t)}+\eta_2\mathcal{I}(t)\big(1-\frac{\mathcal{I}(t)+\mathcal{H}(t)}{N}\big)-\mu_1\mathcal{I}(t)\Big)+\frac{\xi_2^2}{2}\\
&+\Big(1-\frac{1}{\mathcal{V}}\Big)\Big(\varphi\mathcal{I}(t)-\mu_2\mathcal{V}(t)-\frac{\beta\delta\mathcal{H}(t)\mathcal{V}(t)}{1+\alpha\mathcal{V}(t)}\Big)+\frac{\xi_3^2}{2},\\
=&\Gamma+(\eta_1\mathcal{H}+\eta_2\mathcal{I})(1-\frac{\mathcal{H}+\mathcal{I}}{N})+\varphi\mathcal{I}-\mu_0\mathcal{H}-\mu_1\mathcal{I}-\mu_2\mathcal{V}-\frac{\beta\delta\mathcal{H}\mathcal{V}}{1+\alpha\mathcal{V}}-\frac{\Gamma}{\mathcal{H}}-\eta_1(1-\frac{\mathcal{H}+\mathcal{I}}{N})\\
&+(\mu_0+\frac{\xi_1^2}{2})+\frac{\beta\mathcal{V}}{1+\alpha\mathcal{V}}-\frac{\beta\mathcal{H}\mathcal{V}}{\mathcal{I}(1+\alpha\mathcal{V})}-\eta_2(1-\frac{\mathcal{H}+\mathcal{I}}{N})+(\mu_1+\frac{\xi_2^2}{2})-\frac{\varphi\mathcal{I}}{\mathcal{V}}\\
&+\frac{\beta\delta\mathcal{H}}{1+\alpha\mathcal{V}}+(\mu_2+\frac{\xi_3^2}{2}),\\
\leq&\Gamma+\mu_0+\frac{\xi_1^2}{2}+\frac{\beta}{\alpha}+\mu_1+\frac{\xi_2^2}{2}+\mu_2+\frac{\xi_3^2}{2}-\frac{(\eta_1\wedge\eta_2)}{N}(\mathcal{H}+\mathcal{I})^2\\
&+\Big([(\beta\delta+\eta_1)\vee(\eta_2+\varphi)]+\frac{\eta_1+\eta_2}{N}\Big)(\mathcal{H}+\mathcal{I}),\\
\leq&\Gamma+\mu_0+\frac{\xi_1^2}{2}+\frac{\beta}{\alpha}+\mu_1+\frac{\xi_2^2}{2}+\mu_2+\frac{\xi_3^2}{2}+\frac{\Big(N[(\beta\delta+\eta_1)\vee(\eta_2+\varphi)]+\eta_1+\eta_2\Big)^2}{4N(\eta_1\wedge\eta_2)}:=M.
\end{aligned}
$$

The rest of the proof follows the same approach as proving theorem 3.1. □

4.3 Extinction of the HBV

We seek to understand which conditions are adequate for driving the disease to extinction in the system (4.5). We put $\langle f(t)\rangle = \frac{1}{t}\int_0^t f(s)ds$.

Theorem 4.2. *Let $\mathcal{X}(t)$ be a solution of the model (4.5) with initial value $\mathcal{X}(0) \in \mathbb{R}^3$, if*

$$R_0^E = \frac{\frac{\beta\Gamma}{\mu_0} + \frac{\beta\eta_1 N}{4} + \varphi + \eta_2}{(\mu_1 \wedge \mu_2) + \frac{\xi_2^2 \wedge \xi_3^2}{4}} < 1,$$

then $\limsup_{t\to\infty} \dfrac{\ln \mathcal{I}(t) + \mathcal{V}(t)}{t} < 0$ *a.s., namely,* $\mathcal{I}(t), \mathcal{V}(t) \longrightarrow 0$ *exponentially a.s.*

Proof. Integrating from 0 to t the first equation of model (4.5) and dividing by t , we get

$$\langle \mathcal{H}(t)\rangle \leq \frac{1}{\mu_0}\Big(\Gamma + \frac{\eta_1 N}{4} + \frac{\mathcal{H}(0) - \mathcal{H}(t)}{t} + \frac{\xi_1}{t}\int_0^t \mathcal{H}(r)d\mathcal{B}_1(r)\Big). \tag{4.7}$$

Let $Q(t) = \mathcal{V}(t) + \mathcal{I}(t)$.

Applying Itô formula we get

$$\begin{aligned}
d\ln Q(t) &= \frac{1}{Q(t)}dQ(t) - \frac{1}{2Q^2(t)}(dQ(t))^2,\\
d\ln(\mathcal{I}(t)+\mathcal{V}(t)) &= \Big(\Big[(1-\delta)\frac{\beta\mathcal{H}(t)\mathcal{V}(t)}{1+\alpha\mathcal{V}(t)} + \varphi\mathcal{I} + \eta_2\mathcal{I}(t)\big(1 - \frac{\mathcal{I}(t)+\mathcal{H}(t)}{N}\big) - (\mu_1\mathcal{I}(t) + \mu_2\mathcal{V}(t))\Big]\\
&\quad \times \frac{1}{\mathcal{I}(t)+\mathcal{V}(t)} - \frac{\xi_2^2\mathcal{I}^2 + \xi_3^2\mathcal{V}^2}{2(\mathcal{I}+\mathcal{V})^2}\Big)dt + \frac{1}{\mathcal{I}(t)+\mathcal{V}(t)}\Big(\xi_2\mathcal{I}(t)d\mathcal{B}_2(t) + \xi_3\mathcal{V}(t)d\mathcal{B}_3(t)\Big),\\
&\leq \Big(\beta\mathcal{H}(t) + \varphi + \eta_2 - (\mu_1\wedge\mu_2) - \frac{(\xi_2^2\wedge\xi_3^2)(\mathcal{I}^2+\mathcal{V}^2)}{2(\mathcal{I}+\mathcal{V})^2}\Big)dt + \frac{\xi_2\mathcal{I}(t)}{\mathcal{I}(t)+\mathcal{V}(t)}d\mathcal{B}_2(t)\\
&\quad + \frac{\xi_3\mathcal{V}(t)}{\mathcal{I}(t)+\mathcal{V}(t)}d\mathcal{B}_3(t).
\end{aligned}$$

Using the following inequality

$$\mathcal{I}^2 + \mathcal{V}^2 \geq \frac{1}{2}(\mathcal{I}+\mathcal{V})^2.$$

Thus

$$d\ln(\mathcal{I}(t)+\mathcal{V}(t)) \leq \Big(\beta\mathcal{H}(t)+\varphi+\eta_2-(\mu_1\wedge\mu_2)-\frac{\xi_2^2\wedge\xi_3^2}{4}\Big)dt+\frac{\xi_2\mathcal{I}(t)}{\mathcal{I}(t)+\mathcal{V}(t)}d\mathcal{B}_2(t)+\frac{\xi_3\mathcal{V}(t)}{\mathcal{I}(t)+\mathcal{V}(t)}d\mathcal{B}_3(t).$$

Integrating from 0 to t and dividing by t , we obtain

$$\begin{aligned}
\frac{\ln(\mathcal{I}(t)+\mathcal{V}(t))}{t} &\leq \beta\langle\mathcal{H}(t)\rangle + \varphi + \eta_2 - (\mu_1\wedge\mu_2) - \frac{\xi_2^2\wedge\xi_3^2}{4} + \frac{\xi_2}{t}\int_0^t \frac{\mathcal{I}(r)}{\mathcal{I}(r)+\mathcal{V}(r)}d\mathcal{B}_2(r)\\
&\quad + \frac{\xi_3}{t}\int_0^t \frac{\mathcal{V}(r)}{\mathcal{I}(r)+\mathcal{V}(r)}d\mathcal{B}_3(r) + \frac{\ln(\mathcal{I}(0)+\mathcal{V}(0))}{t},
\end{aligned}$$

by using (4.7) we get

$$\frac{\ln(\mathcal{I}(t)+\mathcal{V}(t))}{t} \leq \frac{\beta}{\mu_0}\Big(\Gamma+\frac{\eta_1 N}{4}+\frac{\mathcal{H}(0)-\mathcal{H}(t)}{t}+\frac{\xi_1}{t}\int_0^t \mathcal{H}(r)d\mathcal{B}_1(r)\Big)+\varphi+\eta_2-(\mu_1\wedge\mu_2)-\frac{\xi_2^2\wedge\xi_3^2}{4}$$

$$+\frac{\xi_2}{t}\int_0^t \frac{\mathcal{I}(r)}{\mathcal{I}(r)+\mathcal{V}(r)}d\mathcal{B}_2(r)+\frac{\xi_3}{t}\int_0^t \frac{\mathcal{V}(r)}{\mathcal{I}(r)+\mathcal{V}(r)}d\mathcal{B}_3(r)+\frac{\ln(\mathcal{I}(0)+\mathcal{V}(0))}{t},$$

hence

$$\begin{aligned}\frac{\ln(\mathcal{I}(t)+\mathcal{V}(t))}{t} &\leq \frac{\beta\Gamma}{\mu_0}+\frac{\beta\eta_1 N}{4}+\varphi+\eta_2-(\mu_1\wedge\mu_2)-\frac{\xi_2^2\wedge\xi_3^2}{4}+\frac{\beta}{\mu_0}\Big(\frac{\mathcal{H}(0)}{t}+\frac{\xi_1}{t}\int_0^t \mathcal{H}(r)d\mathcal{B}_1(r)\Big)\\ &+\frac{\xi_2}{t}\int_0^t \frac{\mathcal{I}(r)}{\mathcal{I}(r)+\mathcal{V}(r)}d\mathcal{B}_2(r)+\frac{\xi_3}{t}\int_0^t \frac{\mathcal{V}(r)}{\mathcal{I}(r)+\mathcal{V}(r)}d\mathcal{B}_3(r)+\frac{\ln(\mathcal{I}(0)+\mathcal{V}(0))}{t}.\end{aligned} \tag{4.8}$$

Moreover

$$t^{-1}\int_0^t \mathcal{H}(r)d\mathcal{B}_1(r),\ \ t^{-1}\int_0^t \frac{\mathcal{I}(r)}{\mathcal{I}(r)+\mathcal{V}(r)}d\mathcal{B}_2(r),\ \ t^{-1}\int_0^t \frac{\mathcal{V}(r)}{\mathcal{I}(r)+\mathcal{V}(r)}d\mathcal{B}_3(r)$$

are a continuous local martingale. By Strong Law of Large Numbers lemma, we get

$$\lim_{t\to\infty} t^{-1}\int_0^t \mathcal{H}(r)d\mathcal{B}_1(r)=0,\qquad \lim_{t\to\infty} t^{-1}\int_0^t \frac{\mathcal{I}(r)}{\mathcal{I}(r)+\mathcal{V}(r)}d\mathcal{B}_2(r)=0,$$

$$\lim_{t\to\infty} t^{-1}\int_0^t \frac{\mathcal{V}(r)}{\mathcal{I}(r)+\mathcal{V}(r)}d\mathcal{B}_3(r)=0,\quad a.s.$$

Taking $\limsup_{t\to\infty}$ of (4.8) and if $R_0^E<1$ we obtain

$$\limsup_{t\to\infty}[t^{-1}\ln(\mathcal{I}(t)+\mathcal{V}(t))]\leq\Big((\mu_1\wedge\mu_2)+\frac{\xi_2^2\wedge\xi_3^2}{4}\Big)(R_0^E-1)<0\quad a.s.$$

The proof is finish. □

4.4 Existence of stationary distribution

Based on Hasminskii's theory [39], we demonstrate that under certain moderate conditions applied to the parameters of model (4.5), a stationary distribution exists, indicating that the desease will persist.

Theorem 4.3. *If*

$$R_0^s=\frac{\beta\varphi\mu_2}{\alpha(\mu_0+\frac{\xi_1^2}{2})(\mu_1+\frac{\xi_2^2}{2})(\mu_2+\frac{\xi_3^2}{2})}>1.$$

The system (4.5) has a unique stationary distribution $\pi(.)$ and the ergodicity holds.

Proof. To prove theorem 4.3, we fulfill the conditions of remark 2.1.

Firstly, we show the condition (a). The diffusion matrix of system (4.5) is given by

$$\begin{bmatrix} \xi_1^2\mathcal{H}^2 & 0 & 0 \\ 0 & \xi_2^2\mathcal{I}^2 & 0 \\ 0 & 0 & \xi_3^2\mathcal{V}^2 \end{bmatrix},$$

and

$$\begin{aligned} \sum_{i,j=1}^{3} a_{ij}(\mathcal{H},\mathcal{I},\mathcal{V})\Theta_i\Theta_j &= \xi_1^2\mathcal{H}^2\Theta_1^2 + \xi_2^2\mathcal{V}^2\Theta_2^2 + \xi_3^2\mathcal{V}^2\Theta_3^2, \\ &\geq n|\Theta|^2 \quad \text{for all} \quad (\mathcal{H},\mathcal{I},\mathcal{V}) \in U,\ \Theta \in \mathbb{R}_+^3, \end{aligned}$$

where $n = \min\{\xi_1^2\mathcal{H}^2, \xi_2^2\mathcal{I}^2, \xi_3^2\mathcal{V}^2\}$.

Next, we investigate a condition (b), We will constructing a non-negative C^2-function $\Pi : \mathbb{R}_+^3 \longrightarrow \mathbb{R}_+$.

We define

$$\Pi_1(\mathcal{H},\mathcal{I},\mathcal{V}) = -p_1 \ln \mathcal{H} - p_2 \ln \mathcal{I} - p_3 \ln \mathcal{V} + \mathcal{V} + \mathcal{I} + \mathcal{H},$$

where $p_1, p_2, p_3 > 0$ we will define later.

Using Itô formula we obtain

$$\begin{aligned} L(\mathcal{H}+\mathcal{V}+\mathcal{I}) &= \Gamma + (\eta_1\mathcal{H} + \eta_2\mathcal{I})(1 - \frac{\mathcal{H}+\mathcal{I}}{N}) + \varphi\mathcal{I} - \mu_0\mathcal{H} - \mu_1\mathcal{I} - \mu_2\mathcal{V} - \frac{\beta\delta\mathcal{H}\mathcal{V}}{1+\alpha\mathcal{V}}, \\ L(-\ln \mathcal{H}) &= -\frac{\Gamma}{\mathcal{H}} - \eta_1(1 - \frac{\mathcal{H}+\mathcal{I}}{N}) + (\mu_0 + \frac{\xi_1^2}{2}) + \frac{\beta\mathcal{V}}{1+\alpha\mathcal{V}}, \\ L(-\ln \mathcal{I}) &= -\frac{\beta\mathcal{H}\mathcal{V}}{\mathcal{I}(1+\alpha\mathcal{V})} - \eta_2(1 - \frac{\mathcal{H}+\mathcal{I}}{N}) + (\mu_1 + \frac{\xi_2^2}{2}), \\ L(-\ln \mathcal{V}) &= -\frac{\varphi\mathcal{I}}{\mathcal{V}} + \frac{\beta\delta\mathcal{H}}{1+\alpha\mathcal{V}} + (\mu_2 + \frac{\xi_3^2}{2}). \end{aligned}$$

Consequently

$$\begin{aligned} L\Pi_1 =& \Gamma + (\eta_1\mathcal{H} + \eta_2\mathcal{I})(1 - \frac{\mathcal{H}+\mathcal{I}}{N}) + \varphi\mathcal{I} - \mu_0\mathcal{H} - \mu_1\mathcal{I} - \mu_2\mathcal{V} - \frac{\beta\delta\mathcal{H}\mathcal{V}}{1+\alpha\mathcal{V}} - \frac{p_1\Gamma}{\mathcal{H}} - p_1\eta_1(1 - \frac{\mathcal{H}+\mathcal{I}}{N}) \\ &+ p_1(\mu_0 + \frac{\xi_1^2}{2}) + \frac{p_1\beta\mathcal{V}}{1+\alpha\mathcal{V}} - \frac{p_2\beta\mathcal{H}\mathcal{V}}{\mathcal{I}(1+\alpha\mathcal{V})} - p_2\eta_2(1 - \frac{\mathcal{H}+\mathcal{I}}{N}) + p_2(\mu_1 + \frac{\xi_2^2}{2}) - \frac{p_3\varphi\mathcal{I}}{\mathcal{V}} \\ &+ \frac{p_3\beta\delta\mathcal{H}}{1+\alpha\mathcal{V}} + p_3(\mu_2 + \frac{\xi_3^2}{2}) + \frac{\mu_2}{\alpha}(1+\alpha\mathcal{V}) - \frac{\mu_2}{\alpha}(1+\alpha\mathcal{V}). \end{aligned}$$

Using the inequality $(a_1a_2a_3a_4)^{\frac{1}{4}} \leq \frac{1}{4}(\sum_{l=1}^{4} a_l) \quad \forall a_l > 0 \quad (l = 1,...,4)$,

$$
\begin{aligned}
L\Pi_1 \leq & -4\sqrt[4]{\frac{p_1\Gamma}{\mathcal{H}}\frac{p_2\beta\mathcal{H}\mathcal{V}}{\mathcal{I}(1+\alpha\mathcal{V})}\frac{p_3\varphi\mathcal{I}}{\mathcal{V}}\frac{\mu_2(1+\alpha\mathcal{V})}{\alpha}} + \Gamma + p_1(\mu_0 + \frac{\xi_1^2}{2} + \frac{\beta}{\alpha}) + p_2(\mu_1 + \frac{\xi_2^2}{2}) + p_3(\mu_2 + \frac{\xi_3^2}{2}) \\
& + \frac{\mu_2}{\alpha} - \frac{(\eta_1 \wedge \eta_2)}{N}(\mathcal{H}+\mathcal{I})^2 + \left([(p_3\beta\delta + \eta_1) \vee (\eta_2 + \varphi)] + \frac{p_1\eta_1 + p_2\eta_2}{N}\right)(\mathcal{H}+\mathcal{I}), \\
\leq & -4\sqrt[4]{\frac{p_1\Gamma}{\mathcal{H}}\frac{p_2\beta\mathcal{H}\mathcal{V}}{\mathcal{I}(1+\alpha\mathcal{V})}\frac{p_3\varphi\mathcal{I}}{\mathcal{V}}\frac{\mu_2(1+\alpha\mathcal{V})}{\alpha}} + \Gamma + p_1(\mu_0 + \frac{\xi_1^2}{2} + \frac{\beta}{\alpha}) + p_2(\mu_1 + \frac{\xi_2^2}{2}) + p_3(\mu_2 + \frac{\xi_3^2}{2}) \\
& + \frac{\mu_2}{\alpha} + \left([(p_3\beta\delta + \eta_1) \vee (\eta_2 + \varphi)] + \frac{p_1\eta_1 + p_2\eta_2}{N}\right)(\mathcal{H}+\mathcal{I}), \\
= & -4\sqrt[4]{p_1\Gamma p_2\beta p_3\varphi\frac{\mu_2}{\alpha}} + \Gamma + p_1(\mu_0 + \frac{\xi_1^2}{2} + \frac{\beta}{\alpha}) + p_2(\mu_1 + \frac{\xi_2^2}{2}) + p_3(\mu_2 + \frac{\xi_3^2}{2}) + \frac{\mu_2}{\alpha} \\
& + \left([(p_3\beta\delta + \eta_1) \vee (\eta_2 + \varphi)] + \frac{p_1\eta_1 + p_2\eta_2}{N}\right)(\mathcal{H}+\mathcal{I})
\end{aligned}
$$

Let's put

$$\Gamma = p_1(\mu_0 + \frac{\xi_1^2}{2} + \frac{\beta}{\alpha}) = p_2(\mu_1 + \frac{\xi_2^2}{2}) = p_3(\mu_2 + \frac{\xi_3^2}{2}),$$

then

$$p_1 = \frac{\Gamma}{(\mu_0 + \frac{\xi_1^2}{2} + \frac{\beta}{\alpha})}, \quad p_2 = \frac{\Gamma}{(\mu_1 + \frac{\xi_2^2}{2})}, \quad p_3 = \frac{\Gamma}{(\mu_2 + \frac{\xi_3^2}{2})}.$$

As a result

$$
\begin{aligned}
L\Pi_1 \leq & -4\sqrt[4]{\frac{\Gamma^4\beta\varphi\mu_2}{\alpha(\mu_0 + \frac{\xi_1^2}{2})(\mu_1 + \frac{\xi_2^2}{2})(\mu_2 + \frac{\xi_3^2}{2})}} + 4\Gamma + \frac{\mu_2}{\alpha} \\
& + \left([(p_3\beta\delta + \eta_1) \vee (\eta_2 + \varphi)] + \frac{p_1\eta_1 + p_2\eta_2}{N}\right)(\mathcal{H}+\mathcal{I}), \\
= & -4\Gamma[R_0^s - 1] + \frac{\mu_2}{\alpha} + \left([(p_3\beta\delta + \eta_1) \vee (\eta_2 + \varphi)] + \frac{p_1\eta_1 + p_2\eta_2}{N}\right)(\mathcal{H}+\mathcal{I}).
\end{aligned}
$$

We define

$$\Pi_2(\mathcal{H},\mathcal{I},\mathcal{V}) = p_4(\mathcal{I} + \mathcal{V} + \mathcal{H} - p_1\ln\mathcal{H} - p_2\ln\mathcal{I} - p_3\ln\mathcal{V}) + \mathcal{V} + \mathcal{I} + \mathcal{H} - (\ln\mathcal{H} + \ln\mathcal{I} + \ln\mathcal{V}).$$

Obviously

$$\liminf_{z\to+\infty,(\mathcal{H},\mathcal{I},\mathcal{V})\in\mathbb{R}^3_+\setminus U_z} \Pi_2(\mathcal{H},\mathcal{I},\mathcal{V}) = +\infty,$$

where $U_z =]\frac{1}{z}, z[^3$.

On the other hand

$$\frac{\partial\Pi_2(\mathcal{H},\mathcal{I},\mathcal{V})}{\partial\mathcal{H}} = p_4 + 1 - \frac{p_4p_1 + 1}{\mathcal{H}}, \quad \frac{\partial\Pi_2(\mathcal{H},\mathcal{I},\mathcal{V})}{\partial\mathcal{I}} = p_4 + 1 - \frac{p_4p_2 + 1}{\mathcal{I}},$$

$$\frac{\partial\Pi_2(\mathcal{H},\mathcal{I},\mathcal{V})}{\partial\mathcal{V}} = p_4 + 1 - \frac{p_4p_3 + 1}{\mathcal{V}},$$

the function Π_2 have unique stagnation point $(\mathcal{H}_*,\mathcal{I}_*,\mathcal{V}_*) = \Big(\frac{p_4p_1+1}{p_4+1}, \frac{p_4p_2+1}{p_4+1}, \frac{p_4p_3+1}{p_4+1}\Big)$.
The Hessian matrix of Π_2 at $(\mathcal{H}_*,\mathcal{I}_*,\mathcal{V}_*)$ is given by

$$\begin{bmatrix} \frac{p_4p_1+1}{\mathcal{H}_*^2} & 0 & 0 \\ 0 & \frac{p_4p_2+1}{\mathcal{I}_*^2} & 0 \\ 0 & 0 & \frac{p_4p_3+1}{\mathcal{V}_*^2} \end{bmatrix}.$$

The Hessian matrix is positive definite and Π_2 is continous function then we can say that Π_2 has a single minimum $(\mathcal{H}_*,\mathcal{I}_*,\mathcal{V}_*) \in \mathbb{R}^3_+$.
Let

$$\Pi(\mathcal{H},\mathcal{I},\mathcal{V}) = \Pi_2(\mathcal{H},\mathcal{I},\mathcal{V}) - \Pi_2(\mathcal{H}_*,\mathcal{I}_*,\mathcal{V}_*).$$

Applying Itô formula we obtain

$$\begin{aligned} L\Pi(\mathcal{H},\mathcal{I},\mathcal{V}) \leq & -4p_4\Gamma[R_0^s - 1] + p_4\frac{\mu_2}{\alpha} + p_4\Big([(p_3\beta\delta + \eta_1) \vee (\eta_2 + \varphi)] + \frac{p_1\eta_1 + p_2\eta_2}{N}\Big)(\mathcal{H} + \mathcal{I}) \\ & + \Gamma + (\eta_1\mathcal{H} + \eta_2\mathcal{I})(1 - \frac{\mathcal{H}+\mathcal{I}}{N}) + \varphi\mathcal{I} - \mu_0\mathcal{H} - \mu_1\mathcal{I} - \mu_2\mathcal{V} - \frac{\beta\delta\mathcal{H}\mathcal{V}}{1+\alpha\mathcal{V}} \\ & - \frac{\Gamma}{\mathcal{H}} - \eta_1(1 - \frac{\mathcal{H}+\mathcal{I}}{N}) + (\mu_0 + \frac{\xi_1^2}{2}) + \frac{\beta\mathcal{V}}{1+\alpha\mathcal{V}} - \frac{\beta\mathcal{H}\mathcal{V}}{\mathcal{I}(1+\alpha\mathcal{V})} - \eta_2(1 - \frac{\mathcal{H}+\mathcal{I}}{N}) \\ & + (\mu_1 + \frac{\xi_2^2}{2}) - \frac{\varphi\mathcal{I}}{\mathcal{V}} + \frac{\beta\delta\mathcal{H}}{1+\alpha\mathcal{V}} + (\mu_2 + \frac{\xi_3^2}{2}), \end{aligned}$$

p_4 is a positive constant sufficiently large satisfying

$$-4p_4\Gamma\big[(R_0^s)^{\frac{1}{4}} - 1\big] + E < -2,$$

where

$$E = \Gamma + \mu_0 + \frac{\xi_1^2}{2} + \frac{\beta}{\alpha} + \mu_1 + \frac{\xi_2^2}{2} + \mu_2 + \frac{\xi_3^2}{2} + \frac{\Big(N[(\beta\delta + \eta_1) \vee (\eta_2 + \varphi)] + \eta_1 + \eta_2\Big)^2}{4N(\eta_1 \wedge \eta_2)}.$$

Let $\varepsilon_l > 0, l = 1,2,...,6$, we define a closed bounded set

$$U = \Big\{(\mathcal{H},\mathcal{I},\mathcal{V}) \in \mathbb{R}^3_+ : \varepsilon_1 \leq \mathcal{H} \leq \frac{1}{\varepsilon_2}, \varepsilon_3 \leq \mathcal{I} \leq \frac{1}{\varepsilon_4}, \varepsilon_5 \leq \mathcal{V} \leq \frac{1}{\varepsilon_6}\Big\},$$

we can choose ε_l small positive constants and p_4 sufficiently large such that the following conditions hold

- $W - \frac{\Gamma}{\varepsilon_1} < -1$,
- $-4p_4\Gamma[R_0^s - 1] + E + p_4\frac{\mu_2}{\alpha} + F(H + \varepsilon_3) - \frac{\beta}{\varepsilon_1\varepsilon_5(1+\alpha\mathcal{V})}$,
- $W - \frac{\varphi}{\varepsilon_3} < -1$,

- $W - \frac{\mu_0}{\varepsilon_2} < -1$,
- $W - \frac{\mu_1}{\varepsilon_4} < -1$,
- $W - \frac{\mu_2}{\varepsilon_6} < -1$,

where

$$W = \left\{ p_4 \frac{\mu_2}{\alpha} + \frac{\left(N[(\beta\delta + \eta_1) \vee (\eta_2 + \varphi)] + \eta_1 + \eta_2 + NF \right)^2}{4N(\eta_1 \wedge \eta_2)} + \Gamma + \frac{\xi_1^2 + \xi_2^2 + \xi_3^2}{2} + \frac{\beta}{\alpha} + \mu_0 + \mu_1 + \mu_2 \right\},$$

$$F = p_4 \left([(p_3\beta\delta + \eta_1) \vee (\eta_2 + \varphi)] + \frac{p_1\eta_1 + p_2\eta_2}{N} \right).$$

Next step we show that $L\Pi < 0$ on $\mathbb{R}^3_+ \setminus U$, $\mathbb{R}^3_+ \setminus U = \bigcup_{j=1}^6 U_j$ where

$$U_1 = \left\{ (\mathcal{H},\mathcal{I},\mathcal{V}) \in \mathbb{R}^3_+, 0 < \mathcal{H} < \varepsilon_1 \right\}, \qquad U_2 = \left\{ (\mathcal{H},\mathcal{I},\mathcal{V}) \in \mathbb{R}^3_+, 0 < \mathcal{I} < \varepsilon_3, H \geq \varepsilon_1, V \geq \varepsilon_5 \right\},$$

$$U_3 = \left\{ (\mathcal{H},\mathcal{I},\mathcal{V}) \in \mathbb{R}^3_+, 0 < \mathcal{V} < \varepsilon_5, \mathcal{I} \geq \varepsilon_3 \right\}, \qquad U_4 = \left\{ (\mathcal{H},\mathcal{I},\mathcal{V}) \in \mathbb{R}^3_+, \mathcal{H} > \frac{1}{\varepsilon_2} \right\},$$

$$U_5 = \left\{ (\mathcal{H},\mathcal{I},\mathcal{V}) \in \mathbb{R}^3_+, \mathcal{I} > \frac{1}{\varepsilon_4} \right\}, \qquad U_6 = \left\{ (\mathcal{H},\mathcal{I},\mathcal{V}) \in \mathbb{R}^3_+, \mathcal{V} > \frac{1}{\varepsilon_6} \right\}.$$

Case 1. let $(\mathcal{H},\mathcal{I},\mathcal{V}) \in U_1$

$$\begin{aligned}
L\Pi(\mathcal{H},\mathcal{I},\mathcal{V}) \leq & -4p_4\Gamma[R_0^s - 1] + p_4\frac{\mu_2}{\alpha} + p_4\left([(p_3\beta\delta + \eta_1) \vee (\eta_2 + \varphi)] + \frac{p_1\eta_1 + p_2\eta_2}{N} \right)(\mathcal{H} + \mathcal{I}) \\
& + \Gamma + (\eta_1\mathcal{H} + \eta_2\mathcal{I})(1 - \frac{\mathcal{H} + \mathcal{I}}{N}) + \varphi\mathcal{I} - \mu_0\mathcal{H} - \mu_1\mathcal{I} - \mu_2\mathcal{V} - \frac{\beta\delta\mathcal{H}\mathcal{V}}{1 + \alpha\mathcal{V}} \\
& - \frac{\Gamma}{\mathcal{H}} - \eta_1(1 - \frac{\mathcal{H} + \mathcal{I}}{N}) + (\mu_0 + \frac{\xi_1^2}{2}) + \frac{\beta\mathcal{V}}{1 + \alpha\mathcal{V}} - \frac{\beta\mathcal{H}\mathcal{V}}{\mathcal{I}(1 + \alpha\mathcal{V})} - \eta_2(1 - \frac{\mathcal{H} + \mathcal{I}}{N}) \\
& + (\mu_1 + \frac{\xi_2^2}{2}) - \frac{\varphi\mathcal{I}}{\mathcal{V}} + \frac{\beta\delta\mathcal{H}}{1 + \alpha\mathcal{V}} + (\mu_2 + \frac{\xi_3^2}{2}), \\
& \leq W - \frac{\Gamma}{\mathcal{H}} \leq W - \frac{\Gamma}{\varepsilon_1} < -1.
\end{aligned}$$

Case 2. let $(\mathcal{H},\mathcal{I},\mathcal{V}) \in U_2$

$$\begin{aligned}
L\Pi(\mathcal{H},\mathcal{I},\mathcal{V}) \leq & -4p_4\Gamma[R_0^s - 1] + p_4\frac{\mu_2}{\alpha} + p_4\bigg([(p_3\beta\delta + \eta_1) \vee (\eta_2 + \varphi)] + \frac{p_1\eta_1 + p_2\eta_2}{N}\bigg)(\mathcal{H} + \mathcal{I}) \\
& + \Gamma + (\eta_1\mathcal{H} + \eta_2\mathcal{I})(1 - \frac{\mathcal{H} + \mathcal{I}}{N}) + \varphi\mathcal{I} - \mu_0\mathcal{H} - \mu_1\mathcal{I} - \mu_2\mathcal{V} - \frac{\beta\delta\mathcal{H}\mathcal{V}}{1 + \alpha\mathcal{V}} \\
& - \frac{\Gamma}{\mathcal{H}} - \eta_1(1 - \frac{\mathcal{H} + \mathcal{I}}{N}) + (\mu_0 + \frac{\xi_1^2}{2}) + \frac{\beta\mathcal{V}}{1 + \alpha\mathcal{V}} - \frac{\beta\mathcal{H}\mathcal{V}}{\mathcal{I}(1 + \alpha\mathcal{V})} - \eta_2(1 - \frac{\mathcal{H} + \mathcal{I}}{N}) \\
& + (\mu_1 + \frac{\xi_2^2}{2}) - \frac{\varphi\mathcal{I}}{\mathcal{V}} + \frac{\beta\delta\mathcal{H}}{1 + \alpha\mathcal{V}} + (\mu_2 + \frac{\xi_3^2}{2}), \\
\leq & -4p_4\Gamma[R_0^s - 1] + E + p_4\frac{\mu_2}{\alpha} + F(H + I) - \frac{\beta\mathcal{H}\mathcal{V}}{\mathcal{I}(1 + \alpha\mathcal{V})}, \\
\leq & -4p_4\Gamma[R_0^s - 1] + E + p_4\frac{\mu_2}{\alpha} + F(H + I) - \frac{\beta\varepsilon_1\varepsilon_5}{\varepsilon_3(1 + \alpha\mathcal{V})}.
\end{aligned}$$

We put $\varepsilon_3 = (\varepsilon_1\varepsilon_5)^2$,

$$= -4p_4\Gamma[R_0^s - 1] + E + p_4\frac{\mu_2}{\alpha} + F(H + \varepsilon_3) - \frac{\beta}{\varepsilon_1\varepsilon_5(1 + \alpha\mathcal{V})} < -1.$$

Case 3. let $(\mathcal{H},\mathcal{I},\mathcal{V}) \in U_3$

$$\begin{aligned}
L\Pi(\mathcal{H},\mathcal{I},\mathcal{V}) \leq & -4p_4\Gamma[R_0^s - 1] + p_4\frac{\mu_2}{\alpha} + p_4\bigg([(p_3\beta\delta + \eta_1) \vee (\eta_2 + \varphi)] + \frac{p_1\eta_1 + p_2\eta_2}{N}\bigg)(\mathcal{H} + \mathcal{I}) \\
& + \Gamma + (\eta_1\mathcal{H} + \eta_2\mathcal{I})(1 - \frac{\mathcal{H} + \mathcal{I}}{N}) + \varphi\mathcal{I} - \mu_0\mathcal{H} - \mu_1\mathcal{I} - \mu_2\mathcal{V} - \frac{\beta\delta\mathcal{H}\mathcal{V}}{1 + \alpha\mathcal{V}} \\
& - \frac{\Gamma}{\mathcal{H}} - \eta_1(1 - \frac{\mathcal{H} + \mathcal{I}}{N}) + (\mu_0 + \frac{\xi_1^2}{2}) + \frac{\beta\mathcal{V}}{1 + \alpha\mathcal{V}} - \frac{\beta\mathcal{H}\mathcal{V}}{\mathcal{I}(1 + \alpha\mathcal{V})} - \eta_2(1 - \frac{\mathcal{H} + \mathcal{I}}{N}) \\
& + (\mu_1 + \frac{\xi_2^2}{2}) - \frac{\varphi\mathcal{I}}{\mathcal{V}} + \frac{\beta\delta\mathcal{H}}{1 + \alpha\mathcal{V}} + (\mu_2 + \frac{\xi_3^2}{2}), \\
\leq & W - \frac{\varphi\mathcal{I}}{\mathcal{V}} \leq W - \frac{\varphi\varepsilon_3}{\varepsilon_5}.
\end{aligned}$$

We put $\varepsilon_5 = \varepsilon_3^2$,

$$= W - \frac{\varphi}{\varepsilon_3} < -1.$$

Case 4. let $(\mathcal{H},\mathcal{I},\mathcal{V}) \in U_4$

$$\begin{aligned}
L\Pi(\mathcal{H},\mathcal{I},\mathcal{V}) \leq & -4p_4\Gamma[R_0^s - 1] + p_4\frac{\mu_2}{\alpha} + p_4\bigg([(p_3\beta\delta + \eta_1) \vee (\eta_2 + \varphi)] + \frac{p_1\eta_1 + p_2\eta_2}{N}\bigg)(\mathcal{H} + \mathcal{I}) \\
& + \Gamma + (\eta_1\mathcal{H} + \eta_2\mathcal{I})(1 - \frac{\mathcal{H} + \mathcal{I}}{N}) + \varphi\mathcal{I} - \mu_0\mathcal{H} - \mu_1\mathcal{I} - \mu_2\mathcal{V} - \frac{\beta\delta\mathcal{H}\mathcal{V}}{1 + \alpha\mathcal{V}} \\
& - \frac{\Gamma}{\mathcal{H}} - \eta_1(1 - \frac{\mathcal{H} + \mathcal{I}}{N}) + (\mu_0 + \frac{\xi_1^2}{2}) + \frac{\beta\mathcal{V}}{1 + \alpha\mathcal{V}} - \frac{\beta\mathcal{H}\mathcal{V}}{\mathcal{I}(1 + \alpha\mathcal{V})} - \eta_2(1 - \frac{\mathcal{H} + \mathcal{I}}{N}) \\
& + (\mu_1 + \frac{\xi_2^2}{2}) - \frac{\varphi\mathcal{I}}{\mathcal{V}} + \frac{\beta\delta\mathcal{H}}{1 + \alpha\mathcal{V}} + (\mu_2 + \frac{\xi_3^2}{2}), \\
\leq & W - \mu_0\mathcal{H} \leq W - \frac{\mu_0}{\varepsilon_2} < -1.
\end{aligned}$$

Case 5. let $(\mathcal{H},\mathcal{I},\mathcal{V}) \in U_5$

$$\begin{aligned} L\Pi(\mathcal{H},\mathcal{I},\mathcal{V}) &\leq -4p_4\Gamma[R_0^s - 1] + p_4\frac{\mu_2}{\alpha} + p_4\Big([(p_3\beta\delta + \eta_1) \vee (\eta_2 + \varphi)] + \frac{p_1\eta_1 + p_2\eta_2}{N}\Big)(\mathcal{H} + \mathcal{I}) \\ &+ \Gamma + (\eta_1\mathcal{H} + \eta_2\mathcal{I})(1 - \frac{\mathcal{H} + \mathcal{I}}{N}) + \varphi\mathcal{I} - \mu_0\mathcal{H} - \mu_1\mathcal{I} - \mu_2\mathcal{V} - \frac{\beta\delta\mathcal{H}\mathcal{V}}{1 + \alpha\mathcal{V}} \\ &- \frac{\Gamma}{\mathcal{H}} - \eta_1(1 - \frac{\mathcal{H} + \mathcal{I}}{N}) + (\mu_0 + \frac{\xi_1^2}{2}) + \frac{\beta\mathcal{V}}{1 + \alpha\mathcal{V}} - \frac{\beta\mathcal{H}\mathcal{V}}{\mathcal{I}(1 + \alpha\mathcal{V})} - \eta_2(1 - \frac{\mathcal{H} + \mathcal{I}}{N}) \\ &+ (\mu_1 + \frac{\xi_2^2}{2}) - \frac{\varphi\mathcal{I}}{\mathcal{V}} + \frac{\beta\delta\mathcal{H}}{1 + \alpha\mathcal{V}} + (\mu_2 + \frac{\xi_3^2}{2}), \\ &\leq W - \mu_1\mathcal{I} \leq W - \frac{\mu_0}{\varepsilon_4} < -1. \end{aligned}$$

Case 6. let $(\mathcal{H},\mathcal{I},\mathcal{V}) \in U_6$

$$\begin{aligned} L\Pi(\mathcal{H},\mathcal{I},\mathcal{V}) &\leq -4p_4\Gamma[R_0^s - 1] + p_4\frac{\mu_2}{\alpha} + p_4\Big([(p_3\beta\delta + \eta_1) \vee (\eta_2 + \varphi)] + \frac{p_1\eta_1 + p_2\eta_2}{N}\Big)(\mathcal{H} + \mathcal{I}) \\ &+ \Gamma + (\eta_1\mathcal{H} + \eta_2\mathcal{I})(1 - \frac{\mathcal{H} + \mathcal{I}}{N}) + \varphi\mathcal{I} - \mu_0\mathcal{H} - \mu_1\mathcal{I} - \mu_2\mathcal{V} - \frac{\beta\delta\mathcal{H}\mathcal{V}}{1 + \alpha\mathcal{V}} \\ &- \frac{\Gamma}{\mathcal{H}} - \eta_1(1 - \frac{\mathcal{H} + \mathcal{I}}{N}) + (\mu_0 + \frac{\xi_1^2}{2}) + \frac{\beta\mathcal{V}}{1 + \alpha\mathcal{V}} - \frac{\beta\mathcal{H}\mathcal{V}}{\mathcal{I}(1 + \alpha\mathcal{V})} - \eta_2(1 - \frac{\mathcal{H} + \mathcal{I}}{N}) \\ &+ (\mu_1 + \frac{\xi_2^2}{2}) - \frac{\varphi\mathcal{I}}{\mathcal{V}} + \frac{\beta\delta\mathcal{H}}{1 + \alpha\mathcal{V}} + (\mu_2 + \frac{\xi_3^2}{2}), \\ &\leq W - \mu_2\mathcal{V} \leq W - \frac{\mu_0}{\varepsilon_6} < -1. \end{aligned}$$

According to the above $L\Pi < 0$ for all $(\mathcal{H},\mathcal{I},\mathcal{V}) \in \mathbb{R}^3_+ \setminus U$. Thus the stochastic system (4.5) has a unique ergodic stationary distribution $\mu(.)$. □

4.5 Numerical simulations

We use numerical simulation to demonstrate our above-mentioned results. The discretization of model (4.5) is obtained by applying the Milstein approach [41]

$$\begin{aligned} \mathcal{H}_{j+1} &= \mathcal{H}_j + \Big[\Gamma - \frac{\beta\mathcal{H}_j\mathcal{V}_j}{1 + \alpha\mathcal{V}_j} - \mu_0\mathcal{H}_j + \eta_1\mathcal{H}_j\big(1 - \frac{\mathcal{I}_j + \mathcal{H}_j}{N}\big)\Big]dt + \xi_1\mathcal{H}_j\sqrt{\Delta t}\mathcal{B}_{1_i} + \frac{\xi_1^2}{2}\mathcal{H}_j(\mathcal{B}_{1_j}^2 - 1)\Delta t, \\ \mathcal{I}_{j+1} &= \mathcal{I}_j + \Big[\frac{\beta\mathcal{H}_j\mathcal{V}_j}{1 + \alpha\mathcal{V}_j} + \eta_2\mathcal{I}_j\big(1 - \frac{\mathcal{I}_j + \mathcal{H}_j}{N}\big) - \mu_1\mathcal{I}_j\Big]\Delta t + \xi_2\mathcal{I}_j\sqrt{\Delta t}\mathcal{B}_{2_i} + \frac{\xi_2^2}{2}\mathcal{I}_j(\mathcal{B}_{2_j}^2 - 1)\Delta t, \\ \mathcal{V}_{j+1} &= \mathcal{V}_j + \Big[\varphi\mathcal{I}_j - \mu_2\mathcal{V}_j - \frac{\beta\delta\mathcal{H}_j\mathcal{V}_j}{1 + \alpha\mathcal{V}_j}\Big]\Delta t + \xi_1\mathcal{V}_j\sqrt{\Delta t}\mathcal{B}_{3_i} + \frac{\xi_3^2}{2}\mathcal{V}_j(\mathcal{B}_{3_j}^2 - 1)\Delta t, \end{aligned} \tag{4.9}$$

where $\mathcal{B}_1,\mathcal{B}_2,\mathcal{B}_3$ are normally-distributed $\mathcal{N}(0,1)$ random variables and Δt is step size.

Numerical example for extinction of HBV

To illustrate extinction of **HBV**, we use the parameter in table 4.5 (V1), by calculation we get $R_0^E < 1$, then according to theorem 4.2 **HBV** infetion will extinct. (figure 4.1)

Table 4.2: Parameter's value.

parameters	V1	Source	V2	Source
Γ	$5.04 * 10^5$	[40]	$5.04 * 10^5$	[40]
β	$2 * 10^{-14}$	assumed	0.0014	[35]
μ_0	0.0039	[40]	0.0039	[40]
μ_1	0.0693	[35, 40]	0.0693	[35, 40]
μ_2	0.693	[35, 40]	0.693	[35, 40]
φ	0.06	assumed	280	[35]
δ	0.08	[108, 109]	0.08	[108, 109]
α	0.002	[126]	0.002	[126]
N	$2 * 10^{11}$	[35]	$2 * 10^{11}$	[35]
η_1	1	[35]	1	[35]
η_2	0.01	[32]	0.01	[32]
ξ_1	0.1	assumed	0.1	assumed
ξ_2	0.1	assumed	0.1	assumed
ξ_3	0.1	assumed	0.1	assumed
$\mathcal{H}(0)$	50	[32]	50	[32]
$\mathcal{I}(0)$	0.01	[32]	0.01	[32]
$\mathcal{V}(0)$	0.5	[32]	0.5	[32]

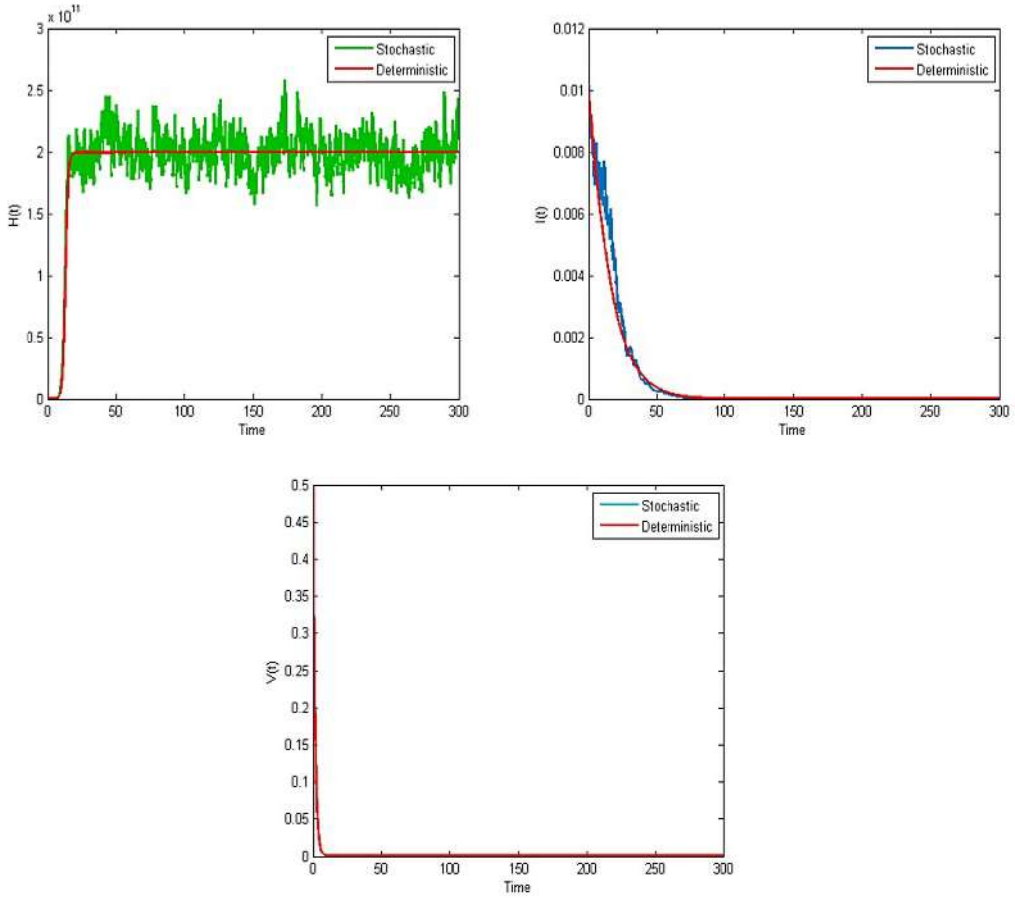

Figure 4.1: The stochastic and deterministic path of solution of model (4.5) based on the parameter set V1.

Numerical example for stationary distribution

In this example, we show the results mentioned above in theorem 4.3. We choose the parameter in table 4.5 (V2), we find that $R_0^S > 1$, thus ensuring that we have the unique stationary distribution as shown in figure 4.2.

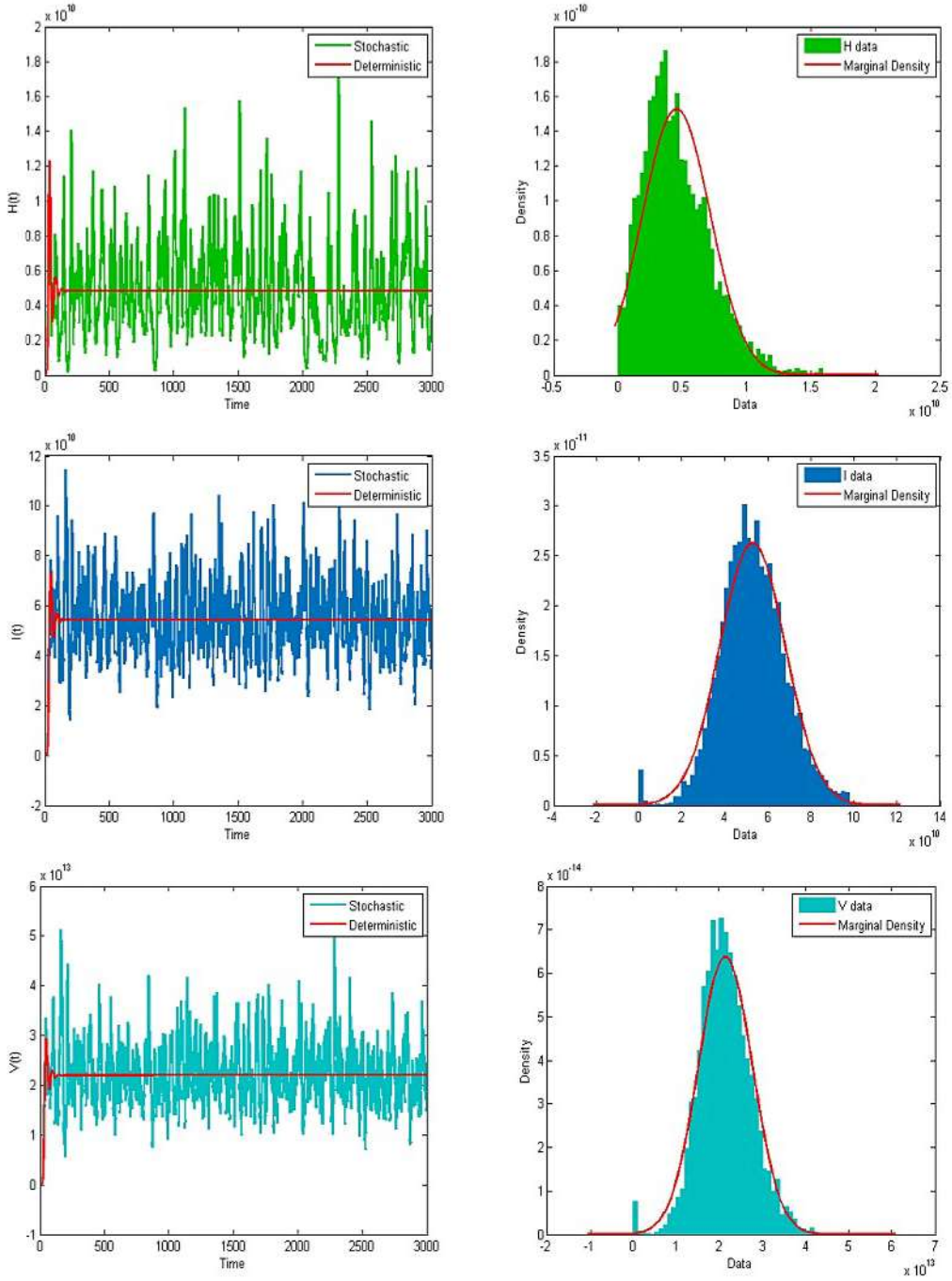

Figure 4.2: Compartement $\mathcal{H}$, $\mathcal{I}$, and $\mathcal{V}$ in the stochastic and deterministic system are simulated in the left hand column. The density function graphs and frequency histogram for $\mathcal{H}$, $\mathcal{I}$, and $\mathcal{V}$ are displayed in the right hand column.

Numerical example of the effect of parameter α

We use the the parameters in table 4.5 (V2). Figure 4.3 illustrate the levels of infected cells and free virus at varying values of α. it is clear that as α increases, both infected cells and free virus

decrease. This suggests that higher values of α can help prevent the spread of the **HBV**.

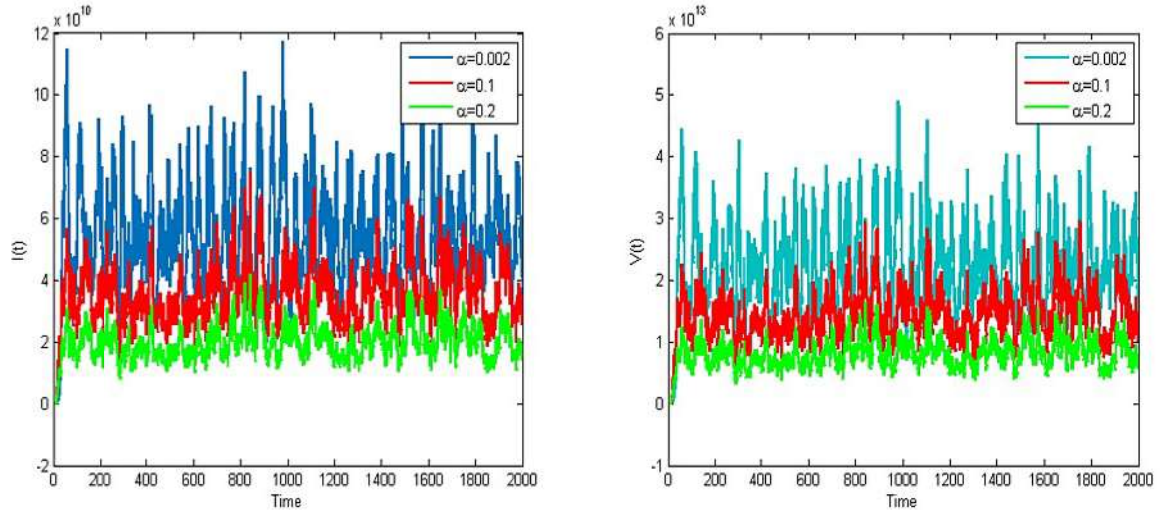

Figure 4.3: Simulation effect of the parameter α on the infected cells and free virus.

4.6 Conclusion

In conclusion, this chapter introduces and analyzes a novel stochastic model for the long-term behavior of the **HBV**, contributing significant insights into its dynamics under uncertainty. By demonstrating the models well-posedness, we ensure that solutions exist globally and remain biologically feasible. The conditions identified for virus extinction and the existence of a unique stationary distribution underscore the potential scenarios under which **HBV** may either be eradicated or persist in a stable state within a host population.

These findings enhance our understanding of **HBV**'s epidemiological behavior in the presence of random fluctuations, which are often encountered in real-world biological systems. The numerical simulations further validate the theoretical predictions, reinforcing the reliability of the model. This work offers a foundation for future studies aimed at developing control strategies for **HBV**, potentially guiding public health interventions and contributing to the broader efforts toward **HBV** elimination.

Chapter 5

Time-Delayed Stochastic Modeling of Epidemic with Crowley-Martin Incidence and Holling Type II Treatment rate

In this part, we consider a time delayed stochastic SIR epidemic model with Crowley-Martin (C-M) incidence rate and Holling Type II treatment rate. First, we prove that the positive global solution exists and is unique. Then, we provide sufficient condition for the extinction and persistence of the disease, and a suitable Lyapunov function is constructed to show the existence of a stationary distribution. At least the numerical simulation is provided to bolster our theoretical results.

5.1 Introduction

The classical SIR compartmental model, introduced by Kermack and McKendrick in 1927 [53], is one of the earliest and most influential frameworks for studying disease transmission. This foundational model, which divides the population into three compartments, has been extensively developed and remains the basis for numerous extensions. These extensions have enabled researchers to more accurately capture the complexities of real-world epidemic dynamics and to simulate various outbreaks with high precision [24, 61, 131]. In recent years, a substantial body of literature has emerged, focusing on the enhancement of the basic SIR model to better reflect the intricacies of disease spread and to assess the effectiveness of intervention strategies [26, 67, 75]. Such advancements provide valuable tools for understanding epidemic behavior and evaluating control measures [98]. However, many of these extensions continue to rely on classical differential

equation models, which inherently assume deterministic behavior and often fail to account for important factors such as memory effects, time delays, and stochastic influences that are commonly observed in real-world epidemics [56]. To achieve a more realistic representation of real-world epidemics, it is essential to develop mathematical models that incorporate both time delays and stochastic effects, as discussed in [23]. Such models are better suited to capture the inherent unpredictability of epidemic outbreaks and the influence of various external factors. For example, time delays can accurately reflect the incubation period between infection and the onset of infectiousness, as well as the duration required for treatment and recovery. These delays significantly impact the dynamics of disease spread and the timing of effective intervention strategies. Furthermore, incorporating stochastic effects allows models to account for the random variability and uncertainties in disease transmission, including fluctuations in contact rates, environmental conditions, and individual immune responses. Stochastic differential equation models offer a more accurate framework for simulating epidemic scenarios, especially in real-world contexts where outcomes are influenced by random events rather than strictly deterministic processes. Considering both time delays and stochasticity is therefore crucial for generating more precise epidemic forecasts and for designing effective control strategies [111].

In classical epidemic models based on differential equations, the treatment rate is often assumed to be either a constant or directly proportional to the number of infected individuals in the population. While this assumption simplifies the mathematical analysis, it overlooks critical real-world constraints faced by healthcare systems, such as limited availability of medical personnel, hospital beds, and medications. In practice, as the number of infections rises, healthcare infrastructure may become overwhelmed, leading to delays or limitations in treatment delivery. Neglecting these limitations can result in inaccurate predictions of disease progression and the development of ineffective public health strategies. Therefore, adopting more realistic modeling approaches that incorporate healthcare capacity constraints and the adaptive nature of treatment availability is essential. In response to these challenges, Wang et al. [119] proposed an SIR epidemic model in which the treatment rate is modeled as a constant, independent of the number of infectious individuals, to better reflect such real-world limitations. This type of treatment rate is represented as follows:

$$\mathcal{H}(I) = b, \quad \text{for } I > 0, \quad \text{and} \quad \mathcal{H}(I) = 0, \quad \text{for } I = 0,$$

Here, b represents a constant treatment rate. This assumption implies that medical resources are either unlimited or regulated externally, resulting in treatment being administered at a fixed rate, regardless of the outbreaks severity or healthcare system capacity. While such a treatment rate

may be useful for theoretical analysis, it fails to reflect the constraints commonly encountered during large-scale epidemics. To address this limitation, Zhang et al. [127] explored a more realistic approach by introducing a treatment function that captures the nonlinear relationship between treatment availability and the number of infected individuals. They incorporated the following continuously differentiable C^1 function into their model:

$$\mathcal{H}(I) = \frac{aI}{1+bI}, \quad a, b \geq 0.$$

In the above function, the ratio $\frac{a}{b}$ represents the maximum treatment capacity that can be delivered within a given time frame. This function, commonly referred to as the HT-II treatment rate, captures the saturation effect of medical resources as infection levels increase within a region. Unlike the assumption of a constant treatment rate-which implies unlimited availability of healthcare services-the HT-II function reflects a more realistic scenario in which the treatment rate initially rises with the number of infected individuals but eventually plateaus as healthcare resources become exhausted. This nonlinear formulation provides a more accurate depiction of the challenges faced by healthcare systems during epidemic outbreaks, especially in settings with limited medical resources. Furthermore, HT-II treatment and incidence rate functions have been incorporated into various epidemiological models to study diseases under constrained healthcare conditions. For example, in [61], researchers applied the HT-II rate function to examine the dynamics of a vector-host disease model under limited treatment capacity. Their results show that including nonlinear treatment and incidence functions yields more realistic and epidemiologically relevant insights into disease transmission and control. By accounting for healthcare limitations, these models produce more accurate forecasts of outbreak progression and support the development of more effective public health intervention strategies.

The infection incidence function in an epidemic model is a critical component that determines the rate at which susceptible individuals become infected. Traditional models often employ a bilinear incidence rate of the form ζSI, where ζ is the transmission coefficient [94, 129]. However, this bilinear formulation falls short in capturing the complexities of real-world disease transmission. One of its main limitations is the inability to account for saturation effects, wherein the rate of new infections does not increase indefinitely with the number of infectious individuals. Such saturation arises due to factors like limited contact opportunities, behavioral changes in response to rising case numbers, and constraints on healthcare resources. To overcome these shortcomings, researchers have proposed various nonlinear incidence functions that more accurately represent the dynamics of infection transmission [18, 30, 62, 87].

The following generalized form of the functional response was proposed by Crowley and Martin

in [21]:

$$\mathcal{G}(S,I) = \frac{\gamma S(t)I(t)}{(1+\alpha_2 I(t))(1+\alpha_1 S(t))}, \quad \alpha_1, \alpha_2 \geq 0.$$

In this formulation, saturation effects are incorporated to account for limited contact opportunities and behavioral adjustments during an epidemic outbreak [27]. The parameters α_1 and α_2 regulate the degree of saturation, ensuring that the infection rate does not grow unbounded as the number of susceptible or infected individuals increases. This is especially relevant in realistic scenarios where factors like immune responses, public health measures, and social distancing impact disease transmission. Such an approach provides a more accurate representation of diseases like COVID-19, tuberculosis, and HIV, where resource limitations and behavioral changes play a critical role in shaping transmission dynamics.

In [121], Wen et al. examined a delayed epidemiological model characterized by a bilinear incidence rate

$$\begin{aligned} S'(t) &= -\gamma I(t)S(t) + \Lambda - \upsilon_S S(t) + \delta e^{-\upsilon_R \iota} I(t-\iota), \\ I'(t) &= \gamma I(t)S(t) - (\upsilon_I + \delta)I(t), \\ R'(t) &= -\upsilon_R R(t) + \delta(I(t) - e^{-\upsilon_R \iota} I(t-\iota)). \end{aligned} \tag{5.1}$$

In [125], model (5.1) was extended to include a saturated incidence rate. The resulting generalized model is outlined in the following model

$$\begin{aligned} S'(t) &= -\frac{\gamma S(t)I(t)}{(1+\alpha_2 I(t))} - \upsilon_S S(t) + \Lambda + \delta e^{-\upsilon_R \iota} I(t-\iota), \\ I'(t) &= -(\upsilon_I + \delta)I(t) + \frac{\gamma I(t)S(t)}{(1+\alpha_2 I(t))}, \\ R'(t) &= -\delta e^{-\upsilon_R \iota} I(t-\iota) - \upsilon_R R(t) + \delta I(t). \end{aligned} \tag{5.2}$$

Here, $S(t)$, $I(t)$, and $R(t)$ represent the numbers of susceptible, infected, and recovered individuals in the population, respectively. The parameter γ denotes the contact rate, Λ is the birth rate, and δ is the recovery rate from infection. The terms υ_S, υ_I, and υ_R correspond to the natural death rates of the susceptible, infected, and recovered individuals, respectively. In [63], the expression $\delta e^{-\upsilon_R \iota} I(t-\iota)$ was introduced to model individuals in the recovery class who have survived natural death and return to the susceptible class, where ι represents the duration of immunity. Moreover, in [131], the following stochastic model was studied:

$$\begin{aligned} dS(t) &= \Big[-\frac{\gamma S(t)I(t)}{(1+\alpha_2 I(t))} - \upsilon_S S(t) + \Lambda + \delta_0 e^{-\upsilon_R \iota} I(t-\iota) \Big] dt - \eta_1 S(t) dW_1(t) - \frac{\eta_4 SI}{1+\alpha_2 I(t)} dW_4, \\ dI(t) &= \Big[-(\upsilon_I + \delta)I(t) + \frac{\gamma S(t)I(t)}{(1+\alpha_2 I(t))} \Big] dt - \eta_2 I(t) dW_2(t) + \frac{\eta_4 SI}{1+\alpha_2 I(t)} dW_4, \\ dR(t) &= \Big[-\delta_0 e^{-\upsilon_R \iota} I(t-\iota) - \upsilon_R R(t) + \delta I(t) \Big] dt - \eta_3 R(t) dW_3(t), \end{aligned} \tag{5.3}$$

where η_j and $W_j(t)$, $(j = 1,2,3,4)$ represents the white noise intensity and the independently Brownian motion respectively, over a complete probability space.

Building on the studies presented in [121, 125], and [131], we developed a more comprehensive epidemic model that integrates the C-M incidence function along with the H-T-II treatment function. Additionally, the condition $\delta \geq \delta_0$ is incorporated into the model formulation

$$\begin{aligned}
dS(t) &= \Big[- \frac{\gamma I(t)S(t)}{(1+\alpha_1 S(t))(1+\alpha_2 I(t))} + \Lambda - \upsilon S(t) + \delta_0 e^{-\upsilon\iota} I(t-\iota) \Big] dt + \eta_1 S(t) dW_1(t), \\
dI(t) &= \Big[- (\upsilon + \delta + \lambda) I(t) + \frac{\gamma S(t) I(t)}{(1+\alpha_1 S(t))(1+\alpha_2 I(t))} - \frac{aI(t)}{1+bI(t)} \Big] dt + \eta_2 I(t) dW_2(t), \\
dR(t) &= \Big[- \upsilon R(t) + \frac{aI(t)}{1+bI(t)} + \delta I(t) - \delta_0 e^{-\upsilon\iota} I(t-\iota) \Big] dt + \eta_3 R(t) dW_3(t).
\end{aligned} \tag{5.4}$$

Here, λ and υ denote the mortality rates due to the disease and natural causes, respectively, while the remaining parameters are as previously defined. Setting $\eta_1 = \eta_2 = \eta_3 = 0$ reduces the model (5.4) to its deterministic form

$$\begin{aligned}
dS(t) &= \Big[- \frac{\gamma I(t)S(t)}{(1+\alpha_1 S(t))(1+\alpha_2 I(t))} + \Lambda - \upsilon S(t) + \delta_0 e^{-\upsilon\iota} I(t-\iota) \Big] dt, \\
dI(t) &= \Big[- (\upsilon + \delta + \lambda) I(t) + \frac{\gamma S(t) I(t)}{(1+\alpha_1 S(t))(1+\alpha_2 I(t))} - \frac{aI(t)}{1+bI(t)} \Big] dt, \\
dR(t) &= \Big[- \upsilon R(t) + \frac{aI(t)}{1+bI(t)} + \delta I(t) - \delta_0 e^{-\upsilon\iota} I(t-\iota) \Big] dt.
\end{aligned} \tag{5.5}$$

Noticing the first two stochastic differential equations in system (5.4) do not depend on the function R, and so we can exclude the third one without loss of generality. Hence, we will only discuss this following system

$$\begin{aligned}
dS(t) &= \Big[- \frac{\gamma I(t)S(t)}{(1+\alpha_1 S(t))(1+\alpha_2 I(t))} + \Lambda - \upsilon S(t) + \delta_0 e^{-\upsilon\iota} I(t-\iota) \Big] dt + \eta_1 S(t) dW_1(t), \\
dI(t) &= \Big[- (\upsilon + \delta + \lambda) I(t) + \frac{\gamma S(t) I(t)}{(1+\alpha_1 S(t))(1+\alpha_2 I(t))} - \frac{aI(t)}{1+bI(t)} \Big] dt + \eta_2 I(t) dW_2(t).
\end{aligned} \tag{5.6}$$

The feasible region is

$$\Delta_{SI} = \Big\{ (S,I) \in \mathbb{R}^2_+ : S + I \leq \frac{\Lambda}{\upsilon} \Big\}.$$

5.2 Global Positive Solution: Existence and Uniqueness

We now present the following theorem to establish the desired results.

Theorem 5.1. *For all* $(S(0), I(0)) \in \mathbb{R}^2_+$ *with* $S(r) \geq 0$ *and* $I(r) \geq 0$, $\forall\ r \in [-\iota, 0[$, *the model* (5.6) *has a unique positive solution* $(S(t), I(t))$. *Additionally,*$(S(t), I(t)) \in \mathbb{R}^2_+$ $\forall t \geq 0$ *a.s.*

Proof. To prove it, we use the same approach using the following Lyapunov function:

$$\aleph : \mathbb{R}^2_+ \to \mathbb{R}_+, \quad \text{where}$$

$$\aleph(S,I) = S + I - h - 1 - (h\ln(\frac{S}{h}) + \ln I) + \delta_0 e^{-\upsilon\iota}\int_{t-\iota}^{t} I(r)dr,$$

where h is positive constants we will define later.

Applying the Itô formula, we get

$$\begin{aligned}
d\aleph(S,I) =&\Big(1-\frac{1}{I}\Big)dI + \Big(1-\frac{h}{S}\Big)dS + \frac{h}{2S^2}(dS)^2 + \frac{1}{2I^2}(dI)^2 + \delta_0 e^{-\upsilon\iota}I(t) - \delta_0 e^{-\upsilon\iota}I(t-\iota),\\
=&\Big(1-\frac{h}{S}\Big)\Big(\Big[\Lambda - \frac{\gamma I(t)S(t)}{(1+\alpha_1 S(t))(1+\alpha_2 I(t))} - \upsilon S(t) + \delta_0 e^{-\upsilon\iota}I(t-\iota)\Big]dt + \eta_1 S(t)dW_1(t)\Big)\\
&+\frac{h}{2S^2}\Big(\Big[\Lambda - \frac{\gamma I(t)S(t)}{(1+\alpha_1 S(t))(1+\alpha_2 I(t))} - \upsilon S(t) + \delta_0 e^{-\upsilon\iota}I(t-\iota)\Big]dt + \eta_1 S(t)dW_1(t)\Big)^2\\
&+\Big(1-\frac{1}{I}\Big)\Big(\Big[\frac{\gamma S(t)I(t)}{(1+\alpha_1 S(t))(1+\alpha_2 I(t))} - \frac{aI(t)}{1+bI(t)} - (\delta+\upsilon+\lambda)I(t)\Big]dt + \eta_2 I(t)dW_2(t)\Big)\\
&+\frac{1}{2I^2}\Big(\Big[\frac{\gamma S(t)I(t)}{(1+\alpha S(t))(1+\sigma I(t))} - \frac{aI}{1+bI} - (\delta+\upsilon+\lambda)I(t)\Big]dt + \eta_2 I(t)dW_2(t)\Big)^2\\
&+\delta_0 e^{-\upsilon\iota}I(t) - \delta_0 e^{-\upsilon\iota}I(t-\iota),\\
=&L\aleph(S,I)dt + \eta_1(S(t)-h)dW_1(t) + \eta_2(I(t)-1)dW_2(t),
\end{aligned}$$

where $L\aleph : \mathbb{R}^2_+ \to \mathbb{R}_+$ is given by

$$\begin{aligned}
L\aleph(S,I) =&\Lambda - \upsilon S(t) - (\upsilon+\delta+\lambda)I + \delta_0 e^{-\upsilon\iota}I(t-\iota) - \frac{aI(t)}{1+bI(t)} - h\delta_0 e^{-\upsilon\iota}\frac{I(t-\iota)}{S} - \frac{h\Lambda}{S}\\
&+\frac{\gamma(hI(t)-S(t))}{(1+\alpha_1 S(t))(1+\alpha_2 I(t))} + \frac{a}{1+bI(t)} + h\upsilon + \upsilon + \lambda + \delta + \frac{h\eta_1^2+\eta_2^2}{2}\\
&+\delta_0 e^{-\upsilon\iota}I(t) - \delta_0 e^{-\upsilon\iota}I(t-\iota),\\
\leq&(\gamma h - [\upsilon+\lambda])I(t) + \Lambda + h\upsilon + \upsilon + a + \lambda + \delta + + \frac{h\eta_1^2+\eta_2^2}{2},\\
&\text{chosing} \quad h = \frac{\upsilon+\lambda}{\gamma} \quad \text{then},\\
\leq&\Lambda + h\upsilon + \upsilon + a + \lambda + \delta + \frac{h\eta_1^2+\eta_2^2}{2} := \tilde{M}.
\end{aligned}$$

Consequently,

$$d\aleph(S,I) \leq \tilde{M}dt + \eta_1(S-h)dW_1(t) + \eta_2(I-1)dW_2(t).$$

The rest of the proof follows the same approach as proving theorem 3.1. □

5.3 Extinction of infection

The goal of this section is to identify the necessary conditions under which the disease dies out in system (5.4).

To this end, we define a parameter:

$$R_0 = \frac{\gamma}{\alpha_1(\upsilon + \lambda + \delta + \frac{\eta_2^2}{2})}.$$

Theorem 5.2. *$(S(t), I(t))$ be a solution of the model (5.6) with $(S(0),I(0)) \in \mathbb{R}^2$, if $R_0 < 1$ then $\limsup_{t\to\infty} \frac{\ln I(t)}{t} < 0$ a.s., namely, $I(t) \longrightarrow 0$ exponentially a.s. Additionaly*

$$\lim_{t\to+\infty} \langle S(t) \rangle = \frac{\Lambda}{\upsilon} \quad a.s.$$

Proof. Let us express the C-M functional as follows:

$$\begin{aligned}
\frac{\gamma S}{(1+\alpha_1 S)(1+\alpha_2 I)} =& \frac{\gamma\Lambda}{\upsilon+\alpha_1\Lambda} - \frac{\gamma\upsilon}{(\upsilon+\alpha_1\Lambda)(1+\alpha_1 S)(1+\alpha_2 I)}\Big(\frac{\Lambda}{\upsilon} - S\Big) \\
&- \frac{\gamma\Lambda\alpha_2 I}{(\upsilon+\alpha_1\Lambda)(1+\alpha_1 S)(1+\alpha_2 I)} - \frac{\gamma\Lambda\alpha_1\alpha_2 SI}{(\upsilon+\alpha_1\Lambda)(1+\alpha_1 S)(1+\alpha_2 I)}, \\
=& \frac{\gamma\Lambda}{\upsilon+\alpha_1\Lambda} + \frac{\gamma\upsilon S}{(\upsilon+\alpha_1\Lambda)(1+\alpha_1 S)(1+\alpha_2 I)} - \frac{\gamma\Lambda}{(\upsilon+\alpha_1\Lambda)(1+\alpha_1 S)(1+\alpha_2 I)} \\
&- \frac{\gamma\Lambda\alpha_2 I}{(\upsilon+\alpha_1\Lambda)(1+\alpha_1 S)(1+\alpha_2 I)} - \frac{\gamma\Lambda\alpha_1\alpha_2 SI}{(\upsilon+\alpha_1\Lambda)(1+\alpha_1 S)(1+\alpha_2 I)}, \\
\leq& \frac{\gamma\Lambda}{\upsilon+\alpha_1\Lambda} + \frac{\gamma\upsilon}{\alpha_1(\upsilon+\alpha_1\Lambda)} - \frac{\gamma\Lambda}{(\upsilon+\alpha_1\Lambda)(1+\alpha_1 S)(1+\alpha_2 I)} \\
&- \frac{\gamma\Lambda\alpha_2 I}{(\upsilon+\alpha_1\Lambda)(1+\alpha_1 S)(1+\alpha_2 I)} - \frac{\gamma\Lambda\alpha_1\alpha_2 SI}{(\upsilon+\alpha_1\Lambda)(1+\alpha_1 S)(1+\alpha_2 I)}.
\end{aligned} \tag{5.7}$$

Applying Itô formula, we get

$$d\ln I = \Big[\frac{\gamma S(t)}{(1+\alpha_1 S(t))(1+\alpha_2 I(t))} - \frac{a}{1+bI(t)} - (\delta+\upsilon+\lambda+\frac{\eta_2^2}{2})\Big]dt + \eta_2 dW_2(t). \tag{5.8}$$

By using (5.7), we obtain

$$\begin{aligned}
d\ln I &\leq \Big[\frac{\gamma\Lambda}{\upsilon+\alpha_1\Lambda} + \frac{\gamma\upsilon}{\alpha_1(\upsilon+\alpha_1\Lambda)} - (\upsilon+\delta+\lambda+\frac{\eta_2^2}{2})\Big]dt + \eta_2 dW_2(t), \\
&= \Big[\frac{\gamma}{\alpha_1} - (\upsilon+\delta+\lambda+\frac{\eta_2^2}{2})\Big]dt + \eta_2 dW_2(t).
\end{aligned}$$

Upon integrating from 0 to t and subsequently dividing by t, one obtains

$$\frac{\ln I(t)}{t} \leq \frac{\gamma}{\alpha_1} - (\upsilon+\delta+\lambda+\frac{\eta_2^2}{2}) + \frac{\eta_2}{t}\int_0^t dW_3(r) + \frac{\ln I(0)}{t}.$$

Moreover $\frac{1}{t}\int_0^t dW_2(r)$ is a continuous local martingale. By lemma 2.1, we obtain

$$\lim_{t\to\infty}\frac{1}{t}\int_0^t dW_2(r)=0 \quad a.s.$$

Taking $\limsup_{t\to\infty}$ of and if $R_0<1$ we get

$$\limsup_{t\to\infty}\frac{\ln I(t)}{t}\leq(\upsilon+\lambda+\delta+\frac{\eta_2^2}{2})(R_0-1)<0.$$

This confirms that $\lim_{t\to\infty} I(t)=0 \quad a.s.$ which implie $\lim_{t\to\infty}\langle I(t)\rangle=0 \quad a.s.$
Next, we consider the following C^2 function:

$$(S(t),I(t))\mapsto I(t)+S(t)+\delta_0 e^{-\upsilon\iota}\int_{t-\iota}^t I(r)dr.$$

Applyin Itô formula, we obtain

$$d\Big[I(t)+S(t)+\delta_0 e^{-\upsilon\iota}\int_{t-\iota}^t I(r)dr\Big]=\Big[-(\upsilon+\delta+\lambda)I(t)-\frac{aI(t)}{1+bI(t)}+\Lambda-\upsilon S(t)+\delta_0 e^{-\upsilon\iota}I(t-\iota)$$

$$+\delta_0 e^{-\upsilon\iota}I(t)-\delta_0 e^{-\upsilon\iota}I(t-\iota)\Big]dt+\eta_1 S(t)dW_1(t)+\eta_2 I(t)dW_2(t).$$

Upon integrating from 0 to t and subsequently dividing by t, one obtains

$$\frac{1}{t}\Big[I(t)+S(t)+\delta_0 e^{-\upsilon\iota}\int_{t-\iota}^t I(r)dr-(I(0)+S(0)+\delta_0 e^{-\upsilon\iota}\int_{-\iota}^0 I(r)dr)\Big]=\Lambda-\upsilon\langle S(t)\rangle$$

$$-(\upsilon+\delta-\delta_0 e^{-\upsilon\iota}+\lambda)\langle I(t)\rangle-\langle\frac{aI(t)}{1+bI(t)}\rangle+\frac{\eta_1}{t}\int_0^t S(r)dW_1(r)+\frac{\eta_2}{t}\int_0^t I(r)dW_2(r),$$

then

$$\langle S(t)\rangle=\frac{\Lambda}{\upsilon}+\frac{1}{\upsilon}\Big[-(\upsilon+\delta-\delta_0 e^{-\upsilon\iota}+\lambda)\langle I(t)\rangle-\langle\frac{aI(t)}{1+bI(t)}\rangle+\epsilon(t)\Big], \tag{5.9}$$

□

where

$$\epsilon(t)=\frac{1}{t}\Big[-(I(t)+S(t)+\delta_0 e^{-\upsilon\iota}\int_{t-\iota}^t I(r)dr)+(I(0)+S(0)+\delta_0 e^{-\upsilon\iota}\int_{-\iota}^0 I(r)dr)$$

$$+\eta_1\int_0^t S(r)dW_1(r)+\eta_2\int_0^t I(r)dW_2(r)\Big],$$

by last result and lemma 2.1, we get

$$\lim_{t\to+\infty}\langle S(t)\rangle=\frac{\Lambda}{\upsilon}\quad a.s.$$

5.4 Persistence of disease

Here, we aim to determine a sufficient criterion for the mean persistence of the disease.

Definition 5.1. For model (5.6), the infected population $I(t)$ are said to be strongly persistent, or just persistent in mean, if

$$\liminf_{t\to\infty} t^{-1}\int_0^t I(r)dr > 0 \quad a.s.$$

Lemma 5.1. *Let $f \in C(\mathbb{R}_+ \times \Omega, \mathbb{R}_+)$ and $F \in C(\mathbb{R}_+ \times \Omega, \mathbb{R})$ such that*

$$\lim_{t\to\infty} \frac{F(t)}{t} = 0 \quad a.s.$$

If $\forall\ t \geq 0$

$$\ln f(t) \geq \kappa_0 t - \kappa\int_0^t f(r)\,dr + F(t) \quad a.s.$$

Then

$$\liminf_{t\to\infty} f(t) \geq \frac{\kappa_0}{\kappa} \quad a.s.,$$

where $\kappa_0 \geq 0$ and $\kappa > 0$.

Theorem 5.3. *For any $(S(0), I(0)) \in \mathbb{R}^2_+$, if*

$$\mathcal{R}_0^p = \frac{\gamma\Lambda}{(\upsilon+\alpha_1\Lambda)(a+\delta+\upsilon+\lambda+\frac{\eta_2^2}{2})} > 1,$$

the disease is persistence in mean. Moreover,

$$\liminf_{t\to\infty}\langle I(t)\rangle \geq \frac{(\mathcal{R}_0^p-1)(\upsilon+\alpha_1\Lambda)(a+\delta+\upsilon+\lambda+\frac{\eta_2^2}{2})}{2\gamma\Lambda\alpha_2+\gamma(a+\upsilon+\delta-\delta_0 e^{-\upsilon\iota}+\lambda)} > 0 \quad a.s.$$

Proof. From the decomposition of C-M functional, we obtain

$$\begin{aligned}\frac{\gamma S}{(1+\alpha_1 S)(1+\alpha_2 I)} \geq& \frac{\gamma\Lambda}{\upsilon+\alpha_1\Lambda} - \frac{\gamma\upsilon}{(\upsilon+\alpha_1\Lambda)}\Big(\frac{\Lambda}{\upsilon}-S\Big) - \frac{\gamma\Lambda\alpha_2 I}{(\upsilon+\alpha_1\Lambda)} - \frac{\gamma\Lambda\alpha_2 I}{(\upsilon+\alpha_1\Lambda)},\\ \geq& \frac{\gamma\upsilon S}{(\upsilon+\alpha_1\Lambda)} - \frac{2\gamma\Lambda\alpha_2 I}{(\upsilon+\alpha_1\Lambda)}.\end{aligned} \tag{5.10}$$

From (5.8), we have

$$d\ln I \geq \Big[\frac{\gamma S(t)}{(1+\alpha_1 S(t))(1+\alpha_2 I(t))} - (a+\delta+\upsilon+\lambda+\frac{\eta_2^2}{2})\Big]dt + \eta_2 dW_2(t), \tag{5.11}$$

sabstituing (5.10) into (5.11), yields

$$d\ln I \geq \Big[\frac{\gamma\upsilon S}{(\upsilon+\alpha_1\Lambda)} - \frac{2\gamma\Lambda\alpha_2 I}{(\upsilon+\alpha_1\Lambda)} - (a+\delta+\upsilon+\lambda+\frac{\eta_2^2}{2})\Big]dt + \eta_2 dW_2(t). \tag{5.12}$$

Integrating (5.12) over $[0,t]$ and from (5.9), we have

$$\ln I \geq \Big[\frac{\gamma\upsilon}{(\upsilon+\alpha_1\Lambda)}.\frac{\Lambda}{\upsilon} - (a+\delta+\upsilon+\lambda+\frac{\eta_2^2}{2})\Big]t - \frac{2\gamma\Lambda\alpha_2}{(\upsilon+\alpha_1\Lambda)}\langle I(t)\rangle t$$
$$- \frac{\gamma(a+\upsilon+\delta-\delta_0 e^{-\upsilon\iota}+\lambda)}{(\upsilon+\alpha_1\Lambda)}\langle I(t)\rangle t + \frac{\gamma}{(\upsilon+\alpha_1\Lambda)}\epsilon(t)t + \int_0^t \eta_2 dW_2(r) + \ln I(0),$$

then

$$\ln I \geq \Big[\frac{\gamma\Lambda}{(\upsilon+\alpha_1\Lambda)} - (a+\delta+\upsilon+\lambda+\frac{\eta_2^2}{2})\Big]t + \tilde{\epsilon}(t)$$
$$- \Big[\frac{2\gamma\Lambda\alpha_2+\gamma(a+\upsilon+\delta-\delta_0 e^{-\upsilon\iota}+\lambda)}{(\upsilon+\alpha_1\Lambda)}\Big]\langle I(t)\rangle t,$$

where

$$\tilde{\epsilon}(t) = \frac{\gamma}{(\upsilon+\alpha_1\Lambda)}\epsilon(t)t + \int_0^t \eta_2 dW_2(r) + \ln I(0),$$

thus, $\lim_{t\to+\infty}\frac{\tilde{\epsilon}(t)}{t} = 0 \quad a.s.$

By lemma 5.1 and if $\mathcal{R}_0^p > 1$, we get

$$\liminf_{t\to\infty}\langle I(t)\rangle \geq \frac{(\mathcal{R}_0^p-1)(\upsilon+\alpha_1\Lambda)(a+\delta+\upsilon+\lambda+\frac{\eta_2^2}{2})}{2\gamma\Lambda\alpha_2+\gamma(a+\upsilon+\delta-\delta_0 e^{-\upsilon\iota}+\lambda)} > 1. \qquad \square$$

5.5 Stationary distribution

We perform the analysis by establishing conditions under which system (5.4) admits a stationary distribution.

Theorem 5.4. *If*

$$\bar{R}_0 := \frac{\gamma}{(\upsilon+\frac{\eta_1^2}{2})(\upsilon+\delta+\lambda+a+\frac{\eta_2^2}{2})} > 1,$$

then, the solution of (5.4) exhibits a unique stationary distribution $\rho(.)$ and satisfies ergodicity.

Proof. The conditions outlined in Remark 2.1 will now be examined. Initially, we show the condition (b), We will constructing a non-negative C^2-function $\mathbb{U}: \mathbb{R}_+^2 \longrightarrow \mathbb{R}_+$.

Let

$$\mathbb{U}_1(S,I) = S + I - c_2\ln I - c_1\ln S,$$

where c_1, c_2, are positive constants we will define later.

Using the Itô formula we have

$$L(S+I) = \Lambda - \upsilon S - (\lambda+\delta+\upsilon)I + \delta_0 e^{-\upsilon\iota}I(t-\iota) - \frac{aI(t)}{1+bI(t)},$$
$$L(\ln S) = \frac{\Lambda}{S} - \frac{\gamma I(t)}{(1+\alpha_1 S(t))(1+\alpha_2 I(t))} - \upsilon + \delta_0 e^{-\upsilon\iota}\frac{I(t-\iota)}{S} - \frac{\eta_1^2}{2},$$
$$L(\ln I) = \frac{\gamma S(t)}{(1+\alpha_1 S(t))(1+\alpha_2 I(t))} - \frac{a}{1+bI(t)} - (\upsilon+\delta+\lambda+\frac{\eta_2^2}{2}).$$

Consequently,

$$\begin{aligned}L\mathbb{U}_1 =&\Lambda - \upsilon S - (\lambda+\delta+\upsilon)I + \delta_0 e^{-\upsilon\iota} I(t-\iota) - \frac{aI(t)}{1+bI(t)} - \frac{c_1\Lambda}{S} + \frac{c_1\gamma I(t)}{(1+\alpha_1 S(t))(1+\alpha_2 I(t))}\\ &- c_1\delta_0 e^{-\upsilon\iota}\frac{I(t-\iota)}{S} + c_1(\upsilon+\frac{\eta_1^2}{2}) - \frac{c_2\gamma S(t)}{(1+\alpha_1 S(t))(1+\alpha_2 I(t))} + \frac{c_2 a}{1+bI(t)}\\ &+ c_2(\upsilon+\delta+\lambda+\frac{\eta_2^2}{2}) + \frac{\upsilon}{\alpha_1\vee\alpha_2}[(1+\alpha_1 S(t))(1+\alpha_2 I(t)) - (1+\alpha_1 S(t))(1+\alpha_2 I(t))].\end{aligned}$$

$$\begin{aligned}L\mathbb{U}_1 \leq& -3\sqrt[3]{\frac{\upsilon\gamma\Lambda c_1 c_2}{\alpha_1\vee\alpha_2}} + \Lambda + c_1(\upsilon+\frac{\eta_1^2}{2}) + c_2(\upsilon+\delta+\lambda+a+\frac{\eta_2^2}{2}) + \delta_0 I(t-\iota)\\ &+ c_1\gamma I + \frac{\upsilon}{\alpha_1\vee\alpha_2} + \frac{\upsilon\alpha_1\alpha_2}{\alpha_1\vee\alpha_2}SI.\end{aligned}$$

Letting

$$\Lambda = c_1(\upsilon+\frac{\eta_1^2}{2}) = c_2(\upsilon+\delta+\lambda+a+\frac{\eta_2^2}{2}),$$

then

$$c_1 = \frac{\Lambda}{(\upsilon+\frac{\eta_1^2}{2})}, \qquad c_2 = \frac{\Lambda}{(\upsilon+\delta+\lambda+a+\frac{\eta_2^2}{2})}.$$

As a result

$$\begin{aligned}L\mathbb{U}_1 \leq& -3\sqrt[3]{\frac{\upsilon\gamma\Lambda^3}{(\alpha_1\vee\alpha_2)(\upsilon+\delta+\lambda+a+\frac{\eta_2^2}{2})(\upsilon+\frac{\eta_1^2}{2})}} + 3\Lambda + \frac{\upsilon}{\alpha_1\vee\alpha_2} + \delta_0 I(t-\iota) + c_1\gamma I + \frac{\upsilon\alpha_1\alpha_2 SI}{\alpha_1\vee\alpha_2},\\ \leq& -3\Lambda\left(\sqrt[3]{\frac{\upsilon\gamma}{(\alpha_1\vee\alpha_2)(\upsilon+\delta+\lambda+a+\frac{\eta_2^2}{2})(\upsilon+\frac{\eta_1^2}{2})}} - 1\right) + \frac{\upsilon}{\alpha_1\vee\alpha_2} + \delta_0 I(t-\iota) + c_1\gamma I\\ &+ \frac{\upsilon\alpha_1\alpha_2}{\alpha_1\vee\alpha_2}SI,\\ =& -3\Lambda\big[(R_0^s)^{\frac{1}{3}} - 1\big] + \frac{\upsilon}{\alpha_1\vee\alpha_2} + \delta_0 I(t-\iota) + c_1\gamma I + \frac{\upsilon\alpha_1\alpha_2}{\alpha_1\vee\alpha_2}SI.\end{aligned}$$

We define

$$\mathbb{U}_2(S,I) = c_3\big(S + I - c_1\ln S - c_2\ln I\big) + I + S - \ln I - \ln S,$$

where c_3 is constant satisfying the following condition

$$-3\Lambda c_3\big[(R_0^s)^{\frac{1}{3}} - 1\big] + \frac{c_3\upsilon}{\alpha_1\vee\alpha_2} + \urcorner_2 < -2,$$

where

$$\urcorner_2 = \Lambda + \frac{\gamma}{\alpha_2} + a + 2\upsilon + \delta + \lambda + \frac{\eta_2^2+\eta_3^2}{2}.$$

Obviously

$$\liminf_{q\to+\infty,(S,I)\in\mathbb{R}_+^2\setminus\mathbb{V}_q} \mathbb{U}_2(S,I) = +\infty,$$

where $\mathbb{V}_q =]\frac{1}{q},q[\times]\frac{1}{q},q[$.

Since: when $q \to +\infty, (S,I) \in \mathbb{R}^2_+ \setminus \mathbb{V}_q$ is exactly equal to $\{0\} \times [0,+\infty[\cup [0,+\infty[\times \{0\}$.

Besides, we have

$$\frac{\partial \mathbb{U}_2(S,I)}{\partial S} = c_3 + 1 - \frac{c_3c_1+1}{S}, \qquad \frac{\partial \mathbb{U}_2(S,I)}{\partial I} = c_3 + 1 - \frac{c_3c_2+1}{I},$$

the function $\mathbb{U}_2$ have unique stagnation point $(S_*,I_*) = \left(\frac{c_3c_1+1}{c_3+1}, \frac{c_3c_2+1}{c_3+1}\right)$ The Hessian matrix of $\mathbb{U}_2$ at (S_*,I_*) is given by

$$\mathbb{H} = \begin{bmatrix} \frac{c_3c_1+1}{S_*^2} & 0 \\ 0 & \frac{c_3c_2+1}{I_*^2} \end{bmatrix}.$$

$\mathbb{H}$ is positive definite and $\mathbb{U}_2$ is continues function then it is clear that $\mathbb{U}_2$ has a unique minimum $(S_*,I_*) \in \mathbb{R}^2_+$.

Let

$$\mathbb{U}(S,I) = \mathbb{U}_2(S,I) - \mathbb{U}_2(S_*,I_*).$$

Utilizing Itô criteria to obtain

$$\begin{aligned} L\mathbb{U}(S,I) =& L\mathbb{U}_2(S,I), \\ \leq& -3c_3\Lambda\left[(R_0^s)^{\frac{1}{3}} - 1\right] + \frac{c_3\upsilon}{\alpha_1 \vee \alpha_2} + (c_3+1)\delta_0 I(t-\iota) + c_3c_1\gamma I + \frac{c_3\upsilon\alpha_1\alpha_2}{\alpha_1 \vee \alpha_2} SI - \upsilon(S+I) \\ &+ \Lambda - (\lambda+\delta)I - \frac{aI(t)}{1+bI(t)} - \frac{\Lambda}{S} + \frac{\gamma I(t)}{(1+\alpha_1 S(t))(1+\alpha_2 I(t))} + \upsilon + \frac{\eta_1^2}{2} \\ &- \frac{\gamma S(t)}{(1+\alpha_1 S(t))(1+\alpha_2 I(t))} - \delta_0 e^{-\upsilon\iota}\frac{I(t-\iota)}{S} + \frac{a}{1+bI(t)} + (\delta + \upsilon + \lambda + \frac{\eta_2^2}{2}). \end{aligned}$$

Let $\varepsilon_l > 0, l = 1,2,3,4$, we give a closed and bounded set

$$\mathbb{V} = \left\{(S,I) \in \mathbb{R}^3_+ : \varepsilon_1 \leq S \leq \frac{1}{\varepsilon_2}, \varepsilon_3 \leq I \leq \frac{1}{\varepsilon_4}\right\}.$$

We can choose a small ε_l, $l = 1,2,3,4$ such that the subsequent criteria holds

- $-\frac{\Lambda}{\varepsilon_1} + \urcorner_1 < -1$,
- $-3\Lambda c_3\left[(R_0^s)^{\frac{1}{3}} - 1\right] + \frac{c_3\upsilon}{\alpha_1\vee\alpha_2} + (c_3+1)\delta_0\varepsilon_3 + c_3c_1\gamma\varepsilon_3 + \frac{c_3\upsilon\alpha_1\alpha_2}{\alpha_1\vee\alpha_2}S\varepsilon_3 + \urcorner_2 < -1$,
- $-\frac{\upsilon}{\varepsilon_2} + \urcorner_1 < -1$,
- $-\frac{\upsilon}{\varepsilon_4} + \urcorner_1 < -1$,

where

$$\urcorner_1 = \sup\left\{\frac{c_3\upsilon}{\alpha_1\vee\alpha_2} + (c_3+1)\delta_0 I(t-\iota) + c_3c_1\gamma I + \frac{c_3\upsilon\alpha_1\alpha_2}{\alpha_1\vee\alpha_2}SI + \Lambda + \frac{\gamma}{\alpha_2} + a + 2\upsilon + \delta + \lambda + \frac{\eta_2^2}{2} + \frac{\eta_3^2}{2}\right\}.$$

Next, we show that $L\mathbb{U} < 0$ on $\mathbb{R}^2_+ \setminus \mathbb{V}$, $\mathbb{R}^2_+ \setminus \mathbb{V} = \bigcup_{j=1}^{4} \mathbb{V}_j$, where

$$\mathbb{V}_1 = \Big\{(S,I) \in \mathbb{R}^2_+, 0 < S < \varepsilon_1\Big\}, \quad \mathbb{V}_2 = \Big\{(S,I) \in \mathbb{R}^2_+, 0 < I < \varepsilon_3\Big\},$$

$$\mathbb{V}_3 = \Big\{(S,I) \in \mathbb{R}^2_+, S > \frac{1}{\varepsilon_2}\Big\}, \quad \mathbb{V}_4 = \Big\{(S,I) \in \mathbb{R}^2_+, I > \frac{1}{\varepsilon_4}\Big\}.$$

Case i. Let $(S,I) \in \mathbb{V}_1$

$$L\mathbb{U}(S,I) \leq \daleth_1 - \frac{\Lambda}{S} \leq \daleth_1 - \frac{\Lambda}{\varepsilon_1} < -1.$$

Case ii. Let $(S,I) \in \mathbb{V}_2$

$$L\mathbb{U}(S,I) \leq -\frac{2}{3}\Lambda c_3\big[(R_0^s)^{\frac{1}{3}} - 1\big](c_3+1)\delta_0\varepsilon_3 + \daleth_2 < -1.$$

Case iii. Let $(S,I) \in \mathbb{V}_3$

$$L\mathbb{U}(S,I) \leq \daleth_1 - \upsilon S \leq \daleth_1 - \frac{\upsilon}{\varepsilon_2} < -1.$$

Case iv. Let $(S,I) \in \mathbb{V}_4$

$$L\mathbb{U}(S,I) \leq \daleth_1 - \upsilon I \leq \daleth_1 - \frac{\upsilon}{\varepsilon_4} < -1.$$

Next, we demonstrate the criteria stated in (a). The diffusion matrix corresponds to (5.4) is as follows

$$\begin{bmatrix} \eta_1^2 S^2 & 0 \\ 0 & \eta_2^2 I^2 \end{bmatrix},$$

and

$$\sum_{i,j=1}^{2} \varsigma_{ij}(S,I)\zeta_i\zeta_j = \eta_1^2 S^2 \zeta_1^2 + \eta_2^2 I^2 \zeta_2^2$$

$$\geq \mathcal{M}|\zeta|^2 \quad \forall (S,I) \in \mathbb{V},\ \zeta \in \mathbb{R}^2_+,$$

where, $\mathcal{M} = \min\{\eta_1^2 S^2, \eta_2^2 I^2\}$.

It follows from the above analysis that model (5.6) possesses a unique ergodic stationary distribution $\rho(.)$. □

5.6 Numerical results

In this part, we present numerical simulations to illustrate the theoretical results.

To approximate solutions of SDEs, we employ the Milstein method. Originally introduced by Grigori N. Milstein in [86], this method provides an effective technique for numerically solving SDEs of the form:

$$d\mathfrak{X}(t) = g(t,\mathfrak{X}(t))dt + h(t,\mathfrak{X}(t))dW(t), \qquad \mathfrak{X}(0) = \mathfrak{X}_0. \tag{5.13}$$

Using the Milstein method as follows:

$$\mathfrak{X}^{n+1} = \mathfrak{X}^n + g(\mathfrak{X}^n, t^n)\Delta t + h(\mathfrak{X}^n, t^n)\Delta W^n + 0.5h(\mathfrak{X}^n, t^n)h'(\mathfrak{X}^n, t^n)((\Delta W^n)^2 - \Delta t), \tag{5.14}$$

where $h'(x,t)$ is the derivative of $h(x,t)$ w.r.t x and $\Delta W = W(t_{n+1}) - W(t_n)$ is the Brownian increment on $[t_n, t_{n+1}]$. Next, we use this method (5.14) to solve the system (5.4) numerically as follows:

$$\begin{aligned}
S^{n+1} &= S^n + \left[\Lambda - \frac{\gamma S^n I^n}{(1+\alpha_1 S^n)(1+\alpha_2 I^n)} - \upsilon S^n + \delta_0 e^{-\upsilon\kappa} I^{n-\kappa}\right]\Delta t + \eta_1 S^n \Delta W^n + 0.5\ \eta_1^2 S^n((\Delta W_1^n)^2 - \Delta t),\\
I^{n+1} &= I^n + \left[\frac{\gamma S^n I^n}{(1+\alpha_1 S^n)(1+\alpha_2 I^n)} - \frac{aI^n}{1+bI^n} - (\upsilon+\delta+\lambda)I^n\right]\Delta t + \eta_2 I^n \Delta W_2^n + 0.5\ \eta_2^2 I^n((\Delta W_2^n)^2 - \Delta t),\\
R^{n+1} &= R^n + \left[\frac{aI^n}{1+bI^n} - \upsilon R^n + \delta I^n - \delta_0 e^{-\upsilon\kappa} I^{n-\kappa}\right]\Delta t + \eta_3 R^n \Delta W_3^n + 0.5\ \eta_3^2 R^n((\Delta W_3^n)^2 - \Delta t).
\end{aligned} \tag{5.15}$$

5.6.1 Numerical Simulation

Several empirical examples are presented to shed light on the following aspects:

- The dynamical behavior of model (5.4) if $R_0 < 1$.
- The existence of stationary distribution of (5.4), if $\bar{R}_0 > 1$.
- How alterations in delay time ι affect the dynamics of disease spread.

Example 5.1. To demonstrate the extinction of the disease in the deterministic and stochastic frameworks, we utilize the following parameter values, partially sourced from [131] : $\gamma = 0.014, \Lambda = 15, \upsilon = 0.03, \iota = 1, \eta_1 = 0.12, \eta_2 = 0.25, \eta_3 = 0.05, \alpha_2 = 0.21, \alpha_1 = 0.21, \delta = 0.25, \delta_0 = 0.023, a = 0.3, b = 0.1, \lambda = 0.03$, then $R_0 = 0.1954 < 1$, and $(S(0), I(0), R(0)) = (2.5, 5.5, 1.7.)$ (See Fig 5.1). According to Fig. 5.1, the infection diminishes over time and ultimately disappears, signifying eradication of the epidemic.

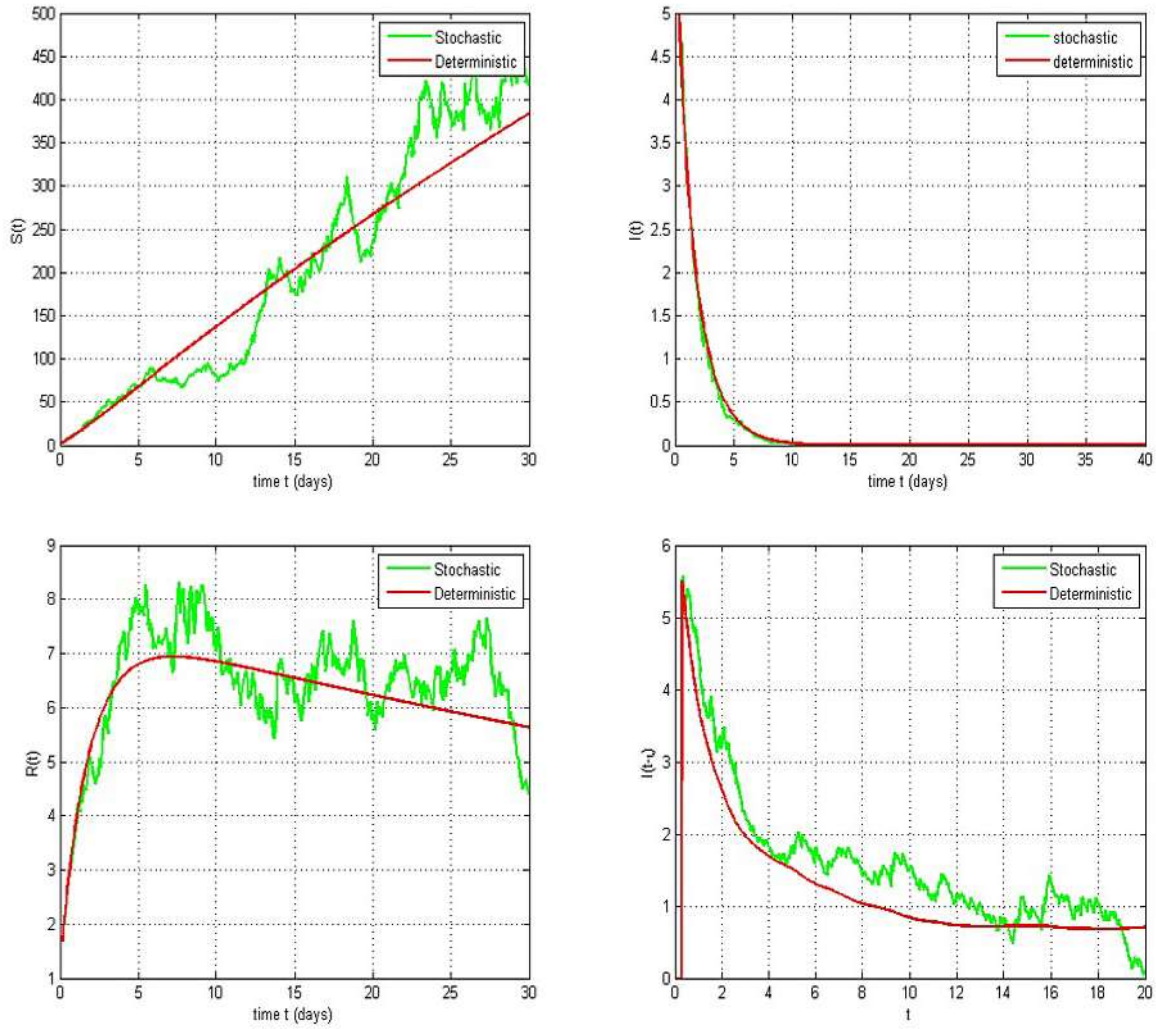

Figure 5.1: Simulated deterministic and stochastic trajectories of model (5.4) based on the parameters in Example 5.1.

Example 5.2. The parameters are selected as follows: $\Lambda = 35, \gamma = 0.659, \upsilon = 0.096, \iota = 0, \eta_1 = 0.0399, \eta_2 = 0.0573, \eta_3 = 0.029, \alpha_1 = 0.029, \alpha_2 = 0.4897, \delta = 0.0458, \delta_0 = 0.0081, a = 0.1, b = 0.001, \lambda = 0.02$, then $\bar{R}_0 = 25.9318 > 1$, with $S(0) = 5.8$, $I(0) = 6.5$, $R(0) = 3.3$. By theorem 5.4 the system (5.4) possesses a unique stationary distribution. (see left column in Fig 5.2). Biologically, this indicates that the disease will continue to circulate within the population and will not die out naturally given the present circumstances.

Fig. 5.3 displays the marginal density functions of S, I, and R, while the right column of Fig. 5.2 presents the corresponding density functions alongside their frequency histograms.

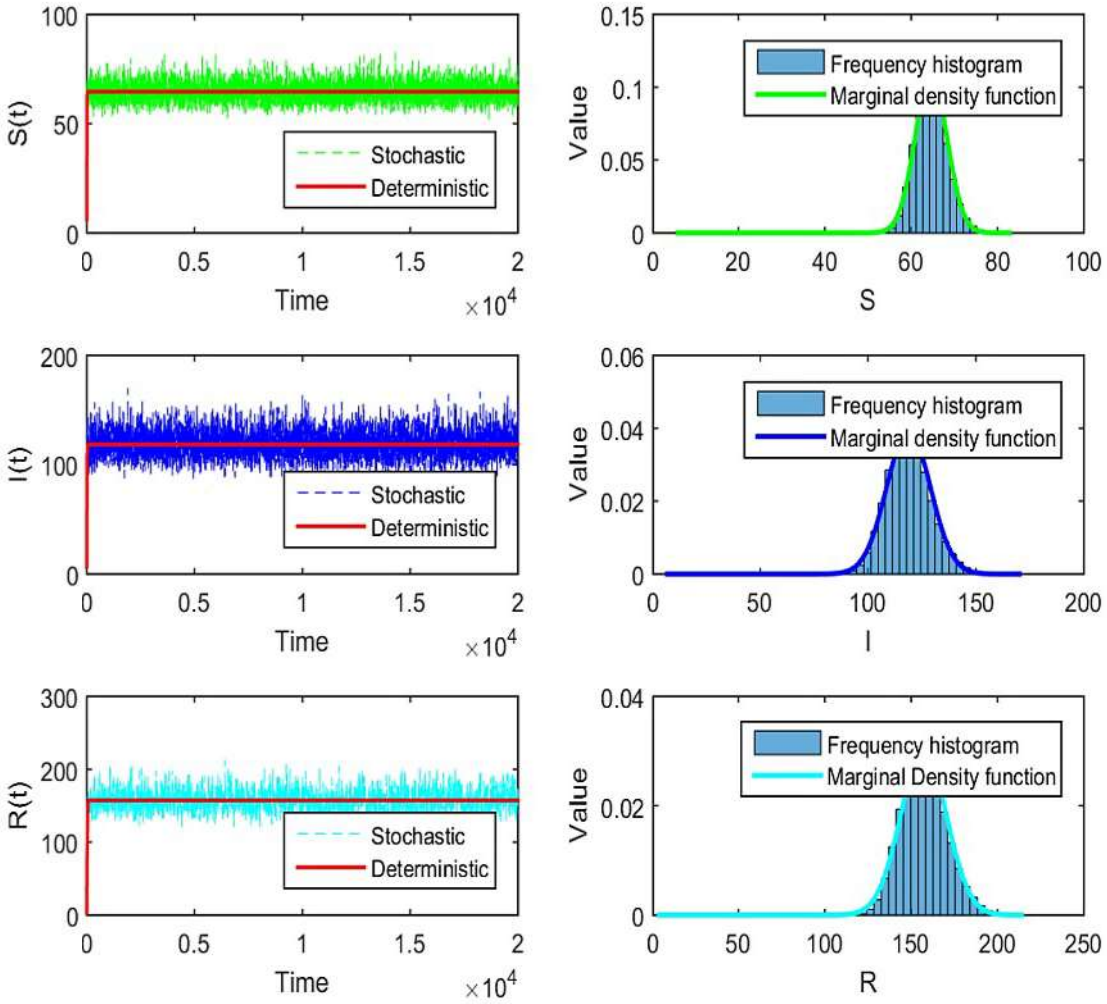

Figure 5.2: Left column: simulations of compartments S, I, and R for the deterministic and stochastic systems. Right column: frequency histograms and marginal density curves for S, I, and R, using the parameters from Example 5.2.

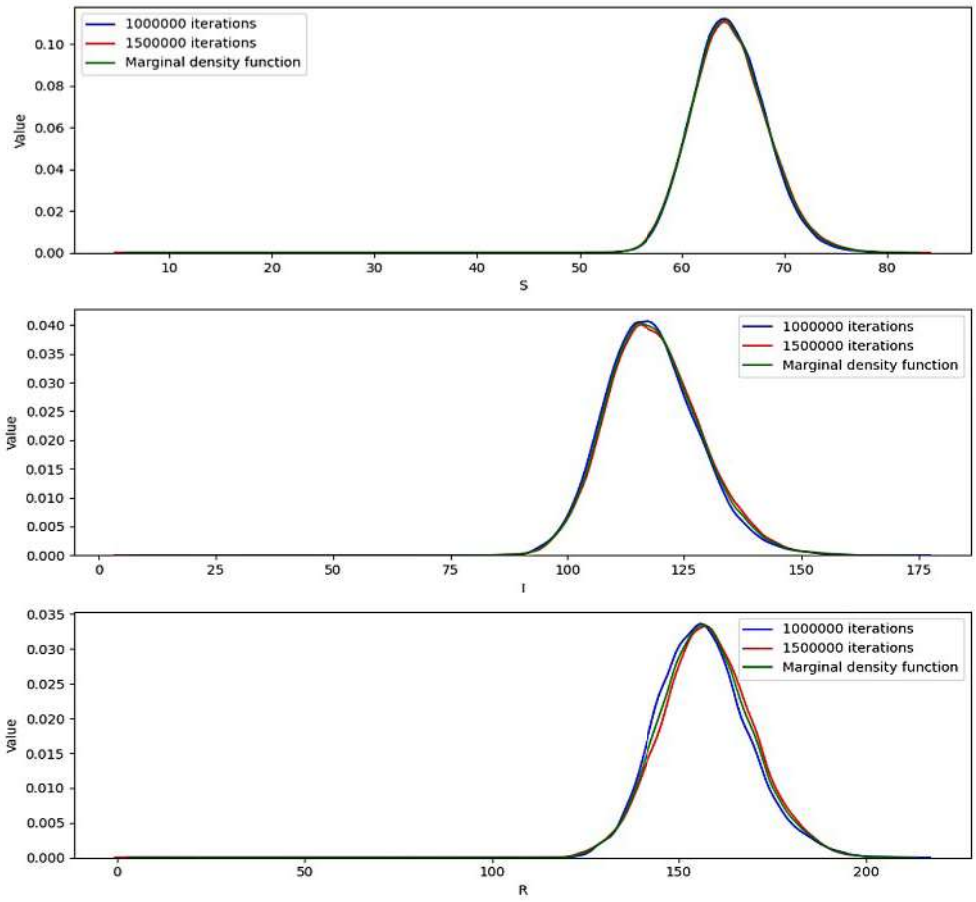

Figure 5.3: Computer simulations for S, I, and R: the marginal density curves are shown in green. At 1,000,000 and 1,500,000 iterations, the frequency histograms of the trajectories are fitted and represented by blue and red lines, respectively.

Example 5.3. We use the following parameters [131]: $\delta = 0.25,\ \Lambda = 15,\ \alpha_2 = 0.1, \alpha_1 = 0.1,$ $\gamma = 0.2,\ \delta_0 = 0.23,\ a = 0.3,\ \upsilon = 0.3,\ b = 1, \lambda = 0.4$, and $(S(0), I(0), R(0)) = (2.5, 0.5, 5.7)$ Also, we use various values of time delay ι, and η_1, η_2, η_3. Fig 5.4-Fig 5.5, show the solution behavior for the model (5.4) with various values of time delay ι, and η_1, η_2, η_3.

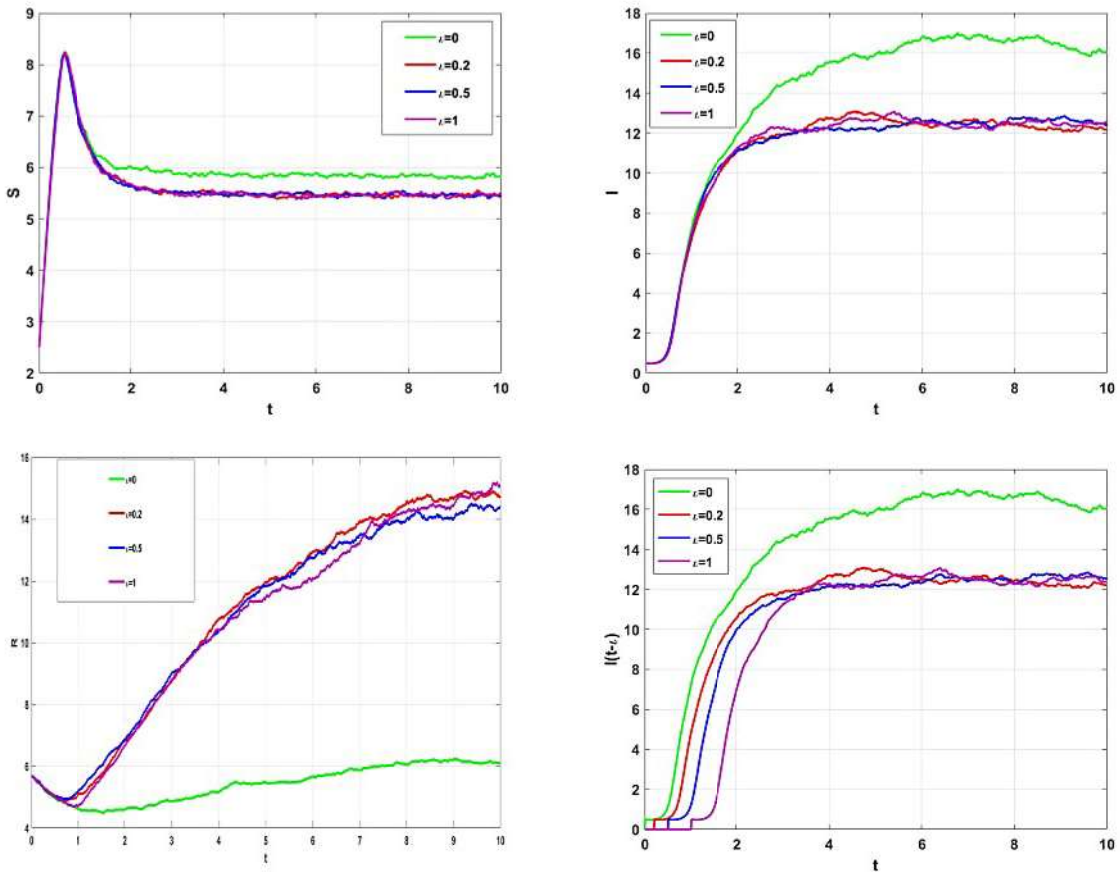

Figure 5.4: Simulation results for model (5.4) under different time delays ι and levels of white noise intensity $\eta_1 = \eta_2 = \eta_3 = 0.02$.

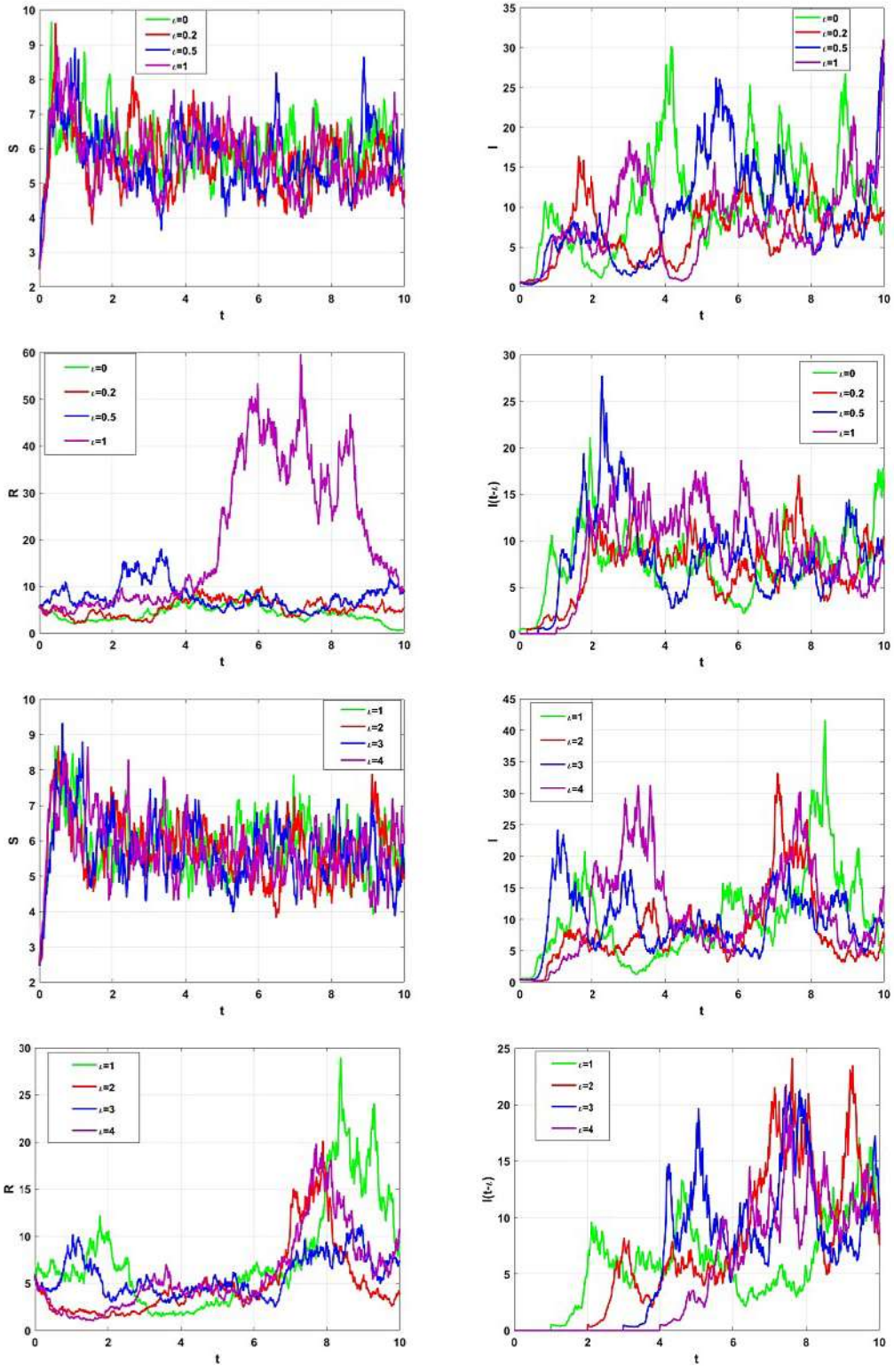

Figure 5.5: Simulation results for model (5.4) under different time delays ι and levels of white noise intensity $\eta_1 = 0.45, \eta_2 = 0.65, \eta_3 = 0.5$.

Our findings indicate that the number of infected individuals reaches its peak when $\iota = 0$, and

gradually declines as ι increases to 0.2, 0.5, and 1. This pattern implies that longer immunity durations are associated with lower infection prevalence. The parameter ι denotes the duration of immunity following recovery, where higher values correspond to prolonged immune protection. When immunity is short-lived, recovered individuals quickly revert to the susceptible class, increasing the likelihood of reinfection and sustaining a high level of infection within the population. Conversely, as ι grows, individuals remain immune for longer periods, which decreases the number of susceptibles and slows the spread of infection. These results underscore the critical role of prolonged immunity-whether through natural recovery, vaccination, or booster doses-in curbing disease transmission and reducing the overall impact of the epidemic.

Through a combination of theoretical analysis and numerical simulations, we found that when $\bar{R}_0 > 1$, a lower intensity of white noise allows model (5.4) to admit a unique ergodic stationary distribution. In contrast, when $R_0 < 1$, higher levels of white noise can drive the disease to extinction. Compared to the deterministic model, the incorporation of stochastic white noise and time delays has a pronounced effect on the persistence and eradication of the disease, thereby enhancing the model's ability to capture complex and realistic epidemic dynamics.

5.7 Conclusion

This study presents a comprehensive analysis of a time-delayed stochastic SIR model incorporating HT-II treatment and C-M incidence, enabling a realistic examination of disease transmission dynamics. By rigorously proving the existence, uniqueness, and stability of solutions, we establish a strong theoretical basis for understanding the models long-term behavior. This foundation ensures biological consistency, which is vital for producing reliable epidemic forecasts. Critical parameters influencing disease extinction were identified, with particular emphasis on transmission rates, treatment efficiency, and the effects of time delays. The analytical derivation of the probability density function offers deeper insight into the stochastic dynamics near the endemic equilibrium, facilitating a more nuanced assessment of disease persistence and fluctuations in infection levels. The theoretical findings were validated through extensive numerical simulations. These simulations demonstrate the significant influence of nonlinear incidence, treatment responses, and temporal delays on disease progression and control. Additionally, they emphasize the importance of accounting for both deterministic and stochastic effects when modeling real-world epidemics. In conclusion, this study not only enriches the theoretical understanding of epidemic behavior under stochastic and delayed influences but also provides practical modeling tools for improving epidemic prediction and intervention strategies. By incorporating more realistic epidemiological

assumptions, the model contributes to more robust and actionable public health planning. Ultimately, the results support the design of targeted control measures aimed at reducing disease incidence and preventing future outbreaks.

Chapter 6

Dynamical analysis of a Tungiasis model for Public Health Education incorporating Lévy process

This chapter focuses on analyzing the long-term behavior of a newly developed stochastic model for Tungiasis, a parasitic skin disease caused by "Tunga penetrans". The proposed model categorizes the population into three groups: susceptible individuals, educated individuals, and infected individuals. We establish the well-posedness of the system by demonstrating the global existence and positivity of solutions. Furthermore, we derive sufficient conditions under which the disease either dies out or continues to persist within the population. To illustrate our theoretical findings, we perform numerical simulations that illustrate and support the analytical results, providing deeper insight into the dynamics of Tungiasis under stochastic influences.

6.1 Introduction

Tungiasis is a parasitic skin condition caused by the infestation of Tunga penetrans, a tiny flea commonly referred to as the chigoe flea or jigger. This disease predominantly affects individuals in tropical and subtropical regions, where the flea thrives in sandy environments. It poses a significant public health challenge in impoverished and rural areas, particularly across sub-Saharan Africa, the Caribbean, and South America [48, 59, 116]. The condition develops when the female flea burrows into the skin, typically on the feet, to feed and lay eggs. This results in severe itching, pain, and inflammation. If left untreated, tungiasis can lead to complications such as secondary bacterial infections, ulcers, and in extreme cases, tetanus or gangrene. Tungiasis primarily impacts

those with limited access to adequate footwear and healthcare. Prevention measures, including proper sanitation, the use of protective footwear, and timely treatment, are crucial in reducing the burden of this neglected tropical disease.

The use of public health education is essential for managing and preventing tungiasis. The impact of health education initiatives can be increased by the public health authority by educating the public about the disease's modes of transmission, modes of spread, and shifts in the number of sick people. Furthermore, the disease's spread can be considerably slowed by public health measures including giving away free pesticides, free shoes, and vaccination campaigns [43].

In biology and disease control, mathematical models are frequently employed and have shown themselves to be an effective tool for researching the spread of infectious illnesses. Researchers create mathematical models to examine the dynamic behavior of infectious illnesses in order to stop their spread [49, 77, 92, 104]. Specifically, Nyang and al. [92] examined a mathematical model of how public health education affects tungiasis

$$\begin{aligned}
\mathcal{S}'(t) &= \Lambda - \beta\mathcal{I}(t)\mathcal{S}(t) - (\epsilon+\mu)\mathcal{S}(t) + \gamma\mathcal{I}(t),\\
\mathcal{E}'(t) &= -\mu\mathcal{E}(t) - \alpha\beta\mathcal{E}(t)\mathcal{I}(t) + \epsilon\mathcal{S}(t),\\
\mathcal{I}'(t) &= \alpha\beta\mathcal{E}(t)\mathcal{I}(t) - (\mu+\sigma+\gamma)\mathcal{I}(t) + \beta\mathcal{I}(t)\mathcal{S}(t),
\end{aligned} \tag{6.1}$$

where $\mathcal{S}(t), \mathcal{E}(t)$, and $\mathcal{I}(t)$, respectively, represent the number of susceptible people, public health educators, and infected people at time t. the parameters are shown in table 6.1. The dynamics of the spread of Tungiasis model (6.1) can be completly analyzed based on the basic reproduction number which the approach described in [113] can compute. It is given as follows

$$R_0^d = \frac{\Lambda\beta(\epsilon\alpha+\mu)}{(\epsilon+\mu)(\sigma+\gamma+\mu)\mu},$$

more precisely, if $R_0^d < 1$, the disease-free equilibrium $P_0 = (\frac{\Lambda}{\mu+\epsilon}, \frac{\epsilon\Lambda}{(\mu+\epsilon)\mu}, 0)$ is globally asymptotically stable. If $R_0^d > 1$ then, P_0 unstable and there exists the endemic equilibrium point $P^* = (\mathcal{S}^*, \mathcal{E}^*, \mathcal{I}^*)$, and it is globally asymptotically stable [92].

Table 6.1: Parameter description.

parameters	Meaning
Λ	the birth rate.
β	the rate of Tungiasis transmission through effective contact.
γ	rate of recovery.
ϵ	education dissemination rate.
σ	death rate due to Tungiasis infection.
α	the impact of public health education on infection prevention, where $\alpha \in [0,1]$.
μ	the disease's mortality rate.
b	Saturation incidence coefficient.

Because of changes in the natural environment, there may be some uncertainties and stochastic occurrences in the spread of infectious diseases. Numerous research have demonstrated that the dynamics of infectious diseases may be investigated and perturbed epidemic models can be formulated using SDEs [4, 76, 120].

In [59], Kong et al. extended the model (6.1) to include a white noise process and get the following stochastic Tungiasis model

$$\begin{aligned} d\mathcal{S}(t) &= \Big[\Lambda - \beta\mathcal{I}(t)\mathcal{S}(t) - (\epsilon+\mu)\mathcal{S}(t) + \gamma\mathcal{I}(t)\Big]dt + \eta_1\mathcal{S}(t)d\mathcal{W}_1(t), \\ d\mathcal{E}(t) &= \Big[-\mu\mathcal{E}(t) - \alpha\beta\mathcal{E}(t)\mathcal{I}(t) + \epsilon\mathcal{S}(t)\Big]dt + \eta_2\mathcal{E}(t)d\mathcal{W}_2(t), \\ d\mathcal{I}(t) &= \Big[\alpha\beta\mathcal{E}(t)\mathcal{I}(t) - (\mu+\sigma+\gamma)\mathcal{I}(t) + \beta\mathcal{I}(t)\mathcal{S}(t)\Big]dt + \eta_3\mathcal{I}(t)d\mathcal{W}_3(t), \end{aligned} \tag{6.2}$$

where $\mathcal{W}_1,\mathcal{W}_2,\mathcal{W}_3$ are Brownian motion independent defined on $(\Omega,\mathcal{F},\{\mathcal{F}_t\}_{t\geq 0},\mathbb{P})$. η_1,η_2,η_3 are the level of white noise intensity.

However, when the population experiences abrupt catastrophic disturbances like earthquakes, storms, and floods, epidemic models that are just disturbed by Gaussian white noise are unable to adequately describe the scenario. Severe environmental change can have a major impact on the epidemic's dynamical behavior [58, 128, 133]. Therefore, in order to investigate and control infectious diseases during these events, the discontinuous Levy process must be used. Based to the Lévy-Itô decomposition [19], a Lévy process is decomposed into the sum of a superposition of centered Poisson processes with varying jump sizes, a Brownian motion and a linear drift. Motivated by what mentioned above and we assume that the incidence rate is saturated [18] and considering that the Tungiasis model is governed by Lévy jumps, then model (6.1) can be

formulated by the following SDEs:

$$\begin{aligned}
d\mathcal{S}(t) &= \Big[\Lambda - \frac{\beta\mathcal{I}(t)\mathcal{S}(t)}{1+b\mathcal{I}(t)} - (\epsilon+\mu)\mathcal{S}(t) + \gamma\mathcal{I}(t)\Big]dt + \eta_1\mathcal{S}(t)d\mathcal{W}_1(t) + \int_{\mathbb{I}}\delta_1(\tau)\mathcal{S}(t^-)\mathcal{N}(dt,d\tau),\\
d\mathcal{E}(t) &= \Big[-\mu\mathcal{E}(t) - \alpha\beta\mathcal{E}(t)\mathcal{I}(t) + \epsilon\mathcal{S}(t)\Big]dt + \eta_2\mathcal{E}(t)d\mathcal{W}_2(t) + \int_{\mathbb{I}}\delta_2(\tau)\mathcal{E}(t^-)\mathcal{N}(dt,d\tau),\\
d\mathcal{I}(t) &= \Big[\alpha\beta\mathcal{E}(t)\mathcal{I}(t) - (\mu+\sigma+\gamma)\mathcal{I}(t) + \frac{\beta\mathcal{I}(t)\mathcal{S}(t)}{1+b\mathcal{I}(t)}\Big]dt + \eta_3\mathcal{I}(t)d\mathcal{W}_3(t) + \int_{\mathbb{I}}\delta_3(\tau)\mathcal{I}(t^-)\mathcal{N}(dt,d\tau),
\end{aligned} \tag{6.3}$$

with

$$\mathcal{Y}(0) = (\mathcal{S}(0),\mathcal{E}(0),\mathcal{I}(0)) \in \mathbb{R}^3_+,$$

where $\mathcal{S}(t^{-1}), \mathcal{E}(t^{-1})$ and $\mathcal{I}(t^{-1})$ are the left limits of $\mathcal{S}(t)$, $\mathcal{E}(t)$ and $\mathcal{I}(t)$, respectively. $\mathcal{P}$ is a Poisson counting measure with compensating martingale $\mathcal{N}$ and characteristic measure π on a measurable subset $\mathbb{I}$ of $]0;\infty[$ satisfying $\pi(\mathbb{I}) < 1$. $\mathcal{W}_1, \mathcal{W}_2, \mathcal{W}_3$ are independent of $\mathcal{P}$. We assume that π is a Lévy measure such that $\mathcal{N}(dt,d\tau) = \mathcal{P}(dt,d\tau) - \pi(\tau)dt$ and $\delta_j : \mathbb{I} \to \mathbb{R}$ $(j = 1,2,3)$ are continuous functions.

6.2 Global Positive Solution: Existence and Uniqueness

In this paper, we adopt the following assumption.

- **H1)** $\delta_j(\tau)$ are a bounded function, $\delta_j(\tau)+1 > 0$ and $\int_{\mathbb{I}}(\delta_j(\tau) - \ln(1+\delta_j(\tau)))\lambda(\tau) < \infty$ $(j = 1,2,3)$, $\tau \in \mathbb{I}$.

We now proceed to show that system (6.3) admits a unique positive solution.

Theorem 6.1. *For all $\mathcal{Y}(0) \in \mathbb{R}^3_+$, there is a unique solution $\mathcal{Y}(t)$ of system (6.3). Morever, $\mathcal{Y}(t)$ will remain in $\mathbb{R}^3_+$, $\forall\, t \geq 0$ a.s.*

Proof. To prove it, we use the same approach using the following Lyapunov function:

$$\Sigma : \mathbb{R}^3_+ \to \mathbb{R}_+, \quad \text{where}$$

$$\Sigma(\mathcal{S},\mathcal{E},\mathcal{I}) = \mathcal{S} + \mathcal{E} + \mathcal{I} - 2 - a - (a\ln\frac{\mathcal{E}}{a} + \ln\mathcal{S} + \ln\mathcal{I}).$$

Applyin the Itô formula, we get

$$\begin{aligned}
d\Sigma(\mathcal{S},\mathcal{E},\mathcal{I}) &= L\Sigma(\mathcal{S},\mathcal{E},\mathcal{I})dt + \eta_1(\mathcal{S}(t)-1)d\mathcal{W}_1(t) + \eta_2(\mathcal{E}(t)-a)d\mathcal{W}_2(t) + \eta_3(\mathcal{I}(t)-1)dW_3(t)\\
&+ \int_{\mathbb{I}}(\mathcal{S}\delta_1(\tau) - \ln(1+\delta_1(\tau)))\mathcal{N}(dt,d\tau) + \int_{\mathbb{I}}(\mathcal{E}\delta_2(\tau) - a\ln(1+\delta_2(\tau)))\mathcal{N}(dt,d\tau)\\
&+ \int_{\mathbb{I}}(\mathcal{I}\delta_3(\tau) - \ln(1+\delta_3(\tau)))\mathcal{N}(dt,d\tau),
\end{aligned}$$

where

$$
\begin{aligned}
L\Sigma(\mathcal{S},\mathcal{E},\mathcal{I}) =& \left(1-\frac{1}{\mathcal{S}}\right)\left(\Lambda-\frac{\beta\mathcal{I}(t)\mathcal{S}(t)}{1+b\mathcal{I}}-(\epsilon+\mu)\mathcal{S}(t)+\gamma\mathcal{I}(t)\right)\\
&+\left(1-\frac{a}{\mathcal{E}}\right)\left(-\mu\mathcal{E}(t)-\alpha\beta\mathcal{E}(t)\mathcal{I}(t)+\epsilon\mathcal{S}(t)\right)\\
&+\left(1-\frac{1}{\mathcal{I}}\right)\left(\alpha\beta\mathcal{E}(t)\mathcal{I}(t)-(\mu+\sigma+\gamma)\mathcal{I}(t)+\frac{\beta\mathcal{I}(t)\mathcal{S}(t)}{1+b\mathcal{I}}\right)+\frac{\eta_1^2+a\eta_2^2+\eta_3^2}{2}\\
&+\int_{\mathbb{I}}\Big[(a\delta_1(\tau)-a\ln(1+\delta_1(\tau)))+(\delta_2(\tau)-\ln(1+\delta_2(\tau)))+(\delta_3(\tau)-\ln(1+\delta_3(\tau)))\Big]\lambda(d\tau),\\
=&\Lambda-\mu(\mathcal{E}+\mathcal{S}+\mathcal{I})-(\gamma+\sigma)\mathcal{I}-\frac{\Lambda}{\mathcal{S}}+\frac{\beta\mathcal{I}}{1+b\mathcal{I}}-\frac{\gamma\mathcal{I}}{\mathcal{S}}+(\epsilon+\mu)-\frac{\beta\mathcal{S}}{1+b\mathcal{I}}-\alpha\beta\mathcal{E}+a\alpha\beta\mathcal{I}\\
&+\sigma+\gamma+\mu+a\mu-\frac{a\epsilon\mathcal{S}}{\mathcal{E}}+\frac{\eta_1^2+a\eta_2^2+\eta_3^2}{2}\\
&+\int_{\mathbb{I}}\Big[(a\delta_1(\tau)-a\ln(1+\delta_1(\tau)))+(\delta_2(\tau)-\ln(1+\delta_2(\tau)))+(\delta_3(\tau)-\ln(1+\delta_3(\tau)))\Big]\lambda(d\tau),\\
&\leq \sigma+\gamma+2\mu+\Lambda+\epsilon+a\mu+\frac{\beta}{b}+(a\alpha\beta-\sigma-\mu-\gamma)\mathcal{I}+3M+\frac{\eta_1^2+a\eta_2^2+\eta_3^2}{2},
\end{aligned}
$$

where

$$
\begin{aligned}
M=\max\Big(&\int_{\mathbb{I}}(\delta_1(\tau)-\ln(1+\delta_1(\tau)))\lambda(\tau),\int_{\mathbb{I}}(a\delta_2(\tau)-a\ln(1+\delta_2(\tau)))\lambda(\tau),\\
&\int_{\mathbb{I}}(\delta_3(\tau)-\ln(1+\delta_3(\tau)))\lambda(\tau)\Big)\geq 0.
\end{aligned}
$$

Choosing $a=\frac{\sigma+\mu+\gamma}{\alpha\beta}$ such that $-(\sigma+\mu+\gamma)+a\alpha\beta=0$, then we have

$$
L\Sigma(\mathcal{S},\mathcal{E},\mathcal{I})\leq a\mu+\Lambda+\epsilon+\sigma+\gamma+2\mu+\frac{\beta}{b}+\frac{\eta_1^2+a\eta_2^2+3M+\eta_3^2}{2}:=M_1,
$$

where $M_1>0$ is a constant. Therefore, we obtain

$$
\begin{aligned}
d\Sigma(\mathcal{S},\mathcal{E},\mathcal{I})\leq& M_1dt+\eta_1(\mathcal{S}(t)-1)d\mathcal{W}_1(t)+\eta_2(\mathcal{E}(t)-a)d\mathcal{W}_2(t)+\eta_3(\mathcal{I}(t)-1)dW_3(t)\\
&+\int_{\mathbb{I}}(\mathcal{S}\delta_1(\tau)-a\ln(1+\delta_1(\tau)))\mathcal{N}(dt,d\tau)+\int_{\mathbb{I}}(\mathcal{E}\delta_2(\tau)-\ln(1+\delta_2(\tau)))\mathcal{N}(dt,d\tau)\\
&+\int_{\mathbb{I}}(\mathcal{I}\delta_3(\tau)-\ln(1+\delta_3(\tau)))\mathcal{N}(dt,d\tau).
\end{aligned}
$$

Integration from 0 to $\tau_k\wedge T=\min\{\tau_k,T\}$ gives

$$
\begin{aligned}
\int_0^{\tau_k\wedge T}d\Sigma(\mathcal{S},\mathcal{E},\mathcal{I})\leq&\int_0^{\tau_k\wedge T}M_1dt+\eta_1\int_0^{\tau_k\wedge T}(\mathcal{S}(t)-1)d\mathcal{W}_1(t)+\int_0^{\tau_k\wedge T}\eta_2(\mathcal{E}(t)-a)d\mathcal{W}_2(t)\\
&+\int_0^{\tau_k\wedge T}\eta_3(\mathcal{I}(t)-1)dW_3(t)+\int_0^{\tau_k\wedge T}\int_{\mathbb{I}}(\mathcal{S}\delta_1(\tau)-a\ln(1+\delta_1(\tau)))\mathcal{N}(dt,d\tau)\\
&+\int_0^{\tau_k\wedge T}\int_{\mathbb{I}}(\mathcal{E}\delta_2(\tau)-\ln(1+\delta_2(\tau)))\mathcal{N}(dt,d\tau)\\
&+\int_0^{\tau_k\wedge T}\int_{\mathbb{I}}(\mathcal{I}\delta_3(\tau)-\ln(1+\delta_3(\tau)))\mathcal{N}(dt,d\tau).
\end{aligned}
$$

Taking expectation, We obtain

$$\mathbb{E}\Big[\Sigma\big(\mathcal{Y}(\tau_k \wedge T)\big)\Big] \leq \Sigma\big(\mathcal{Y}(0)\big) + \mathbb{E}\Big[\int_0^{\tau_k \wedge T} M_1 dr\Big],$$
$$\leq \Sigma\big(\mathcal{Y}(0)\big) + M_1 T.$$

The rest of the proof follows the same approach as proving theorem 3.1. □

6.3 Extinction of the disease

In this subsection, we investigate the condition for the extinction of the disease. We put $\langle \Theta(t) \rangle = \frac{1}{t}\int_0^t \Theta(s)ds$.

Lemma 6.1. *Assume that $\mathcal{Y}(t)$ is a solution to model (6.3) for any initial value, then*

$$\lim_{t\to\infty} \frac{\int_0^t \mathcal{S}(r)d\mathcal{W}_1(r)}{t} = 0, \quad \lim_{t\to\infty} \frac{\int_0^t \mathcal{E}(r)d\mathcal{W}_2(r)}{t} = 0, \quad \lim_{t\to\infty} \frac{\int_0^t \mathcal{I}(r)d\mathcal{W}_3(r)(t)}{t} = 0,$$

$$\lim_{t\to\infty} \frac{\int_0^t \int_{\mathbb{I}} \delta_1(\tau)\mathcal{S}(r)\mathcal{N}(dr,d\tau)}{t} = 0, \quad \lim_{t\to\infty} \frac{\int_0^t \int_{\mathbb{I}} \delta_2(\tau)\mathcal{E}(r)\mathcal{N}(dr,d\tau)}{t} = 0,$$

$$\lim_{t\to\infty} \frac{\int_0^t \int_{\mathbb{I}} \delta_3(\tau)\mathcal{I}(r)\mathcal{N}(dr,d\tau)}{t} = 0 \quad a.s.$$

Morever

$$\lim_{t\to\infty} \frac{\mathcal{S}(t)}{t} = 0, \quad \lim_{t\to\infty} \frac{\mathcal{E}(t)}{t} = 0, \quad \lim_{t\to\infty} \frac{\mathcal{I}(t)}{t} = 0, \quad a.s. \tag{6.4}$$

Proof. The proof follows a similar approach as in [73]. □

Theorem 6.2. *Suppose that **(H1)** holds. Let $\big(\mathcal{S}(t),\mathcal{E}(t),\mathcal{I}(t)\big)$ be a solution of 6.3 with initial value $\mathcal{Y}(0) \in \mathbb{R}^3$, if*

$$R_0^E = \frac{\Lambda\alpha\beta + \Lambda\beta}{(\gamma + \sigma + \mu + \varphi_3)\mu} < 1,$$

where $\varphi_3 = \frac{\eta_3^2}{2} + \int_{\mathbb{I}}(\delta_3(\tau) - \ln(1+\delta_3(\tau)))\lambda(\tau)$,
then $\limsup_{t\to\infty} \frac{\ln \mathcal{I}(t)}{t} < 0$ a.s., namely, $\mathcal{I}(t) \longrightarrow 0$ exponentially a.s. Moreover

$$\lim_{t\to\infty} \langle \mathcal{S}(t) \rangle = \frac{\Lambda}{\mu + \epsilon}, \qquad \lim_{t\to\infty} \langle \mathcal{E}(t) \rangle = \frac{\Lambda\epsilon}{(\mu+\epsilon)\mu} \quad a.s.$$

Proof. Applying Itô formula we get

$$\begin{aligned} d\ln I(t) &= \Big[\frac{\beta\mathcal{S}}{1+b\mathcal{I}} + \alpha\beta\mathcal{E} - (\mu + \sigma + \gamma + \varphi_3)\Big]dt + \eta_3 d\mathcal{W}_3(t) + \int_{\mathbb{I}} \ln(1+\delta_3(\tau))\mathcal{N}(dt,d\tau), \\ &\leq \Big[\beta\mathcal{S} + \alpha\beta\mathcal{E} - (\mu + \sigma + \gamma + \varphi_3)\Big]dt + \eta_3 d\mathcal{W}_3(t) + \int_{\mathbb{I}} \ln(1+\delta_3(\tau))\mathcal{N}(dt,d\tau), \end{aligned} \tag{6.5}$$

where $\varphi_3 = \frac{\eta_3^2}{2} + \int_{\mathbb{I}}(\delta_3(\tau) - \ln(1+\delta_3(\tau)))\lambda(\tau)$.

Integrating (6.5) from 0 to t and dividing by t gives

$$\frac{\ln \mathcal{I}(t)}{t} \leq \beta\langle \mathcal{S}(t)\rangle + \alpha\beta\langle \mathcal{E}(t)\rangle - (\mu+\sigma+\gamma+\varphi_3) + \frac{1}{t}\int_0^t \eta_3 d\mathcal{W}_3(r) + \frac{1}{t}\int_0^t \int_{\mathbb{I}} \ln(1+\delta_3(\tau))\mathcal{N}(dr,d\tau). \quad (6.6)$$

In other hand

$$\begin{aligned} d(\mathcal{S}+\mathcal{I}+\mathcal{E}) &= (\Lambda - \mu[\mathcal{S}+\mathcal{I}+\mathcal{E}] - (\gamma+\sigma)\mathcal{I})dt + \eta_1\mathcal{S}(t)d\mathcal{W}_1(t) + \eta_2\mathcal{E}(t)d\mathcal{W}_2(t) + \eta_3\mathcal{I}(t)d\mathcal{W}_3(t) \\ &\quad + \int_{\mathbb{I}}\Big[\delta_1(\tau)\mathcal{S}(t^-) + \delta_2(\tau)\mathcal{E}(t^-) + \delta_3(\tau)\mathcal{I}(t^-)\Big]\mathcal{N}(dt,d\tau), \\ &\leq (\Lambda - \mu[\mathcal{S}+\mathcal{I}+\mathcal{E}])dt + \eta_1\mathcal{S}(t)d\mathcal{W}_1(t) + \eta_2\mathcal{E}(t)d\mathcal{W}_2(t) + \eta_3\mathcal{I}(t)d\mathcal{W}_3(t) \\ &\quad + \int_{\mathbb{I}}\Big[\delta_1(\tau)\mathcal{S}(t^-) + \delta_2(\tau)\mathcal{E}(t^-) + \delta_3(\tau)\mathcal{I}(t^-)\Big]\mathcal{N}(dt,d\tau). \end{aligned} \quad (6.7)$$

Then, taking integration of (6.7) from 0 to t, dividing by t

$$\begin{aligned} \langle \mathcal{S}(t)+\mathcal{E}(t)+\mathcal{I}(t)\rangle &\leq \frac{\Lambda}{\mu} + \frac{1}{\mu}\Big[\frac{1}{t}\int_0^t \eta_1 d\mathcal{W}_1(r) + \frac{1}{t}\int_0^t \eta_2 d\mathcal{W}_2(r) + \frac{1}{t}\int_0^t \eta_3 d\mathcal{W}_3(r)\Big] \\ &\quad + \frac{1}{\mu}\Big(\frac{1}{t}\int_0^t\int_{\mathbb{I}}\Big[\delta_1(\tau)\mathcal{S}(r) + \delta_2(\tau)\mathcal{E}(r) + \delta_3(\tau)\mathcal{I}(r)\Big]\mathcal{N}(dr,d\tau)\Big), \end{aligned} \quad (6.8)$$

taking lim sup of (6.8). Using Lemma 6.1, we obtain that

$$\limsup_{t\to\infty}\langle \mathcal{S}(t)+\mathcal{E}(t)+\mathcal{I}(t)\rangle \leq \frac{\Lambda}{\mu} \quad a.s.$$

Hence

$$\limsup_{t\to\infty}\langle \mathcal{S}(t)\rangle \leq \frac{\Lambda}{\mu} \quad a.s, \quad \limsup_{t\to\infty}\langle \mathcal{E}(t)\rangle \leq \frac{\Lambda}{\mu} \quad a.s. \quad (6.9)$$

Substituting (6.9) in (6.6) and using lemma 6.1, leads to

$$\limsup_{t\to\infty}\frac{\ln \mathcal{I}(t)}{t} \leq (R_0^E - 1)(\mu+\sigma+\gamma+\varphi_3),$$

if $R_0^E < 1$, then

$$\limsup_{t\to\infty}\frac{\ln \mathcal{I}(t)}{t} \leq 0 \quad a.s,$$

then

$$\lim_{l\to\infty}\mathcal{I}(t) = 0 \quad a.s. \quad (6.10)$$

Additionaly

$$\begin{aligned} d(\mathcal{S}(t)+\mathcal{I}(t)) &= \Big[\Lambda + \alpha\beta\mathcal{I}\mathcal{E}(t) - (\epsilon+\mu)\mathcal{S}(t) - (\mu+\sigma)\mathcal{I}(t)\Big]dt + \eta_1\mathcal{S}(t)d\mathcal{W}_1(t) + \eta_3\mathcal{I}(t)d\mathcal{W}_3(t) \\ &\quad + \int_{\mathbb{I}}\Big[\delta_1(\tau)\mathcal{S}(t^-) + \delta_3(\tau)\mathcal{I}(t^-)\Big]\mathcal{N}(dt,d\tau), \end{aligned} \quad (6.11)$$

taking integration of (6.11) from 0 to t, dividing by t

$$\frac{\mathcal{S}(t)+\mathcal{I}(t)-(\mathcal{S}(0)+\mathcal{I}(0))}{t}=\Lambda+\alpha\beta\langle\mathcal{E}(t)\mathcal{I}(t)\rangle-(\mu+\epsilon)\langle\mathcal{S}(t)\rangle-(\mu+\sigma)\langle\mathcal{I}(t)\rangle+\frac{\eta_1}{t}\int_0^t\mathcal{S}(r)d\mathcal{W}_1(r)$$

$$+\frac{\eta_3}{t}\int_0^t\mathcal{I}(r)d\mathcal{W}_3(r)+\frac{1}{t}\int_0^t\int_{\mathbb{I}}\Big[\delta_1(\tau)\mathcal{S}(r)+\delta_3(\tau)\mathcal{I}(r)\Big]\mathcal{N}(dr,d\tau),$$

then

$$\langle\mathcal{E}(t)\mathcal{I}(t)\rangle=\frac{1}{\alpha\beta}[-\Lambda+(\mu+\epsilon)\langle\mathcal{S}(t)\rangle+(\mu+\sigma)\langle\mathcal{I}(t)\rangle+\Psi_1(t)],\tag{6.12}$$

where

$$\Psi_1(t)=\frac{1}{t}\int_0^t\int_{\mathbb{I}}\Big[\delta_1(\tau)\mathcal{S}(r)+\delta_3(\tau)\mathcal{I}(r)\Big]\mathcal{N}(dr,d\tau)+\frac{\eta_1}{t}\int_0^t\mathcal{S}(r)d\mathcal{W}_1(r)+\frac{\eta_3}{t}\int_0^t\mathcal{I}(r)d\mathcal{W}_3(r)$$

$$+\frac{\mathcal{S}(t)+\mathcal{I}(t)-(\mathcal{S}(0)+\mathcal{I}(0))}{t}.$$

Similarly, based to the second equation of (6.3), we obtain

$$\langle\mathcal{E}(t)\mathcal{I}(t)\rangle=\frac{1}{\alpha\beta}[-\mu\langle\mathcal{E}(t)\rangle+\epsilon\langle\mathcal{S}(t)\rangle+\Psi_2(t)],\tag{6.13}$$

where

$$\Psi_2(t)=\frac{1}{t}\Big[\int_0^t\int_{\mathbb{I}}\delta_2(\tau)\mathcal{E}(r)\mathcal{N}(dr,d\tau)+\eta_2\int_0^t\mathcal{E}(r)d\mathcal{W}_2(r)+\mathcal{E}(0)-\mathcal{E}(t)\Big].$$

Using lemma 6.1, we have

$$\lim_{t\to\infty}\Psi_j(t)=0,\ j=1,2.\ \ a.s.$$

By (6.12) and (6.13), we find

$$\mu(\langle\mathcal{E}(t)\rangle+\langle\mathcal{S}(t)\rangle)=\Lambda+\Psi_2(t)-[\Psi_1(t)+(\mu+\sigma)\mathcal{I}(t)],\tag{6.14}$$

take a limite of (6.14), we get

$$\lim_{t\to\infty}\mu(\langle\mathcal{E}(t)\rangle+\langle\mathcal{S}(t)\rangle)=\Lambda.\tag{6.15}$$

□

In addition, based to the first equation of (6.3), we obtain

$$\langle\mathcal{S}(t)\rangle=\frac{1}{\epsilon+\mu}\Big[\Lambda-\Big\langle\frac{\beta\mathcal{I}(t)\mathcal{S}(t)}{1+b\mathcal{I}(t)}\Big\rangle+\gamma\langle\mathcal{I}(t)\rangle+\Psi_3(t)\Big],$$

$$\leq\frac{1}{\epsilon+\mu}\Big[\Lambda+\gamma\langle\mathcal{I}(t)\rangle+\Psi_3(t)\Big],$$

where

$$\Psi_3=\frac{1}{t}\Big[\int_0^t\int_{\mathbb{I}}\delta_1(\tau)\mathcal{S}(r)\mathcal{N}(dr,d\tau)+\eta_1\int_0^t\mathcal{S}(r)d\mathcal{W}_1(r)+\mathcal{S}(0)-\mathcal{S}(t)\Big].$$

By lemma 6.1, we have

$$\lim_{t\to\infty} \Psi_3 = 0.$$

Hence

$$\lim_{t\to\infty} \langle \mathcal{S}(t) \rangle \leq \frac{\Lambda}{\mu+\epsilon} \quad a.s.$$

In the same way

$$\lim_{t\to\infty} \langle \mathcal{E}(t) \rangle \leq \frac{\Lambda\epsilon}{(\mu+\epsilon)\mu} \quad a.s.$$

From (6.15), we can conclude that

$$\lim_{t\to\infty} \langle \mathcal{S}(t) \rangle = \frac{\Lambda}{\mu+\epsilon} \quad a.s. \quad \text{and} \quad \lim_{t\to\infty} \langle \mathcal{E}(t) \rangle = \frac{\Lambda\epsilon}{(\mu+\epsilon)\mu} \quad a.s.$$

6.4 Persistence of the Diseases

In this section, We will explore the sufficient condition for the disease's persistence in the mean.

Theorem 6.3. *Suppose that (**H1**) hold. If*

$$R_0^P = \frac{(\Lambda\beta)^{\frac{1}{2}} + (\epsilon\alpha\Lambda\beta)^{\frac{1}{2}}}{(\epsilon+\mu+\varphi_1)^{\frac{1}{2}}(2\mu+\varphi_2+\sigma+\gamma+\varphi_3+1)} > 1,$$

then

$$\liminf_{t\to\infty} \langle \mathcal{I}(t) \rangle \geq \frac{(R_0^P-1)(2\mu+\varphi_2+\sigma+\gamma+\varphi_3+1)}{(b+[\alpha+u_1+u_2]\beta)} > 0,$$

where $\varphi_j = \frac{\eta_j^2}{2} + \int_{\mathbb{I}} (\delta_j(\tau) - \ln(1+\delta_j(\tau)))\lambda(\tau), \quad j = 1,2,3.$

Which means that the infected people $\mathcal{I}$ *in model (6.3) is persist in the mean.*

Proof. We define a C^2-function $\Phi_1 : \mathbb{R}^3_+ \to \mathbb{R}$ as follows :

$$\Phi_1(\mathcal{S},\mathcal{E},\mathcal{I}) = (u_1+u_2)\ln\mathcal{S} - \ln\mathcal{E} - \ln\mathcal{I},$$

where u_1, u_2 are non-negative constants to be determined later. It is clear that, the function $\Phi_1(\mathcal{S},\mathcal{E},\mathcal{I})$ has a minimum point $(\mathcal{S}^*,\mathcal{E}^*,\mathcal{I}^*)$ in $\mathbb{R}^3_+$. Thus, define a non-negative C^2-function Φ:

$$\Phi(\mathcal{S},\mathcal{E},\mathcal{I}) = \Phi_1(\mathcal{S},\mathcal{E},\mathcal{I}) - \Phi_1(\mathcal{S}^*,\mathcal{E}^*,\mathcal{I}^*).$$

Using the Ito formula we get

$$d\Phi(\mathcal{S},\mathcal{E},\mathcal{I}) = L\Phi(\mathcal{S},\mathcal{E},\mathcal{I})dt - (u_1+u_2)\eta_1 d\mathcal{W}_1(t) - \eta_2 d\mathcal{W}_2(t) - \eta_3 dW_3(t)$$

$$- \int_{\mathbb{I}} (u_1+u_2)\ln(1+\delta_1(\tau))\mathcal{N}(dt,d\tau) - \int_{\mathbb{I}} \ln(1+\delta_2(\tau))\mathcal{N}(dt,d\tau) - \int_{\mathbb{I}} \ln(1+\delta_3(\tau))\mathcal{N}(dt,d\tau),$$

where

$$
\begin{aligned}
L\Phi(\mathcal{S},\mathcal{E},\mathcal{I}) &= (u_1+u_2)\Big(-\frac{\Lambda}{\mathcal{S}}+\frac{\beta\mathcal{I}}{1+b\mathcal{I}}+(\epsilon+\mu+\frac{\eta_1^2}{2})-\frac{\gamma\mathcal{I}}{\mathcal{S}}\Big)+\Big(\mu+\frac{\eta_2^2}{2}+\alpha\beta\mathcal{I}-\frac{\epsilon\mathcal{S}}{\mathcal{E}}\Big)\\
&+\Big(-\alpha\beta\mathcal{E}+(\mu+\sigma+\gamma+\frac{\eta_3^2}{2})-\frac{\beta\mathcal{S}}{1+b\mathcal{I}}\Big)+\int_{\mathbb{I}}\Big[(u_1+u_2)[\delta_1(\tau)-\ln(1+\delta_1(\tau))]\\
&+[\delta_2(\tau)-\ln(1+\delta_2(\tau))]+[\delta_3(\tau)-\ln(1+\delta_3(\tau))]\Big]\lambda(d\tau),\\
&\leq\Big(-\frac{u_1\Lambda}{\mathcal{S}}-\frac{\beta\mathcal{S}}{1+b\mathcal{I}}-(1+b\mathcal{I})\Big)+\Big(-\frac{\epsilon\mathcal{S}}{\mathcal{E}}-\frac{u_2\Lambda}{\mathcal{S}}-\alpha\beta\mathcal{E}\Big)+(u_1+u_2)(\epsilon+\mu+\frac{\eta_1^2}{2})\\
&+(\mu+\frac{\eta_2^2}{2})+(\mu+\sigma+\gamma+\frac{\eta_3^2}{2})+(u_1+u_2)\beta\mathcal{I}+\alpha\beta\mathcal{I}+(1+b\mathcal{I})\\
&+\int_{\mathbb{I}}\Big[(u_1+u_2)[\delta_1(\tau)-\ln(1+\delta_1(\tau))]+[\delta_2(\tau)-\ln(1+\delta_2(\tau))]\\
&+[\delta_3(\tau)-\ln(1+\delta_3(\tau))]\Big]\lambda(d\tau),\\
&\leq(u_1\Lambda\beta)^{\frac{1}{3}}+(\epsilon u_2\Lambda\alpha\beta)^{\frac{1}{3}}+u_1(\epsilon+\mu+\varphi_1)+u_2(\epsilon+\mu+\varphi_1)+(\mu+\varphi_2)+(\mu+\sigma+\gamma\\
&+\varphi_3+1)+(b+[\alpha+u_1+u_2]\beta)\mathcal{I}. \qquad (6.16)
\end{aligned}
$$

We put

$$
u_1(\epsilon+\mu+\varphi_1)=\frac{\sqrt{\Lambda\beta}}{\sqrt{(\epsilon+\mu+\varphi_1)}},\ \ u_2(\epsilon+\mu+\varphi_1)=\frac{\sqrt{\epsilon\alpha\Lambda\beta}}{\sqrt{(\epsilon+\mu+\varphi_1)}},
$$

then

$$
u_1=\frac{\sqrt{\Lambda\beta}}{\sqrt{(\epsilon+\mu+\varphi_1)}(\epsilon+\mu+\varphi_1)},\ \ u_2=\frac{\sqrt{\epsilon\alpha\Lambda\beta}}{\sqrt{(\epsilon+\mu+\varphi_1)}(\epsilon+\mu+\varphi_1)}. \qquad (6.17)
$$

Substituting (6.17) in (6.16), gives

$$
L\Phi(\mathcal{S},\mathcal{E},\mathcal{I})\leq-\frac{\sqrt{\Lambda\beta}+\sqrt{\epsilon\alpha\Lambda\beta}}{\sqrt{(\epsilon+\mu+\varphi_1)}}+(\mu+\varphi_2+\mu+\sigma+\gamma+\varphi_3+1)+(b+[\alpha+u_1+u_2]\beta)\mathcal{I},
$$

hence

$$
\begin{aligned}
d\Phi(\mathcal{S},\mathcal{E},\mathcal{I})\leq&\Big[-\frac{\sqrt{\Lambda\beta}+\sqrt{\epsilon\alpha\Lambda\beta}}{\sqrt{(\epsilon+\mu+\varphi_1)}}+(\mu+\varphi_2+\mu+\sigma+\gamma+\varphi_3+1)+(b+[\alpha+u_1+u_2]\beta)\mathcal{I}\Big]dt\\
&-(u_1+u_2)\eta_1 d\mathcal{W}_1(t)-\eta_2 d\mathcal{W}_2(t)-\eta_3 dW_3(t)-\int_{\mathbb{I}}(u_1+u_2)\ln(1+\delta_1(\tau))\mathcal{N}(dt,d\tau) \qquad (6.18)\\
&-\int_{\mathbb{I}}\ln(1+\delta_2(\tau))\mathcal{N}(dt,d\tau)-\int_{\mathbb{I}}\ln(1+\delta_3(\tau))\mathcal{N}(dt,d\tau).
\end{aligned}
$$

By integration and divided by t, we find

$$
\begin{aligned}
\frac{\Phi(\mathcal{S}(t),\mathcal{E}(t),\mathcal{I}(t))-\Phi(\mathcal{S}(0),\mathcal{E}(0),\mathcal{I}(0))}{t}\leq&-(\mu+\varphi_2+\mu+\sigma+\gamma+\varphi_3+1)(R_0^P-1)-\Psi(t)\\
&+(b+[\alpha+u_1+u_2]\beta)\langle\mathcal{I}(t)\rangle. \qquad (6.19)
\end{aligned}
$$

Thus

$$\langle \mathcal{I}(t)\rangle \geq \frac{1}{(b+[\alpha+u_1+u_2]\beta)}\Big(\frac{\Phi(\mathcal{S}(t),\mathcal{E}(t),\mathcal{I}(t))-\Phi(\mathcal{S}(0),\mathcal{E}(0),\mathcal{I}(0))}{t}+\Psi(t)+(\mu+\varphi_2+\mu+\sigma+\gamma+\varphi_3+1)(R_0^P-1)\Big), \tag{6.20}$$

where

$$\Psi(t)=\frac{1}{t}\Big[(u_1+u_2)\int_0^t \eta_1 d\mathcal{W}_1(r)+\int_0^t \eta_2 d\mathcal{W}_2(r)+\int_0^t \eta_3 dW_3(r)+\int_0^t\int_{\mathbb{I}}(u_1+u_2)\ln(1+\delta_1(\tau))\mathcal{N}(dr,d\tau)$$
$$+\int_0^t\int_{\mathbb{I}}\ln(1+\delta_2(\tau))\mathcal{N}(dr,d\tau)+\int_0^t\int_{\mathbb{I}}\ln(1+\delta_3(\tau))\mathcal{N}(dr,d\tau)\Big].$$

Similary, $\lim_{t\to\infty}\Psi(t)=0$.

Taking lim inf of (6.20), and if $R_0^P>1$, we obtain

$$\liminf_{t\to\infty}\langle \mathcal{I}(t)\rangle \geq \frac{(R_0^P-1)(\mu+\varphi_2+\mu+\sigma+\gamma+\varphi_3+1)}{(b+[\alpha+u_1+u_2]\beta)}>0.$$

The proof is over. □

6.5 Numerical Simulations

To verify the theoretical results presented above, this section includes several simulation figures. By using the Milstein approach [41, 106], one may obtain the numerical analysis that supports the theoretical results in model (6.3). Here is the discretized equations of our model :

$$\begin{aligned}
\mathcal{S}_{n+1}&=\mathcal{S}_n+\Big[\Lambda-\frac{\beta\mathcal{I}_n\mathcal{S}_n}{1+b\mathcal{I}_n}-(\epsilon+\mu)\mathcal{S}_n+\gamma\mathcal{I}_n\Big]\Delta t+\xi_1\mathcal{S}_n\sqrt{\Delta t}\mathcal{B}_{1_n}+\frac{\xi_1^2}{2}\mathcal{H}_n(\mathcal{B}_{1_n}^2-1)\Delta t-\delta_1\mathcal{S}_n\mathcal{P}_n,\\
\mathcal{E}_{n+1}&=\mathcal{E}_n+\Big[-\mu\mathcal{E}_n-\alpha\beta\mathcal{E}_n\mathcal{I}_n+\epsilon\mathcal{S}_n\Big]\Delta t+\xi_2\mathcal{E}_n\sqrt{\Delta t}\mathcal{B}_{2_n}+\frac{\xi_2^2}{2}\mathcal{E}_n(\mathcal{B}_{2_n}^2-1)\Delta t-\delta_2\mathcal{E}_n\mathcal{P}_n,\\
\mathcal{I}_{n+1}&=\mathcal{I}_n+\Big[\alpha\beta\mathcal{E}_n\mathcal{I}_n-(\mu+\sigma+\gamma)\mathcal{I}_n+\frac{\beta\mathcal{I}_n\mathcal{S}_n}{1+b\mathcal{I}_n}\Big]\Delta t+\xi_1\mathcal{I}_n\sqrt{\Delta t}\mathcal{B}_{3_n}+\frac{\xi_3^2}{2}\mathcal{I}_n(\mathcal{B}_{3_n}^2-1)\Delta t-\delta_3\mathcal{I}_n\mathcal{P}_n,
\end{aligned} \tag{6.21}$$

where $\mathcal{B}_1,\mathcal{B}_2,\mathcal{B}_3$ are normally-distributed $\mathcal{N}(0,1)$ random variables, $\mathcal{P}$ poisson distribution and Δt is step size. Table 6.5 displays the parameter values utilized in the simulation.

Table 6.2: Parameter's value.

parameters	V1	Source
γ	0.427	[44]
β	0.01498	[44]
ϵ	0.01431	[92]
Λ	0.44	[20]
μ	0.016	[20]
σ	0.05	[44]
b	0.8	assumed
α	0.22	assumed
$\mathcal{S}(0)$	0.05	[59]
$\mathcal{E}(0)$	0.8	[59]
$\mathcal{I}(0)$	0.22	[59]

To validate our theorem, a few numerical simulations are then shown. To elucidate the following aspects, a number of empirical examples will be presented:

- The dynamical behavior of Tungiasis model (6.3) if $R_0^E < 1$.
- The dynamical behavior of Tungiasis model (6.3) if $R_0^P > 1$.
- Effect of α and β parameters on the Tungiasis dynamics.

Example 6.1. We choose the parameter in table 6.5 and the following are the stochastic noise intensity: $\delta_1 = 0.01, \delta_2 = 0.02, \eta_1 = 0.1, \eta_2 = 0.2, \eta_3 = 0.4, \delta_3 = 0.08$.
It is straightforward to verify that $R_0^E < 1$ satisfying the condition of Theorem 6.2. The numerical simulation results, presented in Figure 6.1, indicate that the infected $\mathcal{I}(t)$ becomes extinct in both the deterministic and stochastic models. Moreover, for all value of less than 0.01498, $R_0^E < 1$ is achieved, ensuring that the Tungiasis infection will always die out.

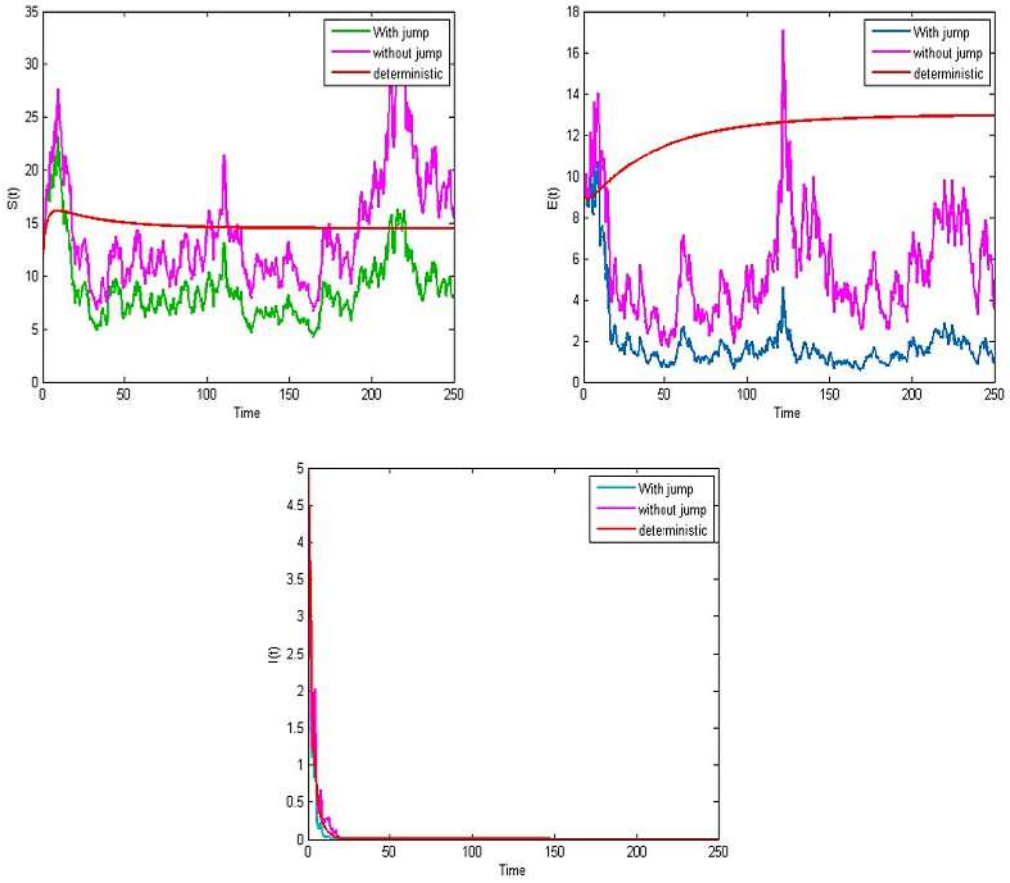

Figure 6.1: The deterministic and stochastic path of solution of model (6.3) with and without jump when $R_0^E < 1$.

Example 6.2. In this example, we increase the connection between $\mathcal{I}$ and $\mathcal{S}$, that is, we increase the value of the parameter $\beta = 0.15$ and keep the same parameters as table 6.5, and the following are the stochastic noise intensity: $\delta_1 = 0.006$,$\delta_2 = 0.003, \eta_1 = 0.05$,$\eta_2 = 0.045, \eta_3 = 0.045, \delta_3 = 0.006$. By calculation we find that $R_0^P > 1$, satisfying the conditions of Theorem 6.3. As stated in Theorem 6.3, the disease exhibits strong persistence, as illustrated in Figure 6.2.

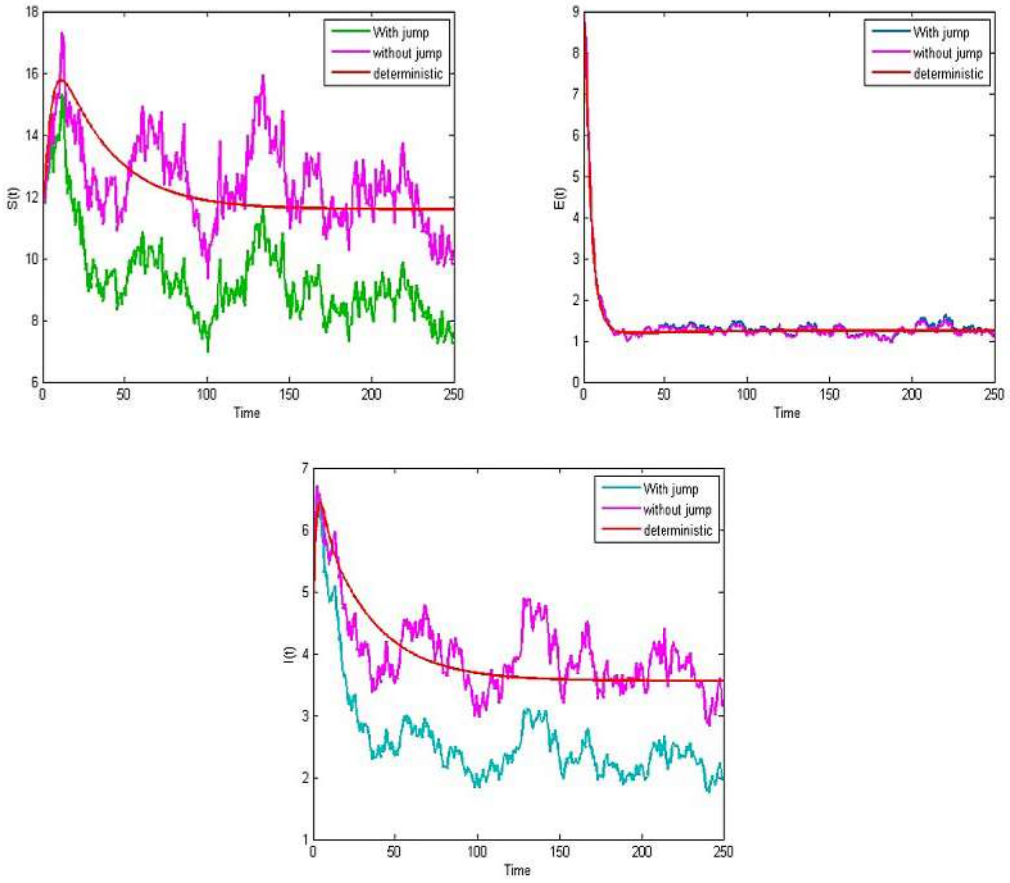

Figure 6.2: Compartement $\mathcal{S}$, $\mathcal{E}$, and $\mathcal{I}$ in the deterministic, stochastic with and without jump are simulated, when $R_0^P > 1$.

When comparing Figures 6.1 and 6.2, it is evident that the contact rate β significantly affects whether the disease persists or goes extinct.

To illustrate the effect of parameters public health education and contact rate on the epedimic outbreak, below we will perform simulation of infected people $\mathcal{I}(t)$ with different values of α and β. The results are shown in figures 6.3 and 6.4.

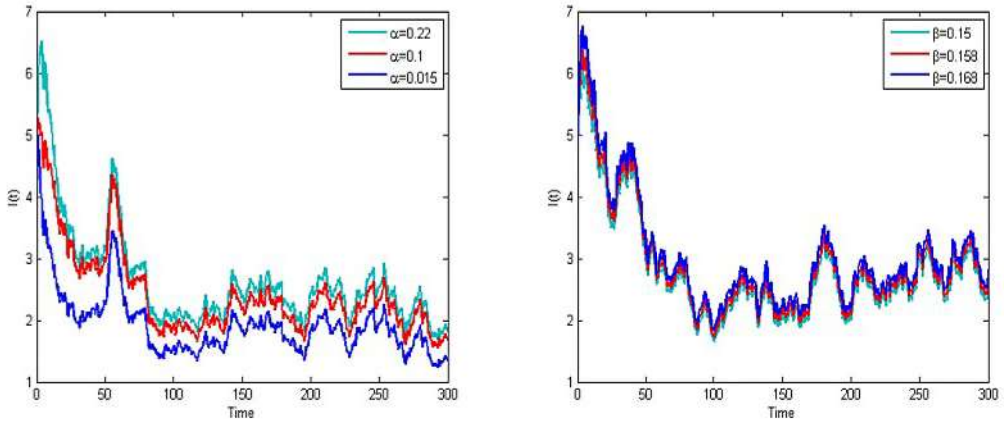

Figure 6.3: Simulation of compartement $\mathcal{I}$ of model (6.3) when $R_0^P > 1$.

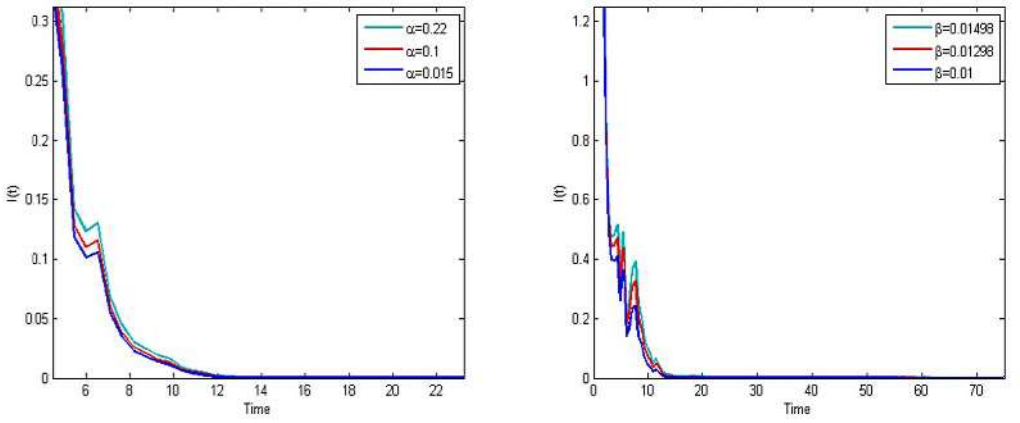

Figure 6.4: Simulation of compartement $\mathcal{I}$ of model (6.3) when $R_0^E < 1$.

6.6 Conclusion

In this chapter, we introduce a stochastic Tunguasis $\mathcal{SEI}$ epidemic model that incorporates the effects of public health education and Lévy noise. We establish the global existence and uniqueness of the systems positive solution and derive sufficient conditions for disease extinction and persistence. To support our theoretical findings, we conduct numerical simulations to examine how various parameters influence disease dynamics. Our results suggest that public health education, contact rate and stochastic fluctuations play crucial roles in determining disease outcomes. Specifically, higher levels of education and stochastic noise, combined with a lower contact rate, increase the likelihood of disease eradication.

This study presents a foundational stochastic dynamical model that aids in understanding

the influence of public health education and stochastic fluctuations on the prevention and control of infectious diseases. From a practical perspective, the findings highlight possible strategies for disease prevention, including enhancing public health awareness, increasing environmental variability, and reducing patient interactions with others.

General conclusion

In this thesis, we have contributed to the modeling and mathematical analysis of several stochastic epidemiological models, aiming to reflect more realistic dynamics of infectious disease spread by incorporating randomness and uncertainty into classical deterministic frameworks. The presence of stochasticity-introduced via white noise and stochastic differential equations-allows a better representation of environmental variability, unpredictable human behavior, and imperfect data reporting, all of which play a significant role in the evolution of epidemics.

The models formulated and analyzed in this work focus on the following key objectives:

- To highlight the necessity of stochastic modeling in capturing the fluctuations and irregularities observed in real epidemic data.
- To explore how stochastic perturbations can influence the disease extinction or persistence, and to determine conditions under which the disease either dies out or stabilizes in a stationary distribution.
- To evaluate the impact of public health strategies-including treatment, vaccination, and behavioral changes-under stochastic dynamics, in order to assess the robustness of control measures in uncertain environments.

Throughout this study, we employed tools from stochastic calculus, particularly Itô's theory, Lyapunov function methods, and numerical simulations, to analyze the existence, uniqueness, and long-term behavior of solutions to the proposed models.

As future directions, we aim to:

- Extend the analysis to more complex stochastic models, including those with switching environments (Markovian switching), delays, or jump processes, which better capture sudden changes in transmission patterns or policy.

- Investigate stochastic fractional models, which merge memory effects with environmental randomness, offering a more comprehensive approach to real-world disease modeling.
- Incorporate data-driven calibration techniques to validate the models using real epidemiological datasets, enabling more accurate predictions and practical recommendations for public health decision-makers.

Our work lays a foundational contribution toward understanding the role of randomness in disease transmission dynamics, and provides a framework for further research into stochastic epidemic modeling in both theoretical and applied contexts.

References bibliography

[1] A. I. Abioye, O. J. Peter, H. A. Ogunseye, F. A. Oguntolu, K. Oshinubi, A. A. Ibrahim, and I. Khan. Mathematical model of covid-19 in nigeria with optimal control. *Results in Physics*, 28:104598, 2021.

[2] A. Ahlbom and S. Norel. *Introduction to Modern Epidemiology*. Epidemiology Resources, 1990.

[3] M. Al-arydah. Mathematical modeling and optimal control for covid-19 with population behavior. *Mathematical Methods in the Applied Sciences*, 46:19184–19198, 2023.

[4] L. Allen. An introduction to stochastic epidemic models. *Mathematical Epidemiology*, 144:81–130, 2008.

[5] R. Alqahtani and A. Ajbar. Study of dynamics of a covid-19 model for saudi arabia with vaccination rate, saturated treatment function and saturated incidence rate. *Mathematics*, 9(23):3134, 2021.

[6] F. Alshammari, F. Akyildiz, M. Khan, A. Din, and P. Sunthrayuth. A stochastic mathematical model for understanding the covid-19 infection using real data. *Symmetry*, 14(12):2521, 2022.

[7] K. Amir, H. Ghulam, Z. Mostafa, Z. Gul, and H. U. Wannasingha. A stochastic sacr epidemic model for hbv transmission. *Journal of Biological Dynamics*, 14(1):788–801, 2020.

[8] D. Anwarud and L. Yongjin. Lévy noise impact on a stochastic hepatitis b epidemic model under real statistical data and its fractal-fractional atangana-baleanu order model. *Physica Scripta*, 2021.

[9] A. Athreya, T. Kolba, and J. C. Mattingly. Propagating lyapunov functions to prove noise induced stabilization. *Electronic Journal of Probability*, 17(96):1–38, 2012.

[10] N. T. J. Bailey. *The Mathematical Theory of Infectious Diseases and its Applications*. Charles Griffin & Co., London and High Wycombe, 2nd edition, 1975.

[11] M. S. Bartlett. Some evolutionary stochastic processes. *Journal of the Royal Statistical Society. Series B (Methodological)*, 11(2):211–229, 1949.

[12] D. Bernoulli. Essaie d'une nouvelle analyse de la mortalité causée par la petite vérole et des avantages de l'inoculation pour la prévenir. *French Royal Academy of Sciences in Paris*, pages 1–45, 1760.

[13] G. A. Bocharov and A. A. Romanyukha. Mathematical model of antiviral immune response iii. influenza a virus infection. *Journal of Theoretical Biology*, 167(4):323–360, 1994.

[14] F. Brauer. Mathematical epidemiology: Past, present, and future. *Infectious Disease Modelling*, 2:113–127, 2017.

[15] F. Brauer and C. Castillo-Chavez. *Mathematical Models in Population Biology and Epidemiology*, volume 40. Springer Science & Business Media, 2013.

[16] Y. Cai, Y. Kang, and W. Wang. A stochastic sirs epidemic model with nonlinear incidence rate. *Applied Mathematics and Computation*, 305:221–240, 2017.

[17] V. Capasso. *Mathematical structures of epidemic systems*, volume 97. Springer Science & Business Media, 2008.

[18] V. Capasso and G. Serio. A generalization of the kermack-mckendrick deterministic epidemic model. *Mathematical Biosciences*, 42(1):43–61, 1978.

[19] C. Chen and Y. Kang. Dynamics of a stochastic multi-strain sis epidemic model driven by levy noise. *Communications in Nonlinear Science and Numerical Simulation*, 42:379–395, 2017.

[20] CIA. *The CIA World Factbook*. Skyhorse Publishing, New York, NY, USA, 2011.

[21] P. H. Crowly and E. K. Martin. Functional responses and interference within and between year classes of a dragonfly population. *Journal of the North American Benthological Society*, 8:211–221, 1989.

[22] D. J. Daley and J. Gani. *Epidemic Modelling: An Introduction*, volume 15. Cambridge University Press, 2001.

[23] A. Din. Bifurcation analysis of a delayed stochastic HBV epidemic model: Cell-to-cell transmission. *Chaos, Solitons & Fractals*, 181:114714, 2024.

[24] A. Din, Y. Li, and A. Yusuf. Delayed hepatitis B epidemic model with stochastic analysis. *Chaos, Solitons & Fractals*, 146, 2021.

[25] X. Duan, S. Yuan, and K. Wang. Dynamics of a diffusive age-structured hbv model with saturating incidence. *Mathematical Biosciences and Engineering*, 13:935–968, 2016.

[26] B. Dubey, A. Patara, P. K. Srivastava, and U. S. Dubey. Modelling and analysis of a SEIR model with different types of nonlinear treatment rates. *Journal of Biological Systems*, 21(3):1350023, 2013.

[27] P. Dubey, B. Dubey, and U. S. Dubey. An SIR model with nonlinear incidence rate and Holling type III treatment rate. In *Applied Analysis in Biological and Physical Sciences*, volume 186 of *Springer Proceedings in Mathematics & Statistics*, pages 63–81. 2016.

[28] D. Ebert, C. D. Zschokke-Rohringer, and H. J. Carius. Dose effects and density-dependent regulation of two microparasites of daphnia magna. *Oecologia*, 122:200–209, 2000.

[29] M. El Fatini and B. Boukanjime. Stochastic analysis of a two delayed epidemic model incorporating Lévy processes with a general non-linear transmission. *Stochastic Analysis and Applications*, 38:387–402, 2020.

[30] M. El Fatini, I. Sekkak, R. Taki, and T. El Guendouz. A control treatment for a stochastic epidemic model with relapse and crowly-martin incidence. *The Journal of Analysis*, 29:713–729, 2021.

[31] W. H. Fleming and R. W. Rishel. *Deterministic and Stochastic Optimal Control*. Springer, New York, 1975.

[32] S. Foko and C. Tadmon. Analysis of a delayed spatiotemporal model of HBV infection with logistic growth. *Applicable Analysis*, 103(13):2283–2327, 2023.

[33] I. M. Foppa. *A Historical Introduction to Mathematical Modeling of Infectious Diseases*. Academic Press, 2017.

[34] T. Gard. *Introduction to Stochastic Differential Equations.* Marcel Dekker, Inc., New York, 1988.

[35] S. A. Gourley, Y. Kuang, and J. D. Nagy. Dynamics of a delay differential equation model of hepatitis b virus infection. *Journal of Biological Dynamics*, 2:140–153, 2008.

[36] A. Gray, D. Greenhalgh, L. Hu, X. Mao, and J. Pan. A stochastic differential equation SIS epidemic model. *SIAM Journal on Applied Mathematics*, 71(3):876–902, 2011.

[37] Y. Gu, S. Ullah, M. A. Khan, M. Y. Alshahrani, M. Abohassan, and M. B. Riaz. Mathematical modeling and stability analysis of the covid-19 with quarantine and isolation. *Results in Physics*, 34:105284, 2022.

[38] Y. E. hadj Moussa, A. Boudaoui, S. Ullah, K. Muzammil, and M. B. Riaz. Application of fractional optimal control theory for the mitigating of novel coronavirus in algeria. *Results in Physics*, 39, 2022.

[39] R. Z. Has'minskii. *Stochastic Stability of Differential Equations.* Sijthoff & Noordhoff, Alphen aan den Rijn, Netherlands, 1980.

[40] K. Hattaf and N. Yousfi. A generalized HBV model with diffusion and two delays. *Computers & Mathematics with Applications*, 69:31–40, 2015.

[41] D. J. Higham. An algorithmic introduction to numerical simulation of stochastic differential equations. *SIAM Review*, 43(3):525–546, 2001.

[42] H. Hui and L. F. Nie. Analysis of a stochastic HBV infection model with nonlinear incidence rate. *Journal of Biological Systems*, 27(3):399–421, 2019.

[43] H. F. Huo and Y. Y. Wang. Impact of media coverage on the drinking dynamics in the scale-free network. *SpringerPlus*, 5(1):204–216, 2016.

[44] IndexMundi. Kenya demographic profile, 2018. Accessed on 18 September 2021.

[45] J. Jacod and A. N. Shiryaev. *Limit Theorems for Stochastic Processes.* Springer, Berlin Heidelberg New York, 1987.

[46] C. Ji, D. Jiang, and N. Shi. Multigroup SIR epidemic model with stochastic perturbation. *Physica A: Statistical Mechanics and its Applications*, 390(10):1747–1762, 2011.

[47] A. Kadri, A. Boudaoui, S. Ullah, et al. A comparative study of deterministic and stochastic computational modeling approaches for analyzing and optimizing COVID-19 control. *Scientific Reports*, 15:11710, 2025.

[48] J. Kahuru, L. Luboobi, and Y. Nkansah-Gyekye. Modelling the dynamics of tungiasis transmission in zoonotic areas. *J. Math. Comput. Sci.*, 7(2):375–399, 2017.

[49] J. Kahuru, L. S. Luboobi, and Y. Nkansah-Gyekye. Optimal control techniques on a mathematical model for the dynamics of tungiasis in a community. *International Journal of Mathematics and Mathematical Sciences*, 2017, 2017.

[50] M. I. Kamien and N. L. Schwartz. *Dynamic Optimization: The Calculus of Variations and Optimal Control in Economics and Management.* North-Holland, 1991.

[51] M. J. Keeling and P. Rohani. *Modeling Infectious Diseases in Humans and Animals.* Princeton University Press, 2007.

[52] D. G. Kendall. Branching processes since 1873. *Journal of the London Mathematical Society*, 1(1):385–406, 1966.

[53] W. O. Kermack and A. G. McKendrick. A contribution to the mathematical theory of epidemics. *Proceedings of the Royal Society of London. Series A, Containing Papers of a Mathematical and Physical Character*, 115(772):700–721, 1927.

[54] W. O. Kermack and A. G. McKendrick. Contributions to the mathematical theory of epidemics. ii.the problem of endemicity. *Proceedings of the Royal Society of London. Series A, Containing Papers of a Mathematical and Physical Character*, 138(834):55–83, 1932.

[55] W. O. Kermack and A. G. McKendrick. Contributions to the mathematical theory of epidemics. iii.further studies of the problem of endemicity. *Proceedings of the Royal Society of London. Series A, Containing Papers of a Mathematical and Physical Character*, 141(843):94–122, 1933.

[56] M. A. Khan, M. Ismail, S. Ullah, and M. Farhan. Fractional order SIR model with generalized incidence rate. *AIMS Mathematics*, 5(3):1856–1880, 2020.

[57] R. Khasminskii. *Stochastic Stability of Differential Equations*, volume 66. Springer Science & Business Media, 2011.

[58] D. Kiouach and Y. Sabbar. Dynamic characterization of a stochastic sir infectious disease model with dual perturbation. *International Journal of Biomathematics*, 2020.

[59] L. Kong, L. Li, S. Kang, Y. Liu, and W. Feng. Dynamic behavior of a stochastic tungiasis model for public health education. *Discrete Dynamics in Nature and Society*, 2022, 2022.

[60] A. E. Koufi, J. Adnani, A. Bennar, and N. Yousfi. Dynamics of a stochastic sir epidemic model driven by levy jumps with saturated incidence rate and saturated treatment function. *Stochastic Analysis and Applications*, pages 1–19, 2021.

[61] A. Kumar and Nilam. Stability of a time delayed SIR epidemic model along with nonlinear incidence rate and Holling type-II treatment rate. *International Journal of Computational Methods*, 15(6):1850055, 2018.

[62] A. Kumar and Nilam. Dynamic behavior of an SIR epidemic model along with time delay; crowley-martin type incidence rate and holling type ii treatment. *International Jornal of Nonlinear Science and Numerical Simulation*, 20(7-8):757–771, 2019.

[63] Y. N. Kyrychko and K. B. Blyuss. Global properties of a delayed SIR model with temporary immunity and nonlinear incidence rate. *Nonlinear Analysis: Real World Applications*, 6:495–507, 2005.

[64] W. Lee. Hepatitis b virus infection. *New England Journal of Medicine*, 337:1733–1745, 1997.

[65] S. Lenhart and J. T. Workman. *Optimal Control Applied to Biological Models.* Chapman & Hall/CRC Mathematical and Computational Biology Series. Chapman & Hall/CRC, Boca Raton, FL, 2007.

[66] D. Lestari, F. Adi-Kusumo, N. Megawati, and N. Susyanto. A minimum principle for stochastic control of hepatitis c epidemic model. *Boundary Value Problems*, page 52, 2023.

[67] D. Li, F. Wei, and X. Mao. Stationary distribution and density function of a stochastic SVIR epidemic model. *Journal of the Franklin Institute*, 359(16):9422–9449, 2022.

[68] J. Li, K. Wang, and Y. Yang. Dynamical behaviors of an HBV infection model with logistic hepatocyte growth. *Mathematical and Computer Modelling*, 54:704–711, 2011.

[69] X. Li, D. Jiang, and X. Mao. Population dynamical behavior of lotka volterra system under regime switching. *Journal of Computational and Applied Mathematics*, 232(2):427–448, 2009.

[70] X. Li and X. Mao. Population dynamical behavior of non autonomous lotka–volterra competitive system with random perturbation. *Discrete and Continuous Dynamical Systems - Series A*, 24(2):523–545, 2009.

[71] M. Liu and M. Fan. Permanence of stochastic lotka–volterra systems. *Journal of Nonlinear Science*, 27(2):425–452, 2017.

[72] P. Liu and X. Tan. Dynamics analysis of a class of stochastic seir models with saturation incidence rate. *Symmetry*, 14(11):2414, 2022.

[73] Q. Liu, Q. Chen, and D. Jiang. The threshold of a stochastic delayed sir epidemic model with temporary immunity. *Phys. A Stat. Mech. Its Appl.*, 450:115–125, 2016.

[74] Q. Liu, D. Jiang, N. Shi, and T. Hayat. Dynamics of a stochastic delayed SIR epidemic model with vaccination and double diseases driven by Lévy jumps. *Physica A: Statistical Mechanics and its Applications*, 492:2010–2018, 2018.

[75] Z. Liu. Dynamics of positive solutions to SIR and SEIR epidemic models with saturated incidence rates. *Nonlinear Analysis: Real World Applications*, 14:1286–1299, 2013.

[76] T. Luzyanina and G. Bocharov. Stochastic modeling of the impact of random forcing on persistent hepatitis b virus infection. *Math. Comput. Simul.*, 96:54–65, 2014.

[77] W. Lv, L. Liu, and S. J. Zhuang. Dynamics and optimal control in transmission of tungiasis diseases. *International Journal of Biomathematics*, 15(2):1–25, 2021.

[78] Z. Ma. *Dynamical modeling and analysis of epidemics.* World Scientific, 2009.

[79] X. Mao. *Stochastic Differential Equations and Applications.* Horwood, Chichester, UK, 2nd edition, 2007.

[80] X. Mao, G. Marion, and E. Renshaw. Environmental brownian noise suppresses explosions in population dynamics. *Stochastic Processes and their Applications*, 97(1):95–110, 2002.

[81] X. Mao and C. Yuan. *Stochastic Differential Equations with Markovian Switching.* Imperial College Press, London, 2006.

[82] M. Martcheva. *An Introduction to Mathematical Epidemiology.* Springer, 2015.

[83] J. Mattingly, A. Stuart, and D. Higham. Ergodicity for sdes and approximations: locally lipschitz vector fields and degenerate noise. *Stochastic Processes and their Applications*, 101(2):185–232, 2002.

[84] S. Meyn and R. Tweedie. Stability of markovian processes iii: Foster-lyapunov criteria for continuous-time processes. *Advances in Applied Probability*, 25(3):518–548, 1993.

[85] Y. L. Michael. *An Introduction to Mathematical Modeling of Infectious Diseases*. Springer, 2018.

[86] G. N. Mil'shtein. Approximate integration of stochastic differential equations. *Teoriya Veroyatnostei i ee Primeneniya*, 19(3):583–588, 1974.

[87] M. Milunovi and M. Krsti. Long time behavior of a two diffusion stochastic SIR epidemic model with nonlinear incidence and treatment. *Filomat*, 36(8):2829–2846, 2022.

[88] L. Min, Y. Su, and Y. Kuang. Mathematical analysis of a basic virus infection model with application to HBV infection. *Rocky Mountain Journal of Mathematics*, 38:1–13, 2008.

[89] K. Moriyama, H. Okamoto, F. Tsuda, et al. Reduced precore transcription and enhanced core-pregenomic transcription of hepatitis b virus dna after replacement of the precore-core promoter with sequences associated with e antigen-seronegative persistent infections. *Virology*, 226:269–280, 1996.

[90] M. A. Nowak, S. Bonhoeffer, A. M. Hill, R. Boehme, H. C. Thomas, and H. McDade. Viral dynamics in hepatitis b virus infection. *Proceedings of the National Academy of Sciences*, 93:4398–4402, 1996.

[91] M. A. Nowak and R. M. May. *Virus Dynamics*. Oxford University Press, Oxford, 2000.

[92] R. A. Nyanginja, D. N. Angwenyi, C. M. Musyoka, and T. O. Orwa. Mathematical modeling of the effects of public health education on tungiasis-a neglected disease with many challenges in endemic communities. *Advances in Difference Equations*, 426:1–19, 2018.

[93] H. Parhusip, S. Trihandaru, B. A. A. Wicaksono, D. Indrajaya, Y. Sardjono, and O. Vyas. Susceptible vaccine infected removed (svir) model for covid-19 cases in indonesia. *Science and Technology Indonesia*, 7(3), 2022.

[94] M. Parsamanesh and M. Erfanian. Global dynamics of an epidemic model with standard incidence rate and vaccination strategy. *Chaos, Solitons & Fractals*, 117:192–199, 2018.

[95] L. S. Pontryagin, V. G. Boltyanskii, R. V. Gamkrelidze, and E. F. Mishchenko. *The Mathematical Theory of Optimal Processes.* Interscience Publishers John Wiley & Sons, Inc., New York-London, 1962.

[96] P. E. Protter. *Stochastic Integration and Differential Equations*, volume 21 of *Stochastic Modelling and Applied Probability.* Springer, Berlin Heidelberg New York, 2nd edition, 2003.

[97] S. Rajasekar and M. Pitchaimani. Ergodic stationary distribution and extinction of a stochastic sirs epidemic model with logistic growth and nonlinear incidence. *Applied Mathematics and Computation*, 377:125143, 2020.

[98] F. A. Rihan, H. J. Alsakaji, and C. Rajivganthi. Stochastic SIRC epidemic model with time-delay for COVID-19. *Advances in Difference Equations*, 2020.

[99] A. Safarishahrbijari, T. Lawrence, R. Lomotey, J. Liu, C. Waldner, and N. Osgood. Particle filtering in a seirv simulation model of h1n1 influenza. In *2015 Winter Simulation Conference (WSC)*, pages 1240–1251. IEEE, 2015.

[100] M. Samsuzzoha, M. Singh, and D. Lucy. Uncertainty and sensitivity analysis of the basic reproduction number of a vaccinated epidemic model of influenza. *Applied Mathematical Modelling*, 37:903–915, 2013.

[101] K. Sato. *Lévy processes and infinitely divisible distributions.* Cambridge University Press, 1999.

[102] A. Schuster, M.)ielecke, V. Raharimanga, et al. High-resolution infrared thermography: a new tool to assess tungiasis-associated inflammation of the skin. *Tropical Medicine and Health*, 45(23):23–13, 2017.

[103] A. Settati and A. Lahrouz. Stationary distribution of stochastic population systems under regime switching. *Applied Mathematics and Computation*, 244:235–243, 2014.

[104] S. M. Simelane, P. G. Dlamini, F. J. Osaye, G. Obaido, B. Ogbukiri, K. Aruleba, C. M. Jones, C. W. Chukwu, and O. F. Egbelowo. Modeling the impact of public health education on tungiasis dynamics with saturated treatment: Insight through the caputo fractional derivative. *Mathematical Biosciences and Engineering*, 20(5):7696–7720, 2023.

[105] X. Song and A. U. Neumann. Global stability and periodic solution of the viral dynamics. *Journal of Mathematical Analysis and Applications*, 329:281–297, 2007.

[106] Y. Song, P. Liu, and A. Din. A novel stochastic model for human norovirus dynamics: Vaccination impact with lévy noise. *Fractal Fract.*, 8:349, 2024.

[107] G. Strang. *Linear Algebra and Its Applications.* Thomson Learning, Inc., 1988.

[108] C. Tadmon and S. Foko. Modeling and mathematical analysis of an initial boundary value problem for hepatitis b virus infection. *Journal of Mathematical Analysis and Applications*, 474:309–350, 2019.

[109] C. Tadmon and S. Foko. Non-standard finite difference method applied to an initial boundary value problem describing hepatitis b virus infection. *Journal of Difference Equations and Applications*, 26:122–139, 2020.

[110] P. Tankov. *Financial modelling with jump processes.* Chapman and Hall/CRC, 2003.

[111] E. Tornatore, S. M. Buccellato, and P. Vetro. Stability of stochastic SIR system. *Physica A: Statistical Mechanics and its Applications*, 354:111–126, 2005.

[112] A. Tridane, K. Hattaf, R. Yafia, and F. A. Rihan. Mathematical modeling of HBV with antiviral therapy for the immunocompromised patients. *Communications in Mathematical Biology and Neuroscience*, page 20, 2016.

[113] P. van den Driessche and J. Watmough. Reproduction numbers and sub-threshold endemic equilibria for compartmental models of disease transmission. *Mathematical Biosciences*, 180:29–48, 2002.

[114] J. VanderPlank. Analysis of epidemics. In J. G. Horsfall and A. E. Dimond, editors, *Plant Pathology III*, pages 229–289. Academic Press, New York, USA, 1960.

[115] J. VanderPlank. *Plant Diseases: Epidemics and Control.* Academic Press, New York, 1963.

[116] S. Veraldi and M. Valsecchi. Imported tungiasis: a report of 19 cases and review of the literature. *International Journal of Dermatology*, 46(10):1061–1066, 2007.

[117] C. Wang, P. W. Horby, F. G. Hayden, and G. F. Gao. A novel coronavirus outbreak of global health concern. *The Lancet*, 395(10223):470–473, 2020.

[118] P. Wang and J. Jia. Stationary distribution of a stochastic sird epidemic model of ebola with double saturated incidence rates and vaccination. *Advances in Difference Equations*, 2019.

[119] W. Wang and S. Ruan. Bifurcation in an epidemic model with constant removal rates of the infectives. *Journal of Mathematical Analysis and Applications*, 291:775–793, 2004.

[120] X. Wang, Y. Tan, Y. Cali, K. Wang, and W. Wang. Dynamic stochastic hbv infection model with cell-to-cell transmission and immune response. *Mathematical biosciences and engineering*, 18(1):616–642, 2020.

[121] L. Wen and X. Yang. Global stability of a delayed SIRS model with temporary immunity. *Chaos, Solitons & Fractals*, 38:221–226, 2008.

[122] World Health Organization. Hepatitis b. http://www.who.int/mediacentre/factsheets/fs204/en/, revised October 2000.

[123] Worldometers. Algeria COVID-19 coronavirus statistic. https://www.worldometers.info/coronavirus/country/algeria/, revised March 2023.

[124] F. Xie, M. Shan, X. Lian, and W. Wang. Periodic solution of a stochastic HBV infection model with logistic hepatocyte growth. *Applied Mathematics and Computation*, 293:630–641, 2016.

[125] R. Xu, Z. Ma, and Z. Wang. Global stability of a delayed SIRS epidemic model with saturation incidence and temporary immunity. *Computers & Mathematics with Applications*, 59:3211–3221, 2010.

[126] R. Xu and Z. J. Ma. An hbv model with diffusion and time delay. *Journal of Theoretical Biology*, 257:449–509, 2009.

[127] X. Zhang and X. Liu. Backward bifurcation of an epidemic model with saturated treatment function. *Journal of Mathematical Analysis and Applications*, 348:433–443, 2008.

[128] X. Zhang and K. Wang. Stochastic sir model with jumps. *Applied Mathematics letters*, 26(8):867–874, 2013.

[129] W. Zhao, J. Liu, M. Chi, et al. Dynamics analysis of stochastic epidemic models with standard incidence. *Advances in Difference Equations*, page 22, 2019.

[130] Y. Zhao and D. Jiang. The threshold of a stochastic SIRS epidemic model with saturated incidence. *Applied Mathematics Letters*, 34:90–93, 2014.

[131] X. Zhong, S. Guo, and M. Peng. Stability of stochastic SIRS epidemic models with saturated incidence rates and delay. *Stochastic Analysis and Applications*, 35(1):1–26, 2017.

[132] Y. Zhou, Z. Ma, and F. Brauer. A discrete epidemic model for sars transmission and control in china. *Mathematical and Computer Modelling*, 40(13):1491–1506, 2004.

[133] Y. Zhou and W. Zhang. Threshold of a stochastic sir epidemic model with levy jumps. *Physica A*, 446:204–2016, 2016.

[134] C. Zhu and G. Yin. Asymptotic properties of hybrid diffusion systems. *SIAM Journal on Control and Optimization*, 46:1155–1179, 2007.

[135] V. M. Zolotarev. *One-dimensional stable distributions*, volume 65 of *Translations of Mathematical Monographs*. American Mathematical Society, 1986.

[136] B. Øksendal and A. Sulem. *Applied Stochastic Control of Jump Diffusions*. Springer-Verlag, Berlin, 2nd edition, 2007.

ملخص

تُعد النماذج الرياضية، بدعم من المحاكاة الحاسوبية، أدوات قيّمة لتطوير واختبار النظريات المتعلقة بالأنظمة البيولوجية المعقدة التي تشمل الأمراض. فهي تتيح تقييم الفرضيات الكمية، وتقدير قيم المعلمات الأساسية من المعطيات الواقعية، وتحليل الحساسية لهذة المعلمات ، إضافةً إلى تطبيق استراتيجيات التحكم الأمثل في بعض المعلمات. وتُعتبر النمذجة ضرورية بشكل خاص في علم الأوبئة، حيث غالبا ما تكون آليات انتشار المرض غير مفهومة بالكامل، كما أن إجراء التجارب ليس ممكنا في معظم الحالات.

تركز هذه الرسالة على دراسة بعض الأنظمة الديناميكية غير الخطية التي تصف انتشار الأمراض المعدية. وينصب اهتمامنا الرئيسي على تحليل النماذج الوبائية العشوائية، وخصوصا النماذج العشوائية القائمة على تقسيم السكان إلى فئات. تتضمن هذه النماذج، سواء كانت تحتوي على تأخيرات زمنية أو لا، تأثير نوعين محددين من الضوضاء البيئية: الضوضاء البيضاء الغاوسية وضوضاء ليفي. والهدف من ذلك هو دراسة كيفية تأثير هذه الأنواع من العمليات العشوائية على ديناميكيات المرض، مما يساهم في تعميق فهمنا لنمذجة الأوبئة. لقد كنا مهتمين بإثبات وجود حل إيجابي، تفرده، انقراض الوباء، وجود توزيع ثابت، الاستمرار في المتوسط وتوضيح النتائج من خلال المحاكاة العددية.

كلمات مفتاحية: علم الأوبئة، نموذج وبائي عشوائي، ضوضاء بيضاء، ضوضاء ليفي ، إنقراض الوباء، الدوام في المتوسط، التوزيع الثابت، الإرجودية .

Abstract

Mathematical models, supported by computer simulations, are valuable tools for developing and testing theories related to complex biological systems involving diseases. They facilitate the evaluation of quantitative hypotheses, estimation of key parameters from rael data, sensitivity analysis with respect to parameter changes, and the implementation of optimal control strategies for certain parameters. Modeling is particularly vital in epidemiology, where the underlying complexity of disease transmission is often not fully understood, and conducting experimental studies is generally not feasible.

This thesis focuses on the investigation of some nonlinear dynamical systems that describe the spread of infectious diseases. Our main interest lies in the analysis of stochastic epidemic models, especially those based on compartmental frameworks. These models, with or without time delays, incorporate the effects of two specific types of environmental noise: Gaussian white noise and Lévy noise. The objective is to examine how these types of stochastic disturbances influence disease dynamics, thereby contributing to a deeper understanding of epidemic modeling. We were interested in proving the existence of a positive solution, its uniqueness, the extinction of the epidemic, the existence of a stationary distribution , the persistence in mean and illustrate the results by numerical simulation.

Key words: *Epidemiology, Stochastic epidemic model, White nose, Lévy noise, Extinction of desease, Persistence in mean, Stationary distribution, Ergodicity.*

Résumé

Les modèles mathématiques, soutenus par des simulations informatiques, sont des outils précieux pour développer et tester des théories relatives à des systèmes biologiques complexes impliquant des maladies. Ils facilitent l'évaluation d'hypothèses quantitatives, l'estimation des paramètres clés à partir des données reèl, l'analyse de sensibilité par rapport aux variations des paramètres, ainsi que la mise en œuvre de stratégies de contrôle optimal pour certains paramètres. La modélisation est particulièrement essentielle en épidémiologie, où la complexité sous-jacente de la transmission des maladies est souvent mal comprise, et où la réalisation d'études expérimentales n'est généralement pas faisable.

Cette thèse porte sur l'étude de certains systèmes dynamiques non linéaires décrivant la propagation des maladies infectieuses. Notre principal intérêt réside dans l'analyse des modèles épidémiques stochastiques, notamment ceux fondés sur des cadres compartimentaux. Ces modèles, avec ou sans délais temporels, intègrent les effets de deux types spécifiques de bruits environnementaux : le bruit blanc gaussien et le bruit de Lévy. L'objectif est d'examiner comment ces types de perturbations stochastiques influencent la dynamique des maladies, contribuant ainsi à une compréhension plus approfondie de la modélisation épidémique. Nous nous sommes intéressés à démontrer l'existence d'une solution positive, son unicité, l'extinction de l'épidémie, l'existence d'une distribution stationnaire, la persistance en moyenne, et à illustrer les résultats par des simulations numériques.

Mots clés : *Épidémiologie , Modèle épidémique stochastique, Bruite blanch, Bruite Lévy, , Extinction de la maladie , Persistance en moyenne , Distribution stationnaire , Ergodicité*